Remote Sensing Series 38

Mathias Kneubühler

Spectral Assessment of Crop Phenology Based on Spring Wheat and Winter Barley

Remote Sensing Laboratories
Department of Geography
University of Zurich, 2002

Spectral Assessment of Crop Phenology
Mathias Kneubühler

Die vorliegende Arbeit wurde von der Mathematisch-naturwissenschaftlichen Fakultät der Universität Zürich im Sommersemester 2002 aufgrund der Gutachten von Prof. Dr. K. I. Itten und Prof. Dr. K. Staenz, CCRS Ottawa (Canada), als Dissertation angenommen.

Remote Sensing Laboratories
Department of Geography
University of Zürich
Winterthurerstrasse 190
CH-8057 Zürich
Switzerland

http://www.geo.unizh.ch

Printed by the *Druckerei der Zentralstelle der Studentenschaft der Universität Zürich*

ISBN 3-03703-004-6

Summary

The goal of this work is to evaluate the potential of spectroscopy data for the retrieval of biophysical and biochemical parameters to track the main development stages of cereals relevant for agricultural purposes and precision farming needs. The investigated cultivars are spring wheat and winter barley. Emphasis is put on the parameters' suitability to monitor crop stands over a whole range of phenological stages. A methodology of field- and laboratory data acquisition during a cropping cycle is developed. Empirical, semi-empirical and statistical methods are applied to retrieve vitality-related parameters from spectroradiometric data. Data collection is based on widely accepted, operational techniques and instruments.

Agricultural crops pass through a series of phenological stages in which the plant's physiology, reflected by its biochemistry and structural characteristics, constantly changes. Information on crop growth status is important for agricultural management (e.g., time-specific crop management) and the emerging needs of precision crop management (e.g., variable rate application of fertilizer).

The fundamentals of remote sensing applications in support of agricultural management are summarized in the beginning of this work, resulting in the selection of four key parameters to be investigated during a whole vegetation period. They are leaf area index (LAI), fraction of absorbed photosynthetically active radiation (FAPAR), leaf chlorophyll content and water content. Field data acquisition was performed between April and August 1999 on two test fields located in the Limpach valley in northwestern Switzerland. Biological, developmental and economical aspects of wheat and barley on the one hand, and the basics of crop phenology and its characterization, together with a test site description on the other hand, complete this work's context.

Empirical, semi-emipirical and statistical methods of parameter retrieval from spectroradiometric data are implemented. Many of these methods were originally developed under laboratory conditions or from modelling approaches, reported to work on the leaf level, applied to canopies other than cereals, or never used for parameter retrieval over a whole range of phenological stages. LAI is determined using a simplified reflectance model based on an inverse exponential relation between the weighted difference vegetation index (WDVI) and LAI. FAPAR is calculated from LAI using an exponential relation. Spectral ratios involving wavelengths in the visible and near-infrared region of the electromagnetic spectrum are used to calculate leaf chlorophyll content. Plant water content is determined using stepwise multiple linear regression. Leaf- and grain water retrieval is addressed, too.

The section on data acquisition presents a methodology for spectroradiometric data takes and acquisition of plant vitality parameters over a cropping cycle. Such a plan is a prerequisite for the successful retrieval of quantitative information from spectral data. It must incorporate temporal and spatial sampling considerations. Field- and laboratory measurements are based on commonly available and widely accepted instruments. Data characterization by means of statistics is performed for all phenological stages observed, in order to assess infield variabilities of the acquired data sets. An approach for the determination of the sample size to be collected, that includes a mean sample value with a certain probability within a given confidence interval, is presented.

The results of vitality-related vegetation parameter retrieval are discussed according to the methods' respective feasibility. An accuracy assessment is performed. During the crops' growing phase, LAI determination from spectral data can be performed at relative rms errors around 20%. Less accurate results are found for the senescing phase in case of weed infestation and dense canopy structure. FAPAR can be derived from LAI data over the whole cropping cycle at a relative rms error around 8% for a joint data set of both cultivars. The use of wavelengths ratios that involve the visible and near-infrared spectral region to track leaf chlorophyll content turns out not to be successful. It is mainly green biomass (green LAI) that drives the spectral response of a vegetation canopy in this wavelength region. Since spectroradiometric measurements of a crop canopy, as recorded by a remote sensing device, do not represent single leaves, but a whole plant, the extraction of plant water content from spectroradiometric data is more promising than it is the case for leaf water content. Plant water retrieval can be performed at rms errors between 3% and 8%. These results are obtained from stepwise multiple linear regression. During the reproductive phase, grain water content can be linearly correlated to plant water content, given the absence of precipitation.

This work has shown that monitoring the main development stages of cereals by the use of selected vegetation parameters is possible. A suitability characterization of the investigated parameters for phenological observations finds LAI to be a key parameter to track plant vitality. FAPAR is strongly correlated to LAI. Plant water content is judged the most promising vegetation parameter to be used for phenological studies. Determination of leaf chlorophyll content from remote sensing data over a vegetation period suffers from spectral dominance of plant structural effects.

The findings of the 1999 field campaign are applied to a HyMap imaging spectrometer data set, acquired in July 1999. It covers the two test fields, which allows to retrieve the cultivars' current LAI, FAPAR and plant water

content. Image based hyperspectral remote sensing data bears the potential of providing spatially distributed, timely information of a certain regional extent. Such sensors, whether they are air- or spaceborne, can support phenological monitoring of large areas to meet the growing needs of precision farming.

Zusammenfassung (German)

Das Ziel dieser Arbeit liegt in der Evaluation des Potenzials hyperspektraler Daten für die Herleitung biophysikalischer und biochemischer Parameter, um die hauptsächlichen Entwicklungsstadien von in der Landwirtschaft und speziell im Zusammenhang mit teilschlagbezogener Bewirtschaftung von Kulturland ("Precision Farming") wichtigen Getreidearten verfolgen zu können. Die untersuchten Getreidearten sind Sommerweizen und Wintergerste. Spezielles Gewicht wird auf die Charakterisierung der einzelnen Parameter hinsichtlich ihrer Eignung zur phänologischen Überwachung der Kulturen über eine Vegetationsperiode gelegt. In der Arbeit wird eine Methodik zur Erhebung von Feld- und Labordaten vorgestellt. Empirische, semi-empirische und statistische Methoden gelangen zur Anwendung, um die vitalitätsbezogenen Parameter aus hyperspektralen Daten herzuleiten. Die Datenerhebung basiert auf allgemein akzeptierten, operationellen Techniken und Instrumenten.

Landwirtschaftliche Kulturen durchlaufen eine Reihe phänologischer Stadien, in denen sich die Pflanzenphysiologie wandelt, was sich in biochemischen und strukturellen Veränderungen der Pflanze manifestiert. Informationen bezüglich des Wachstumszustandes sind wichtig für zeitkritische landwirtschaftliche Tätigkeiten, wie auch in Bezug auf die wachsenden Bedürfnisse auf dem Gebiet des "Precision Farming".

Die Grundlagen fernerkundlicher Anwendungen in der Landwirtschaft werden zu Beginn der Arbeit dargelegt, woraus sich die Auswahl von vier während einer Vegetationsperiode untersuchten Schlüsselparametern ergibt. Diese Parameter sind der Blattflächenindex (LAI), der Anteil absorbierter, photosynthetisch aktiver Strahlung (FAPAR), der Blattchlorophyllgehalt sowie der Wassergehalt. Die Datenerhebung im Feld wurde zwischen April und August 1999 an zwei ausgewählten Testfeldern im Limpachtal (Kanton Solothurn) durchgeführt. Biologische, wachstumsbezogene sowie wirtschaftliche Aspekte von Weizen und Gerste auf der einen Seite, und die Phänologie von Getreide, deren Parametrisierung sowie eine Beschreibung des Testgebietes

auf der anderen Seite, vervollständigen den Kontext der Arbeit.

Für die Herleitung der Vitalitätsparameter aus spektroradiometrischen Daten wurden empirische, semi-empirische und statistische Methoden implementiert. Viele dieser Methoden wurden ursprünglich unter Laborbedingungen oder durch Modellierung entwickelt, eignen sich insbesondere für Einzelblätter, wurden nie auf Getreideflächen angewendet oder sind noch nie für die Parameterherleitung über mehrere Phänologiestadien verwendet worden. Der LAI wird mittels eines einfachen Reflektanzmodells, das auf einer inversen, exponentiellen Beziehung zwischen dem "Weighted Difference Vegetation Index" (WDVI) und dem LAI beruht, hergeleitet. FAPAR wird über eine exponentielle Beziehung aus dem LAI berechnet. Spektrale Ratios von Wellenlängen im sichtbaren und nahinfraroten Bereich des elektromagnetischen Spektrums werden für die Herleitung des Blattchlorophyllgehaltes verwendet. Der Pflanzenwassergehalt wird mittels "Stepwise Multiple Linear Regression" bestimmt. Die Herleitung von Blatt- und Kornwassergehalt wird ebenfalls diskutiert.

Das Kapitel über Datenerhebung enthält eine Methodik für Spektrometermessungen und zur Erfassung von Vitalitätsparametern über eine Vegetationsperiode. Sie ist Voraussetzung für eine darauf folgende, erfolgreiche Herleitung quantitativer Information aus Spektraldaten. Feld- und Labormessungen basieren auf allgemein akzeptierten und weit verbreiteten Instrumenten. Die Datencharakterisierung umfasst eine statistische Aufbereitung der Daten mit dem Ziel, Variabilitäten innerhalb des Feldes zu jedem erhobenen phänologischen Zeitpunkt zu erfassen. Eine Methode zur Bestimmung der notwendigen Stichprobengrösse, deren Mittelwert mit einer bestimmten Vertrauenswahrscheinlichkeit in einem gegebenen Vertrauensintervall liegt, wird präsentiert.

Die Resultate der Herleitung vitalitätsbezogener Vegetationsparameter werden in Bezug auf die Eignung der jeweiligen Methode und deren Genauigkeit diskutiert. Während der Wachstumsphase kann der LAI aus Spektraldaten mit einem relativen RMS-Fehler um 20% hergeleitet werden. In der Seneszenzphase sind die Genauigkeiten im Falle von Unkraut oder dichter Pflanzendecke geringer. FAPAR kann aus dem LAI über die Vegetationsperiode mittels eines gemeinsamen Datensatzes beider Kulturen mit einem relativen RMS-Fehler um 8% bestimmt werden. Die Verwendung von Wellenlängenratios im sichtbaren und nahinfraroten Bereich zur Herleitung von Blattchlorophyll über mehrere Phänologiestadien ist nicht erfolgreich. Das spektrale Verhalten einer Vegetationsdecke in diesem Wellenlängenbereich wird in erster Linie durch die grüne Biomasse (grüner LAI) und nicht durch Chlorophyll bestimmt. Spektroradiometrische Messungen einer Vegetationsdecke, wie sie

von einem Fernerkundungssensor gemacht werden, repräsentieren nicht Einzelblätter, sondern die gesamte Pflanze. Deshalb ist die Herleitung des Pflanzenwassergehaltes erfolgversprechender als jene des Blattwassergehaltes. Der Pflanzenwassergehalt kann über die Vegetationsperiode mit RMS-Fehlern zwischen 3% und 8% hergeleitet werden. In niederschlagsfreien Zeiten besteht in der reproduktiven Phase ein starker linearer Zusammenhang zwischen Pflanzen- und Kornwassergehalt.

Die vorliegende Arbeit zeigt, dass die Überwachung der hauptsächlichen phänologischen Stadien von Getreide mittels ausgewählter Vegetationsparameter möglich ist. Eine Charakterisierung der Eignung der untersuchten Parameter in Bezug auf phänologische Untersuchungen zeigt, dass der LAI einen Schlüsselparameter darstellt, um die Pflanzenvitalität zu erfassen. FAPAR ist stark mit dem LAI korreliert. Der Pflanzenwassergehalt wird aber als der vielversprechendste Parameter für Phänologiestudien bewertet. Die Bestimmung des Blattchlorophyllgehaltes aus Spektraldaten im sichtbaren und nahinfraroten Wellenlängenbereich wird durch die spektrale Dominanz struktureller Effekte der Pflanzendecke verunmöglicht.

Die Resultate der Feldmesskampagne von 1999 werden auf Daten des abbildenden Spektrometers HyMap angewendet, welche im Juli 1999 aufgenommen wurden. Der Datensatz umfasst die beiden Testfelder von Sommerweizen und Wintergerste, was die Bestimmung von momentanem LAI, FAPAR und Pflanzenwassergehalt innerhalb der Felder erlaubt. Abbildende hyperspektrale Fernerkundungsdaten vermögen Information bestimmten regionalen Ausmasses eines momentanen Zustandes mit räumlichem Bezug wiederzugeben. Deren Sensoren, seien sie flugzeug- oder satellitengestützt, können einen Beitrag zur phänologischen Überwachung grosser Gebiete leisten, um den wachsenden Bedürfnissen des "Precision Farming" gerecht zu werden.

Table of Contents

The cover page shows the observed spring wheat field in the Limpach valley (northwestern Switzerland) during the 1999 cropping cycle. The phenological stages, represented by Zadoks' decimal code (DC), are (from top left to bottom right): DC11, DC13, DC30, DC59, DC 69, DC71-75, DC75, DC75-85, DC87.

List of Figures

List of Tables

Chapter 1

Introduction

1.1 Problem Description

The goal of this work is to evaluate the potential of spectroscopy data for the retrieval of biophysical and biochemical parameters to track the main development stages of cereals relevant for agricultural purposes and precision farming needs. Emphasis is put on the parameters' suitability to monitor crop stands over a whole range of phenological stages. A methodology of field- and laboratory data acquisition during a cropping cycle is developed. Empirical, semi-empirical and statistical methods are applied to retrieve vitality-related parameters from spectroradiometric data. Data collection is based on widely accepted, operational techniques and instruments.

Agricultural crops pass through a series of phenological stages from sowing until harvest. Phenology, as defined by the U.S. International Biological Program Phenology Committee, is *"the study of the timing of recurring biological events, the causes of their timing with regard to biotic and abiotic forces, and the interrelation among phases of the same or different species"* [89].

Much attention has been paid to the application of remote sensing techniques in agriculture from the time when such data first became available [14]. Detailed knowledge about biochemical composition and structure of the vegetation cover is mandatory to take appropriate actions in agricultural management. Vegetation cover characteristics are needed for precision farming purposes or ecological studies to optimize profitability, sustainability and protection of the environment.

The plant's physiological state, reflected by its biochemistry and structural characteristics, constantly changes. This results in spectral changes observable by a remote sensing device. Knowledge of the stage of crop development is necessary for time-specific crop management during crucial periods (e.g. grain filling in cereals or harvest).

While measurements of canopy characteristics of agricultural crops using conventional field sampling methods are time-consuming and expensive, the use of remotely sensed spectroscopy data bears a high potential for extraction of biochemical and biophysical parameters. Spectroscopy data not only accounts for the spatial variability of the surface but also expands the spectral

domain towards small and specific absorption features. It allows to relate measured spectral radiance to the chemical composition of vegetation as well as to the biophysical characteristics.

The following methodological problems have to be addressed to solve the scientific question of this work:

- The selection of vitality-related vegetation parameters:
  The plants' transition from the *vegetative* through the *reproductive* to the *senescing phase* is described by a number of parameters that depend on plant vitality. These parameters are leaf area index (LAI), fraction of absorbed photosynthetically active radiation (FAPAR), chlorophyll content and water content.
- The selection and application of parameter retrieval methods:
  Retrieval methods include empirical, semi-empirical and statistical approaches and their error assessment.
- The definition of a standardized data acquisition process:
  Data acquisition is performed using widely accepted, operational techniques.

The observed parameters are characterized with respect to their suitability to track the stages of crop development. Two different types of cereals, commonly grown in Switzerland, are selected: spring wheat and winter barley. The selection of two independent, but comparable study objects allows to give answer to the question, whether a certain cultivar must be treated separately when assessing its vitality or whether species of the same family may be seen as one set of data.

The abovementioned issues of this work, together with their theoretical background, describe a methodology to assess crop phenology through vitality-related vegetation parameters, based on real data from field measurements.

1.2 The Potential of Remote Sensing in Agriculture

Remote sensing techniques have the potential to provide spectral and spatial information quantitatively, instantaneously and non-destructively. Information on vegetation status generally, and on cultivated land specifically, is of growing importance in an ecological, political as well as economical sense. Remote Sensing can provide three basic types of information required for agricultural management [98]:

- Information on seasonally stable conditions.
- Information on seasonally variable conditions.
- Information required to detect the cause of infield variability and to develop a management strategy.

Seasonally stable conditions only need to be determined preseason and updated if necessary, because they are relatively constant throughout the crop growing season. Products like crop yield maps or soil fertility maps represent an important basis for precision crop management (PCM) systems. Since they are collected over several growing seasons, they reflect the relative productivity of a field over time and help to determine seasonally stable management units.

Soil moisture, weed or insect infestation, crop stress and plant diseases denote changing conditions during the growing season that require management actions. Remote sensing is not only a tool to monitor seasonally variable conditions and support decision management, but is also capable to detect disease infestation before it becomes visible to the human eye. Especially spectroscopy data has proven to be useful for vegetation parameter retrieval and crop diagnosis like nutrient deficiencies detection.

Having information about yield variability available, it remains to understand the relation between crop and soil variability and management strategies, in order to make management and application decisions. Especially imaging spectrometers yield the potential of determining the cause of soil and crop variability. Remote sensing information can improve the capacity and accuracy of decision support systems (DSS) and agronomic models by providing accurate input information, or as a means of within-season calibration or validation. Successful integration of remotely sensed data into crop growth models depends on relating remote sensing measurements with common model inputs or on refining models to link existing remote sensing information to the unavailable data needed for the model.

The availability of appropriate remote sensing data for a critical period of crop development is the most difficult requirement for an operational

application in PCM. Coarse spatial and spectral resolution, insufficient locational accuracy and long repeat cycles have been the main drawbacks to operational use of such data. The requirements of a remote sensing system in the optical domain for precision agriculture applications are discussed in Chapter 2.5.

1.3 The Structure of this Work

This work addresses the question whether the main development stages of an agricultural crop stand can be tracked by selected biophysical and biochemical vegetation parameters, using a standardized methodology of data acquisition and empirical, semi-empirical and statistical methods of parameter retrieval from field spectroscopy data. Field- and laboratory data collection is performed using widely accepted, operational techniques. The investigations are based on ground truth data of spring wheat and winter barley. A number of problems discussed, together with the methodology of data acquisition, equally apply to a range of other agricultural crops.

A compilation of remote sensing applications to agriculture, and the potential of spectroscopy data in support of precision crop management are presented in Chapter 2. The fundamentals of radiative transfer in single leaves and plants are discussed in this chapter, too. Based on plant physiology considerations, vitality-related vegetation parameters, to be retrieved from spectral data, are defined.

Chapter 3 deals with biological, phenological and economical aspects of the cultivars under investigation. Beside a test site description, a widely accepted method for phenological characterization of growth stages of cereals, that is used in this work, is introduced.

Retrieval of the vegetation parameters under investigation is based on a number of empirical, semi-empirical and statistical methods, that are described in Chapter 4. The applied methods are presented in their respective context from literature.

The data basis of this work is introduced in Chapter 5. In the first part of this chapter, a methodology for acquisition of field- and laboratory data is proposed. It deals with sampling strategy considerations and the optimal performance of field- and laboratory measurements. The second part presents the entire data sets acquired during the 1999 field campaign. Measured mean values and the variations present within the data are given for all measurement days over the phenological cycle. The third part deals with a method to determine the minimum sample size to be collected in the field for statistical

relevance of a data set.

The results of vegetation parameter retrieval from spectroscopy data to track the main phenological stages of the observed cultivars are discussed extensively in Chapter 6. Parametrization of the retrieval approaches for the two cultivars is followed by accuracy considerations. Finally, parameter retrieval is performed on a HyMap imaging spectrometer data set by applying the found empirical, semi-empirical and statistical relations from the field measurements.

Chapter 7 draws conclusions on the results achieved in this work. By summarizing the suitability of the observed vitality parameters for observation of the main stages of crop development over a phenological cycle, it addresses this work's main question.

Useful facts about the two agricultural fields investigated are given in the appendix, together with factory specifications of the used instruments.

Chapter 2

Remote Sensing of Agriculture

2.1 Introduction

Remote sensing applications in support of agricultural managment have a long tradition. The contributions of remote sensing to agriculture are manifold, bearing a great potential to serve as a means of information in the emerging and fast growing domain of precision crop management. Remote sensing requirements, system specifications and data integration into agricultural management are addressed in this chapter.

The fundamentals of radiative transfer in leaves and plant canopies are summarized in the second part of this chapter. Variations in radiative transfer over a cropping cycle, which are detectable by a remote sensing device, are caused by biophysical and biochemical parameters. Finally, the selection of parameters investigated in this work to track phenology is discussed.

2.2 A Historical Review

In the early 1970's, american scientists tracked the rapid spread of Southern Leaf Corn Blight across the southern and eastern cornbelts of the United States, that caused devastating damages [13]. Imaging data from airborne cameras and multispectral scanners was used to detect infested corn stands, monitor the desease from changing spectral properties of the plants, and map the dimensions of the affected areas. It could be demonstrated that remote sensing of agricultural areas offers regional and fast information that can be used as decision support input.

The CITARS Project (Crop Identification Technology Assessment for Remote Sensing) of 1973 investigated the potential of remote sensing to identify different crop types in agricultural areas. For the first time, multispectral sensor (MSS) data from a LANDSAT satellite (ERTS-1) was available. The influence of climate, soil, agricultural practice, acreage and phenology on classification accuracy was studied [16].

Remote sensing applications in agriculture in the late 1970's and early 1980's focused mainly on the use of multispectral images for crop classification, inventory mapping and crop production. The feasibility of using

satellite-based multispectral data for estimation of wheat production from actual crop acreage was demonstrated by the Large Area Crop Inventory Experiment (LACIE) and AGRISTARS [93]. They both produced methods that are still in use today for regional crop identification, acreage estimation as well as condition assessment, and defined the physics of relations between spectral measurements and biophysical properties of crop canopies and soils [98]. Many studies in the 1980's relate multispectral reflectances of crop canopies to basic physiological processes like photosynthesis and plant stand parameters such as leaf area index (LAI) or chlorophyll content [14][126]. Vegetation indices that measure vegetation density or cover, photosynthetically active biomass, LAI or green leaf density to portend yield, were developed [7][134]. Some indices were modified to correct for soil background [7][27][28][68].

These empirical studies have been complemented by modelling efforts of leaf- and canopy reflectance for retrieval of biophysical and biochemical parameters from reflectance data [57][71][128]. In 1985, Bauer [13] presented a framework that used optical remote sensing for crop condition assessment. It involved spectral indices (e.g., greenness) or parameters estimated from spectral data (e.g., LAI) of LANDSAT Thematic Mapper (TM) as input to crop growth and yield models, in combination with meteorological, soil and other crop data.

A growing number of satellite launches in the last three decades made multispectral images available to a large community of users. Five MSS were launched since 1972. On LANDSAT 4 and 5, launched in 1982 and 1984, respectively, they were operated together with TM, offering better radiometric and spatial resolution and seven spectral bands. The french SPOT HRV, launched in 1986, 1990, 1993 and 1998 have an additional panchromatic band with a spatial resolution of 10 m. The first Indian Remote Sensing Satellite (IRS) was launched in 1988. LISS-III on IRS-1C nowadays records multispectral data at a spatial resolution of 23 m and panchromatic data at 5.8 m ground resolution. The Enhanced Thematic Mapper Plus (ETM+) on LANDSAT 7 was launched in 1999.

The growing need for quantitative studies on biogeophysical and -chemical processes in ecosystem functioning on the one hand, and vegetation analysis on the other hand, made both higher spectral and spatial resolution necessary, together with improved radiometric performance and accurate geolocation. The 1990's can be regarded as the decade of the emergence of airborne hyperspectral sensors like AVIRIS, DAIS, CASI and HyMap, although prototypes were already designed in the 1970's. A summary on common airborne imaging spectrometers is given by Strobl [121].

The airborne imaging spectrometer APEX (Airborne PRISM Experiment), a joint Swiss/Belgian project with ESA's support, is currently built to close the gap between ground based point measurements and spaceborne imaging spectrometer data acquisition [111][113]. It is designed to be a pushbroom imager with up to 300 spectral bands in the 400-2500 nm wavelength region.

The 36-channels MODIS on TERRA, launched in December 1999, and the 220-channels HYPERION on the EO-1 platform, brought into space in November 2000, mark the beginning of hyperspectral data acquisition from space.

The successful launch of IKONOS-2 in 1999 dramatically increased spatial resolution of remotely sensed data from space. For the first time, it made available multispectral data products of 4 m and panchromatic data of 1 m ground resolution at a programmable repetition rate of less than three days to a large community of users.

The directionality of spectral reflectance and their impact on parameter retrieval from remote sensing data has drawn much attention, although the first instrument in space, capable of acquiring directionally dependent spectral information, POLDER on ADEOS-I, was only operational for eight months in 1996 [45][82]. MISR on the TERRA platform offers data of four spectral bands from nine different pushbroom cameras, each in a different viewing angle.

Upcoming and planned spaceborne systems show four main trends, all meeting certain needs in vegetation analysis and agricultural remote sensing. The following compilation of present and future sensors is not intended to be complete:

- Enhanced multispectral systems at moderate resolutions between 10 to 30 m, together with a high resolution PAN sensor meet the requirements of vegetation cover studies at regional scale.
  The VEGETATION system on SPOT-4 and SPOT-5, operating in four spectral bands at a ground resolution of 1 km, offers daily information for resource management and environmental monitoring at global scale.
- Multispectral systems at high spatial resolution between 1 m (PAN) and 4 m (MSS) meet the spatial requirements of precision agriculture applications. QUICKBIRD-2, designed to acquire panchromatic data at a ground resolution of 0.6 m and multispectral data from the visible and near-infrared region at a resolution of 2.5 m, was susccessfully brought into orbit in October 2001. ORBVIEW-3, which operates in the same spectral regions at ground resolutions of 1 m and 4 m, is planned to be launched in early 2002. The launch of ORBVIEW-4 failed in September 2001.

- Multiangular systems meet the growing needs for spectral information of a target observed under different directions. Multi-directional data helps to determine structural parameters of vegetation canopies. Systems designed to acquire data from differing viewing directions are POLDER on ADEOS-2 and ESA's hyperspectral sensor CHRIS on PROBA. While PROBA was successfully launched in October 2001, the launch of ADEOS-2 is scheduled for late 2002.
- Hyperspectral systems bear the potential of data acquisition for quantitative analysis. Quantification of a remotely sensed effect (e.g., infestation, stress, ripeness) is essential in precision agriculture. The use of a (limited) number of sufficiently small spectral bands (generally ≤ 10 nm) allows for identification of spectral features caused by the observed effect. COIS on NEMO, and ARIES-1 are hyperspectral sensors planned to be brought into space in the near future. MERIS on ENVISAT was launched successfully on March 1st 2002. WARFIGHTER, an imaging spectrometer of 280 channels on board of ORBVIEW-4 was lost due to launch failure.

  Future hyperspectral sensors will be designed for specific applications, resulting in a reduced number of small spectral bands. Such sensors are called superspectral. MERIS' mission objectives can be met by only 15 spectral bands, the smallest bandwidth being 2.5 nm.

Despite an emerging fleet of satellites providing frequent, high-resolution data with quick turnaround and delivery time to users, together with a growing number of crop growth simulation models [63][102][119], airborne systems will continue to play an important role in agricultural remote sensing because of their flexible use.

2.3 Contribution of Remote Sensing to Agriculture

Since the development of remote sensing nearly sixty years ago, there has been a wide range of applications for agricultural management. Improvements in spatial, spectral and temporal resolution of available data products together with the precision agriculture revolution have meant an increase in the availability of services and products that help to manage agricultural operation more efficiently and profitably. Beside of land use and land cover applications for crop inventory and crop production, as performed in the late 1970s and early 1980s, image-based remote sensing offers the potential to provide

spatially and temporally distributed information for agricultural management. Johannson et al. [74] present the following areas in agriculture for remote sensing technology as a management assistance tool:

- crop anomaly detection,
- soil properties or soil inventory,
- crop stress detection,
- crop yield detection,
- nutrient detection,
- detection of crop injury,
- land use / land cover,
- regulation compliance, and
- weather data.

Advances in agricultural management technology, such as variable-rate production input applications, together with advances in global positioning systems (GPS) and geographic information systems (GIS) provide powerful analysis tools for agricultural management. Moran et al. [98] identified eight areas in which remote sensing technology can provide information for precision crop management (PCM) that is currently inadequate or completely unavailable (Tab. 2.1).

Table 2.1 Remote sensing (RS) as a source of information for precision crop management applications [98].

Context of Remote Sensing Input	Contribution of Remote Sensing
Converting point samples to field maps	Combination of on-site measurements of soil and crop properties with RS data to produce accurate, timely maps of soil and crops characteristics for defining precision management units.
Mapping crop yield	Combination of RS information with semi-empirical, statistical or modelling approaches to predict final yield.
Mapping soil variability	Generation of soil-type maps from either bare soil- or full crop cover RS data.
Monitoring seasonally variable soil and crop characteristics	Characterization of soil moisture content, phenological stage, biomass and yield production, evapotranspiration rate, nutrient deficiencies, disease, weed infestation or insect infestation.

Table 2.1 Remote sensing (RS) as a source of information for precision crop management applications [98].

Context of Remote Sensing Input	Contribution of Remote Sensing
Determining the cause of the soil / crop variability	Combination of RS data with agro-meteorological models to determine the cause of variability. Determination of the cause of variability from hyperspectral RS data. Provision of accurate input information for agricultural decision support systems (DSS).
Mapping spatially distributed information on meteorological / climate conditions	Generation of local or regional maps of meteorological parameters like insolation, PAR or rainfall from RS data of coarse spatial and fine temporal resolution.
Producing fine-resolution digital elevation data	Generation of fine-resolution DEMs from stereo- or laserscanner RS data.
Addressing time-critical crop management (TCCM) applications	Identification and quick assessment of the extent of damage. Definition of management units for damage control.

2.4 The Current State of Precision Crop Management

Precision crop management (PCM), site-specific crop management (SSCM), variable rate technology (VRT), precision farming and precision agriculture are terms that are all used interchangeably to refer to a developing agricultural management system that promotes variable management practices within a field according to site or soil conditions. Robert et al. [105] define PCM as an information and technology based agricultural management system to identify, analyze and manage site-soil spatial and temporal variability within fields for optimum profitability, sustainability and protection of the environment. PCM is a knowledge-based system integrating different information technologies like grid sampling, positioning technologies (GPS), geographic information systems (GIS), remote sensing, yield monitor sensors, variable rate applicators (VRA) and crop simulation models. Packing these components into decision-support systems or intelligent farm equipment yields the potential for increased crop productivity, reduced chemical use and reduction in environmental degradation [90].

Precision agriculture relies heavily on positional accuracy. Yield and moisture monitors continuously measure yields and moisture content of the grain while harvesting. Combined with a GPS, they produce a yield map for a given field. Together with soil attribute data, within-field micro

meteorological data and terrain information (DEM), site-specific yield maps can be produced in a GIS. The GIS is the basis for agricultural decision making and management. Its input can either come from various grid sampling techniques [34] or from remote sensing data. Remotely sensed information can provide valuable information for crop management applications as:

- time-critical crop management (TCCM) support like crop condition maps. They allow to monitor changes in crop conditions and pest infestations within fields. Such maps serve as information input for variable rate application of fertilizers, seeds and pestizides within the field.
- decision tool for next year's cropping cycle. Time-series help to define recurrent within-field management units.
- input into crop simulation models. They serve as a decision support tool to make prescriptions for cultural practices that optimize crop growth and yields.

Variable application rates are either specified by a controller unit based on information from a GIS or from tractor-based sensors controlling rate application in near-real time and knowledge of field location as provided by real time differential GPS. Several near-real time sensors have been developed for soil organic matter, soil nitrate levels or soil clay content and thickness. Research has been done into the development of sensors for weed discrimination and crop nitrogen statement assessment [98].

User information requirements and system specifications needed for successful adoption of remote sensing products and services in precision agriculture applications are discussed in Chapter 2.5. Critical factors include timely delivery of remote sensing products and services, agronomic liability, accuracy standards and grower's return on investment [19]. Whether image based remote sensing technology is included in upcoming PCM systems depends on the ability of commercial image providers, engineers and scientists to meet the stringent PCM requirements for quantitative, validated information products [99].

2.5 Remote Sensing Requirements for Agricultural Management

In agriculture, as anywhere else, information is valuable when it leads to improved management decisions. In crop production, this means better crop yields and quality, lower costs and reduced agricultural pollution, all leading to more profitable, more sustainable agricultural management. For remote

sensing, as for any information technology to be profitable to a business, the information, value when adopting the technique, must outstrip its costs. Remote sensing technologies represent an emergent alternative to conventional sampling methods [123]. Sensing performs automated data collection using intensive sampling. It frequently relies on a variable that is correlated with the attribute of management interest.

PCM systems for agricultural management require information on seasonally stable and variable crop conditions and for the detection of the cause of infield variability (Chapter 1.2). Typical parameters used in these systems are acreage by crop type, nutrient availability, soil characteristics, extent of fungal, insect or weed infestation and crop phenology. While the collection of these parameters is time consuming and limited to punctual surveys, remote sensing allows large and continuous radiometric measurements that can provide quantitative information on biophysical and biochemical characteristics of a plant canopy. Parameters retrievable by remote sensing systems must have an impact on the spectral signal of vegetation canopies. Biophysical parameters (e.g., LAI, crop height) affect broader spectral regions and are easier to determine, whereas biochemical concentrations (e.g., nitrogen, lignin) are difficult to detect because of their narrow spectral features, only detectable by hyperspectral sensors, and masking by plant water.

The utility of remote sensing technology for PCM is determined by the measurement accuracy of crop conditions, the location accuracy, the spatial and spectral characteristics, the frequency of revisit periods, and the timeliness of availability. In order to be successful, an image based remote sensing system for PCM must meet certain user information requirements, as summarized in Tab. 2.2.

Measurement accuracies of 70-75% of most crop or soil conditions are considered by data users to be sufficient to implement PCM and improve agricultural profitability.

Differing requirements of spatial resolution for agricultural management can be found in literature [11][92][99]. The spatial resolution of a management unit depends upon the management operation and the equipment used. Gradients of soil parameters vary across short distances so that fertilizer rates may need to change every 10-20 m for nutrients such as nitrogen. The width of tractor-mounted field equipment used for variable rate application is nearly 7 m. Therefore it is economical to manage crop and soil units with a nominal size of 10 m [99].

Location accuracy depends, like spatial resolution, upon agricultural management. It can differ in levels of location accuracy for PCM (from ’plant

specific' to several meters) or in positional accuracy of equipment. Variable rate granular spreaders of a 7 m swath width result in a pointing accuracy of approximately 2 m [99].

The spectral specifications of an optical remote sensing system for agricultural management should meet both requirements of the wavelength range needed and the spectral resolution. To monitor biophysical and biochemical parameters, the visible (VIS), near-infrared (NIR) and short-wave-infrared (SWIR) regions of the electromagnetic spectrum are most promising. Little information can be found in literature on the spectral bandwidth needed for PCM applications. The width of spectral bands is defined by the width of absorption features to be detected. Baret [11] proposes spectral band widths of 10 nm. Apart of the red edge region, he suggests broader spectral bands for the VIS and NIR region because of only a small number of absorption features in these wavelength regions.

Product delivery time desired by data users is 24 hours, preferably 12 hours at 100% reliability. Time-critical crop management (TCCM) operations that require immediate management need a 12 hour turnaround time. Delivery times of one week are only useful for providing data into a GIS for the next year's cropping cycle.

Weekly revisit periods are considered sufficient for agricultural management in general, except for irrigation scheduling (twice a week). But taking into account meteorological conditions, overpass frequencies of one to three days [11] or three days [99] are proposed to guarantee usable data on a weekly basis. More quantitative remote sensing products, offering an accurate assessment of the cause of an anomaly and suggesting a management activity, are reported to raise the request in more frequent coverage.

Table 2.2 User information requirements for PCM.

User Information Category *Parameter of interest*	Factors to be Considered	Requirements
Measurement accuracy *Physical measurement of crop or soil conditions*	- Accuracy needed to improve profitability	70 - 75% [99]
Spatial resolution *Optimal management unit*	- Management operation - Fertilizer rates need to change every 10-20 m - Dimension of field equipment used (1-10 m)	3-4 m optimal, up to 10 m [92] 10 m [99] 5-20 m [11]

Table 2.2 User information requirements for PCM.

User Information Category *Parameter of interest*	Factors to be Considered	Requirements
Location accuracy *Georegistration*	- Level of location accuracy for PCM	1 cm (plant-specific) to several meters (soil parameter. gradients) [99]
	- Positional accuracy of field equipment used (tractor, spreader)	2 m [99]
Spectral characteristics *Spectral range* *Spectral band width* *Wavelength stability*	- Wavelengths relevant for specific application	VIS, NIR, SWIR (crop biomass, ground cover determination, pests, weed and stress conditions) [92]
	- Spectral feature width	10 nm [11]
	- Wavelength calibration	± 0.5 nm [11]
Product delivery time *Timeliness of availability*	- Time-criticism of application	Less than 24 h, preferably 12 h for TCCM [99] 72 h [92]
Revisit period *Overpass frequency*	- Kind of application - Processing level of delivered products - Meteorological conditions	Weekly [11][92] Twice a week to biweekly [99] 3 days [99]

Tab. 2.3 gives a short summary of specifications for an optical remote sensing system for agricultural management, based on the user requirements of Tab. 2.2.

Table 2.3 Specifications for an optical remote sensing system for PCM, based on the user requirements given in Tab. 2.2.

User Information Category	System Specifications
Algorithm accuracy	70-75%
Pixel size	2-5 m
Georegistration accuracy	1 pixel
Spectral characteristics - Spectral range - Spectral band width - Wavelength stability	 VIS, NIR, SWIR 10 nm ±0.5 nm

Table 2.3 Specifications for an optical remote sensing system for PCM, based on the user requirements given in Tab. 2.2.

User Information Category	System Specifications
Product delivery time	< 24h
Revisit period	3 days

2.6 Integration of Remote Sensing into Agricultural Management

Integration of remote sensing data into agricultural management not only depends on successful realization of user information requirements and system specifications (Chapter 2.5), but also on coupling existing crop process models and remote sensing data. Decision making in agricultural management of single fields is based on quantitative information on observed infield variabilities caused by stress, nutrient deficiencies, infestations or phenological stage of the crops. Beside using empirical, semi-empirical or statistical approaches, such information can be obtained from crop growth simulation models. These models summarize analytical knowledge of plant physiology into mathematical equations that describe the primary physiological mechanisms of crop growth (e.g., photosynthesis, respiration) and phenology. Furthermore, the plants' interactions with the underlying environmental factors (e.g., soil, moisture, nutrients) are included. Model state variables, such as developmental phase, plant dry mass or LAI are linked to input variables including weather, location and management [43].

Coupling crop growth models with remote sensing data is reported to show improved results in comparison to using pure agronomy models without remote sensing information [100]. Data integration into growth models can include (a) direct use of a driving variable, (b) updating of a state variable (e.g., LAI), (c) forcing of a model step to meet a certain state or (d) recalibration of the model by adjusting its parameters to obtain a simulation in agreement with the variable (e.g., LAI) derived from the observation [43][91].

Crop growth models describe the relationship between physiological processes in plants and environmental factors such as solar irradiation, temperature and water and nutrient availability. They compute the daily growth and development rate of a crop from emergence till maturity. Examples of crop models using remote sensing information as an input parameter are GRAMI [91], AFRCWHEAT-2 [102], a modified version of CERES-Wheat [12], and SUCROS [30][119]. Since temperature and photoperiod are the driving forces of plant growth, typical input parameters for

these models are mean daily temperature, solar radiation, sowing date and latitude. Common output parameters are grain yield, biomass growth or phenological development. LAI is regarded as an important physical plant characteristic because photosynthesis takes place in the green plant parts. It is normally calculated by multiplying the leaf area per plant by the planting density and is fundamental for daily gross assimilation of a canopy [119].

Crop growth models often appear to fail when severe disturbances of the growing conditions occurr (e.g., diseases, drought, frost). In this case, remote sensing data can be used to update and recalibrate the model. In addition, such data bears the potential to enable growth models to take into account the spatial variability of a field. Recent efforts have been undertaken to scale models from the site-scale to a regional scale [63]. Such considerations become necessary when it comes to decision making on climate change effects and its impacts on national or worldwide cereal production. Upscaling the knowledge of local vegetation characteristics to larger areas can be based on remote sensing in cases where missing spatial and spectral information is needed to run crop models. Such models that are adjusted to regional instead of field scale topics are linked to radiative transfer models, known as SVAT (Soil-Vegetation-Atmosphere Transfer) models [129].

2.7 Radiative Transfer in Plants

2.7.1 Optical Properties of Plant Leaves

A first theory of possible paths for light rays entering a leaf has been formulated by Willstätter and Stoll in 1918 [135]. It is the basis for spectral reflectance, transmittance and absorbtance measurements of Gates et al. [53], Allen et al. [1], Suits [122] and Sinclair et al. [117]. As basic optical laws of refraction, absorption and reflection can be applied to leaves, incident radiation on a leaf surface can be reflected, transmitted or absorbed. Leaf optical properties are a function of leaf structure, water content and concentration of biochemicals [35][52][53][132].

Leaf surface reflection is a combination of diffuse and specular reflection. It is not lambertian and strongly depends on the physiological state of the leaf surface. According to Willstätter and Stoll's theory, light diffusion is mainly due to total reflections which occur in the spongy mesophyll of a leaf, where the orientation of the cell walls and the differences in refractive indices of cell walls and intercellular air spaces provide suitable interfaces for critical reflection. Radiation is eventually reflected back and exits the leaf as diffuse

reflectance [59].

Light diffusion within leaves strongly depends on leaf morphology. Leaves of monocotyledonous plants (Poaceae, e.g., cereals) have a homogeneous mesophyll structure with only few intercellular air spaces. The mesophyll of dicotyledonous leaves (e.g., leguminous plants) consists of palisade cells and spongy parenchyma cells, with randomly oriented cell walls and a large number of air-cell interfaces. These leaves reflect more incident radiation because of the spongy parenchyma's scattering ability [116]. Gates et al. [53] assume that the near-infrared reflectance is a function of the cell shape and size as well as the amount of intercellular space. Therefore, morphological differences between leaves of monocotyledons and dicotyledons cause higher reflectances in the case of dicotyledonous leaves. Allen et al. [2] and Kumar and Silva [80] reexamined Willstätter and Stoll's theory by applying a ray tracing technique and introducing more intercellular air spaces than accounted for in the spongy mesophyll. They concluded that the theory underestimated leaf reflectance. Their work is the basis of today's understanding of diffuse reflectance within a leaf.

Absorption of electromagnetic radiation is mainly caused by pigments occurring in the vacuoles and chloroplasts of green leaves [127] and certain molecules. The two processes causing absorption are electronic transitions and vibrations of polyatomic molecules. Electronic transitions on the one hand result in the formation of an electronically excited state. Since these transitions consume a lot of energy, only shorter wavelengths (400-1000 nm) are concerned. The molecules which absorb light in this spectral domain are the foliar pigments chlorophyll a and b, carotenoids and brown pigments [127]. Chloropyll acts as a photoreceptor and catalysator for photosynthesis. Carotenoids can be divided into oxygen-free carotenes (α - and β - form) and into xantophylls which contain fixed oxygen. The β -carotenes transfer energy towards chlorophyll and protect chlorophyll a from photooxydation [85]. Vibrations of polyatomic molecules on the other hand are caused by absorption of light from chemical compounds like water, cellulose, lignin, starch, pectins, waxes, tannins and nitrogens.

Electromagnetic radiation which is not being reflected or absorbed transmits the leaf. Because of multiple scattering within the leaf, it is of diffuse character. Transmittance of a leaf is therefore determined by leaf morphology, leaf thickness and the amount of leaf pigments.

2.7.2 Spectral Characteristics of Plant Leaves

Reflectance, transmittance and absorptance by leaves are determined by the concentration of pigments and water, along with the internal leaf cell structure. As reported by Bauer [14], these physiological and morphological quantities depend on leaf type, stage of development, senescence and stress. Taking into account the optical properties of plant leaves (Chapter 2.7.1), the shape of a leaf spectrum can be described according to the three 'classical' spectral regions over the 400-2500 nm wavelength range. This range is generally covered by spectroradiometers in the optical domain of the electromagnetic spectrum.

2.7.2.1 Visible Region (400-700 nm)

The visible region of the electromagnetic spectrum is characterized by strong absorption of the foliar pigments chlorophyll and carotenoids. All pigments show absorption maxima between 300-500 nm; only chlorophyll absorbs in the red wavelengths, as well [132]. Principal absorption peaks of extracted chlorophyll a are reported to occur at 430 nm and 660 nm, those of chlorophyll b at 455 nm and 640 nm. Because of the difference in refractive indices between the extract solvent and leaf water, these peaks shift approximately 20 nm toward longer wavelengths when measured in vivo [132]. Lichtenthaler [85] demonstrates the varying wavelength position of maximum absorption depending on the solvent used for chlorophyll extraction. Slightly differing absorption maxima for chlorophyll can be found in literature [35][69]. Chlorophyll a and b are about ten times more concentrated than carotenoids [127]. Carotenoids exhibit overlapping absorption features with chlorophyll. Therefore, the effect of carotenoid absorption in green leaves is masked and becomes only visible during senescence, when chlorophylls degrade faster than carotenoids. Main absorption features of carotenoids lie between 435 nm and 455 nm [85]. Zur et al. [138] report a prominent peak in reflectance spectra of senescing and mature leaves near 520 nm that can be attributed to carotenoids absorption. Chlorophyll absorption decreases rapidly above 670 nm and scattering effects within the leaf cause a strong increase in reflectance between 670 nm and 780 nm, known as the red edge of a vegetation spectrum. Gates et al. [53] and Horler et al. [66] report an apparent spectral shift of the inflection point of the red edge for single leaves as a result of changes in chlorophyll concentration with phenological development.

2.7.2.2 Near-Infrared Region (700-1300 nm)

Since absorption in the near-infrared region is low, light penetrates deeper into the leaf tissue. Spectral characteristics in this region are determined by internal leaf structure [54][117], resulting in high reflectance and transmittance. Minor water absorption features around 975 nm and 1175 nm [35][38][69] significantly vary in shape and depth depending on cellular arrangement within the leaf and hydration state [132]. During plant development, the most important changes in near-infrared reflectance appear during maturation and senescence. As leaves mature and senesce, air spaces in the mesophyll increase, cell geometry changes and moisture content decreases, resulting in higher reflectance values. A similar effect is induced by severe drought stress [127].

2.7.2.3 Shortwave-Infrared Region (1300-2500 nm)

Radiative transfer in the shortwave-infrared region depends mainly on leaf water content and other foliar biochemical components. The main water absorption bands are located around 1450 nm, 1940 nm and 2500 nm, but the overall shape of this wavelength region is strongly influenced by water. Based on the 'plate model' developed by Allen et al. [1], Gausman et al. [54] introduced the concepts of void area index (VAI) and equivalent water thickness (EWT) to explain the effect of intercellular air spaces and leaf water content on reflectance and transmittance. Their concepts were considered in radiative transfer models like PROSPECT [71]. Dehydration increases reflectance and transmittance in the shortwave-infrared region. When the leaf dehydrates, other foliar constituents like cellulose, lignin or starch, whose absorption were masked by water, appear [127].

Curran et al. [35] and Fourty et al. [52] present compilations of known absorption features of biochemical components, together with their wavelength positions and the absorption mechanism.

2.7.3 Optical Properties of Vegetation Canopies

The reflectance of individual leaves is not sufficient to describe the remotely sensed reflectance of a vegetation canopy [69], which makes it extremely difficult to study the role of tissue and structural attributes that determine canopy radiative transfer characteristics [5]. Beside of leaf optical properties, the contribution of stem and litter optical properties, canopy structural attributes and solar and sensor view angles to vegetation reflectance must be

taken into account, since they largely modify the biochemical absorption signal of a single leaf. The vegetation canopy reflectance ρ_{canopy}, acquired by a remote sensing device, can be described by the following relationship [5]:

$$\rho_{canopy} = f(Geometry, Structure, Biochemistry, Geochemistry) \quad (2.1)$$

The first parameter, describing the geometry between sun, ground and observer, includes the influences of solar and sensor view azimuth and zenith angle. The structure parameter accounts for canopy materials and architecture (i.e., the horizontal distribution of species, canopy height, leaf area index (LAI), non-photosynthetic vegetation index (NPVI), leaf angle distribution (LAD) of both photosynthetically active and non-photosynthetic vegetation). The third parameter includes the chemical components of the tissues (i.e., carbon, nitrogen, water, lignin, sugar and starch), where geochemistry accounts for the mineral and moisture properties of the soil surface.

Modelling canopy spectral properties is often based on optical properties of single leaves that are combined with structural characteristics. Baret et al. [9][10] and Jacquemoud et al. [73] summarize the various approaches for modelling leaf- and canopy optical properties to retrieve biophysical and biochemical parameters from spectral data. LAI is considered the primary factor controlling the optical properties of a canopy, with the most pronounced effect in the near-infrared and the smallest effect in the visible region of the electromagnetic spectrum. High LAI canopies allow weak-level biochemical information to be enhanced at canopy scale via multiple scattering [5]. Since the near-infrared region has the strongest multiple scattering in green foliage, this region is capable to enhance the leaf-level signal, making it often impossible to discriminate between structural and biochemical effects (see Chapter 6.4.3). As a prominent example, increasing LAI values result in a deepening and widening of the chlorophyll absorption feature and an increased reflectance in the near-infrared region.

2.8 Selection of Vegetation Parameters to be Retrieved

The selection of biophysical and biochemical parameters to be investigated in this work is driven by their ability to track the phenological development of a plant. This implies detectable gradients of the observed data over time. In addition, it must be possible to ascertain them by means of reflectance measurements from a remote sensing device. The measurement of the parameters in the field and the laboratory should be possible using widely accepted and operational methods.

A plant's photosynthetic activity or light interception, which is responsible for dry matter accumulation and final yield, is dependent on its vitality. Vitality of an agricultural crop stand is driven by its genetic material and environmental factors. It decreases with transition from the *vegetative* through the *reproductive* to the *senescing phase*. Water- and nutrient stress cause physiological and phenological changes in the plant organism leading to reduced vitality.

Four key parameters reflecting a crop stand's vitality are defined and investigated in this work. They are given in Tab. 2.4. They are leaf area index (LAI), fraction of absorbed photosynthetically active radiation (FAPAR), leaf chlorophyll content and water content.

The fraction of absorbed photosynthetically active radiation (FAPAR) is strongly correlated to leaf area and amount of photosynthetically active pigments [8][26]. Physiological changes in plants influence photosynthetic activity and therefore FAPAR. While the vitality of single leaves correlates to the amount of photosynthetically active pigments (besides of water and nutrients), the amount of green leaves per unit area (LAI) must be considered additionally when assessing the vitality of a whole plant or even crop stand. Nitrogen, a major nutrient, is closely associated with chlorophyll. The plant's nitrogen status is therefore detectable from chlorophyll measurements. The question whether strongly correlating parameters could substitute each other when tracking a crop's phenological development will be addressed in Chapter 7. Thermal data like soil- and foliage temperature is not considered in this work, but water content of leaves, grains, as well as of whole plants is being investigated, since water status is a driving force of plant vitality.

The parameters of Tab. 2.4 correspond with a subpart of key process parameters, that were defined by the Land-Surface Processes and Interactions Mission (LSPIM) of the 1999 ESA Earth Explorer Core missions to characterize primary production [47]. They are ranked as important input parameters into land-surface process models. Their importance is reconfirmed in ESA's SPECTRA Report [48], where LAI is considered the main canopy structural parameter and chlorophyll content and water content the main leaf characteristics. Although FAPAR is ranked as a secondary parameter, it is an important input parameter to growth models. Other parameters mentioned in the report are not investigated in this work, since they describe either soil characteristics or are closely related to parameters under investigation (e.g., fractional cover (*f*cover), which is related to LAI).

Table 2.4 Key parameters selected to track vitality of the observed cereals.

Key Parameter	Biophysical	Biochemical
Leaf area index (LAI)	x	
Fraction of absorbed photosyntheticall active radiation (FAPAR)	x	
Chlorophyll content		x
Water content		x

In the following section, the relevance of the above chosen vegetation parameters for tracking the development of winter barley and spring wheat is shortly described.

2.8.1 Leaf Area Index (LAI)

The leaf area index is defined as the total one-sided leaf area per unit soil area [14]. Depending on its definition, the leaf area index includes only the green leaves or the dead leaves as well. The green leaf area is of major importance in plant growth. It is strongly coupled to biomass production and crop yield. Kimes et al. [77] found that the green leaf area index is the agronomic parameter best correlating with spectral data. Remote sensing can provide data about the spatial distribution of the green leaf area which is a main driving parameter in many crop growth models. Such models simulate the leaf area for calculating biomass production and yield prediction (Chapter 2.6). Successful determination of LAI from remote sensing data can supply data needed to validate or update models at high spatial and temporal resolution.

Photosynthesis processes take place in the green plant parts, i.e. the area containing chlorophyll. Physiological changes during a vegetation period affect both single leaves and total leaf area, thus allowing phenological stages to be monitored by means of spectral data.

2.8.2 Fraction of Absorbed Photosynthetically Active Radiation (FAPAR)

Plants absorb solar radiation mainly in the 400 to 700 nm region for photosynthetic purposes. Absorbed photosynthetically active radiation (APAR) is defined as the amount of photosynthetically active radiation (PAR) absorbed by a vegetation canopy. Contrary to canopy PAR absorption, which is a measure of radiant flux absorbed, a canopy's capacity to absorb PAR can be described by fractional APAR, abbreviated as FAPAR or FPAR [58]. A

plant's capacity to absorb incoming radiation for biomass production is dependent on its physiological state and therefore related to its phenological stage. The APAR is particularly interesting from an agronomical point of view, since plant growth occurs through diurnal integration of APAR. Estimating APAR over an interval of time (e.g., daily APAR) requires both incident PAR and FAPAR. Daily APAR for crops is reported to be reliably computed from FAPAR measurements near solar noon and daily incident PAR [40]. FAPAR can be estimated from a remote sensing platform and its temporal and spatial variations can be related to net primary production (NPP) and CO_2 exchange.

2.8.3 Chlorophyll Content

The primary plant pigments chlorophyll a and b are the engine of plant biomass production and the resulting crop yield. Chlorophyll content in higher plant leaves changes throughout the different stages of plant development [56][66][126]. Determination of chlorophyll content bears the potential for detection of physiological states and stresses in plants. Remote estimation of canopy chlorophyll content is more promising than of leaf chlorophyll content, since a remote sensor acquires spectral data of a whole vegetation canopy. Biochemical estimates at leaf level are reported to be strongly correlated to LAI estimates [32]. Therefore, a precise derivation of leaf area index is necessary for accurate chlorophyll estimation at leaf level. In addition, a close relationship between leaf chlorophyll content and nitrogen fertilization level yields the potential of using hyperspectral data for nitrogen management [95].

2.8.4 Water Content

The amount of plant-, leaf- and grain water content of cereals strongly decreases during the growing season. Early studies on leaf water status [53][116][126] or vegetation canopy water status [49][65][70] revealed relationships with spectral reflectance data. Since variations in leaf internal structure, canopy architecture and the contribution of the soil background, as a result of aging and water stress, cause reflectance differences, they contribute to the difficulty of relating reflectance measurements to the quantity of an absorbing medium, such as water. Nevertheless, accurate estimation of water content is of growing importance in the *generative* and *reproductive phase*. Water stress can affect the processes of grain initiation, fertilization and grain-fill [109]. The different ripening stages of grain are characterized by their respective grain water content. The assessment of harvest ripeness is

crucial to the farmer from an organizational and economical point of view. Remote sensing can offer spatial information on plant water status needed for decision making purposes.

Chapter 3

Agricultural Context

3.1 Introduction

This chapter summarizes biological, developmental and economical aspects of wheat and barley, which are considered as background information on the study objects. A commonly used decimal code for crop development characterization, introduced in this chapter, serves as a basis for the compilation of main phenological stages of the observed fields, as well as for phenological considerations to be found in the following chapters. A short description of the Limpach valley test site is given, focusing on climate and soil aspects of the region, as well as meteorological facts of the most recent years.

3.2 The Study Objects - Wheat and Barley

The two cereals investigated in this work are spring wheat and winter barley. Wheat is the most important cool-temperate cereal in the world, being produced mainly between 30°N and 60°N and 27°S and 40°S. It is followed by barley which tends to replace wheat where the annual precipitation is too low or erratic for satisfactory wheat yields or where the growing season is too short for wheat.

3.2.1 Biological Aspects

3.2.2.1 Wheat

Wheat belongs to the tribe *Triticae* of the family *Poaceae*. This tribe also contains barley, rye and the wheat-rye hybrid triticale. The genus *Triticum* consists of many species and sub-species including the primitive wheats emmer and einkorn from which today's modern wheats originate. Most of todays intensive cultivars is *Triticum aestivum* (common wheat). *Triticum durum* and *Triticum spelta* (spelt) is of less importance [109]. Wheat cultivars are divided into winter and spring types of which many varieties exist [96]. True winter types require ten weeks of temperatures between 0°C and 8°C (vernalization time) to trigger floral initiation, but many modern winter wheats

have a low vernalization requirement. Autumn sown wheats typically yield 25% more than spring sown types, but spring wheat is typically of higher quality than winter cultivars. True spring wheats, having no vernalization requirement, are sown in spring and harvested in the same year. Spring wheat is harvested later than winter wheat and was traditionally sown when it became too late to sow winter wheat. More than 95% of wheat grown in Switzerland is winter wheat.

3.2.3.2 Barley

Like wheat, barley belongs to the *Triticae* tribe of the *Poaceae* family. Barley (*Hordeum*) is believed to be the earliest grain taken into cultivation. *Hordeum vulgare* cultivars are divided into winter and spring, and four to six- and two-row ears types. These divisions are based on the presence or absence of particular genes. 'Winter' and 'spring' refer to certain genotypic characteristics and not necessarily to the date of sowing [108]. Barley, which is more tolerant of drought than wheat can be grown where the mean annual rainfall exceeds 250 mm. The growing season of spring barley is shorter than the one of winter cultivars. Therefore, spring barley is predominantly grown in northern areas and mediterranean regions. Barley is harvested before wheat.

3.2.4 Developmental Aspects

Like other cereals, wheat and barley pass through a series of phases of development. A plant's development is subdivided into a *vegetative,* a *generative* and a *reproductive phase*. *Germination, seedling growth* and *tillering* are processes of the *vegetative phase, stem elongation, booting, inflorescence emergence* and *flowering* occur in the *generative phase* and the different *ripening* stages define the *reproductive phase* (c.f., Tab. 7.4 on page 130).

The two environmental variables dominating phenology are temperature (thermal time, [°Cd]) and photoperiod (sum of day-length and civil twilight). Daylength has an important influence on the plants' development mainly in the *reproductive phase*, whereas temperature is essential for the transition from the *vegetative* to the *generative phase*. Successful crop growth can only take place if there is sufficient time between *sowing* and *harvest* to meet the plants' energy requirements. The annual thermal time (air temperature) above an appropriate base temperature must exceed a certain value. Typical amounts of thermal time requirements for winter cultivars at 45° latitude range from 2000-2400°Cd, those of spring cultivars from 1800-2000°Cd [79][108][109]. The type of cultivar is the main cause of variation in the time to maturity.

Most studies describe morphological changes using Zadoks' growth stage

scale (Chapter 3.3). Stem apex development is the driving force for the consequently visible external morphological changes [137].

Some work has been done on the timing of crop development [79][108][109] although data for Switzerland is rare. Systematic phytophenological data has been collected in Switzerland since 1951 by Meteo Swiss (formerly Swiss Meteorological Institute). Today, 70 phenological phases are studied by observing 37 different plants at approximately 160 stations in various Swiss regions and altitudes [42]. Records for wheat and barley contain the dates of *inflorescence emergence* and *harvest*. Since 1996, phenological data of agricultural crops is no longer recorded by Meteo Swiss because of lacking interest in behalf of the agricultural community. These observations are now partly performed by research stations like the Swiss Federal Research Station for Agroecology and Agriculture (FAL). Their interest is mainly on the deviation of inflorescence emergence of certain varieties from standard cultivars and therefore not on the absolute date of main phenological stages.

Parametrization of the stages for input into crop growth models, mean phase length and the importance of each period in its effect on yield are described in Russell [108] and Russell et al. [109]. Meteorological conditions can affect wheat growth during all development stages. While soil water deficit and extreme temperatures (both minimum and maximum temperatures) are a threat to the stages from *sowing* to *flowering*, heavy and frequent rain affects *grain filling*, *ripening* and *harvesting*. Optimal conditions for *harvesting* are a grain moisture content of 15% (DC [1)]92) and less than 1.5 mm of rain on the day before *harvest*. In reality, cereals are often harvested at a grain moisture content of 15-20% resulting in additional costs to the farmer for artificial drying. Maximum precipitation acceptable on the day before *harvest* is driven by the potential evapotranspiration rate of a region [109].

3.2.5 Economical Aspects

World wheat production of the year 2000 is around 580 million tons, of which 105 million tons were grown in the European Union. Worldwide barley production totals 133 million tons. 52 million tons are grown in the EU [50].

The Swiss wheat production of the year 2000 amounts to almost 553’000 tons. The barley production is around 283’000 tons (Tab. 3.1). Wheat is both being produced for bread-making (like rye and spelt) and fodder purposes, depending on its quality. The quality is defined by the hectoliter weight, protein content and alpha-amylase-level (expressed by the Hagberg falling

[1)] Decimal code

number) of the harvested grain [109]. Barley is mainly grown as animal fodder supply (like oat, triticale and corn). Growing barley for brewing purposes is not profitable in Switzerland, because low protein content is needed, which means absence of fertilizer, resulting in low yields per hectare.

Wheat is grown on more than 90% of Switzerland's agricultural land designated for bread-making cereals, whereas barley makes up almost 60% of the acreage for fodder cereals (another 26% is used for corn farming).

Table 3.1 Acreage and prduction of wheat and barley in Switzerland from 1996-2000 [114].

Cereal	1996	1997	1998	1999	2000
Winter wheat					
- Agricultural area [ha]	93'447	92'432	92'917	86'261	89'779
- Production [t]	626'095	573'078	594'669	465'809	529'696
Spring wheat					
- Agricultural area [ha]	3'100	3'000	3'000	6'600	4'330
- Production [t]	18'910	15'900	16'200	32'340	22'949
Winter barley					
- Agricultural area [ha]	45'305	42'664	43'020	43'842	42'021
- Production [t]	299'013	285'849	301'140	236'747	264'732
Spring Barley					
- Agricultural area [ha]	5'754	5'451	6'000	5'100	3'720
- Production [t]	33'373	29'981	33'600	23'460	18'600

Wheat cultivars cover more than 30% of Switzerland's acreage for agricultural products. Barley is grown on over 15% of this area.

3.3 Characterization of Growth Stages of Cereals

Most studies dealing with crop development stages nowadays use a decimal code (DC) proposed by Zadoks et al. [137] which takes into account morphological changes of the plant. The first digit of this two-digit code refers to the principal stage of development beginning with germination (stage 0) and ending with grain ripening (stage 9). The second digit between 0 and 9 subdivides each principal growth stage. A second digit value of 5 usually indicates the midpoint of the principal stage (Tab. 3.2). This decimal code bases on scales developed by Keller et al. [75] and Large [84], which themselves base on a scale proposed by Feekes in 1941. An intercomparison of the different codes, together with a detailed characterization of the growth stages of Tab. 3.2 is given in Tab. 7.4 on page 130.

Table 3.2 Zadoks' decimal code (DC) and mean durations of the growth stages for winter barley and spring wheat over a 15 years period (1968-1983) [79].

Growth Stage	DC	Winter Barley (Mean Duration in Days)	Spring Wheat (Mean Duration in Days)
Germination	00-09	10-13	18
Seedling growth	10-19	28-33	24-25
Tillering	20-29	33-36	8-9
Stem elongation	30-39	154-156[1)]	25-28
Booting	40-49	4-6	4-5
Inflorescence emergence	50-59	5-6	5-7
Anthesis (flowering)	60-69	5-6	9
Milk development	70-79	26-28	28-30
Dough development	80-89	13-15	13-15
Ripening	90-99	2-3	2
Harvest	≥ 92	1-3	1-3

[1)] including a vernalization time of 125-127 days

3.4 Test Site Description

Data acquisition from April 1999 to August 1999 was performed on a winter barley field and a spring wheat field in the Limpach valley (470 m.a.sl.), which is an intensively cultivated agricultural area in nortwestern Switzerland. It ranges almost 10 km from its southwestern beginning near the village of Wengi to its northeastern end near Brittern. The two test fields are situated close to the village of Oberramsern in the Swiss Canton of Solothurn. Most of the land in the Limpach valley is used as arable land for crop production (c.f., Fig. 6.26 on page 120).

The winter barley and spring wheat fields, visible from Fig. 3.1, have an acreage of 1.4 ha and 1.84 ha, respectively. Their surface can be considered as flat. Winter barley of the selected variety Lyric [96] is characterized by a very high hectoliter weight, but poor stem rigidity. Spring barley of the variety Balmi [96] was chosen for bread making purposes since it has very high baking quality and a very high stem rigidity. The fields' treatment by the farmer is summarized in Tab. 7.1 and Tab. 7.2 on page 129. Winter barley was treated in an extensive manner, following the regulations of integrated production [115]. Extensively cultivated cereals are not treated with fungicides, herbicides and growth regulators. In 1998, their acreage made up almost half of the agricultural area designated to cereal growth in Switzerland [22]. Because of minor yield, the farmer gets subsidies from the government.

Figure 3.1 Partial view of the observed spring wheat (left) and winter barley field (right), situated near the village of Oberramsern in the Limpach valley. The photograph of the spring wheat field was taken on July 5th 1999 (DC 71-75), the one of the winter barley field on May 18th 1999 (DC 55-59).

The climate of the Limpach valley can be regarded as typical for the Swiss Midlands. Precipitation is even to moderatly dry. The vegetation period lasts between 210-230 days. The summer months are characterized by hot temperatures and occasional dry periods [46]. The basic material of the valley's plane is of postglacial sandy to clayey-silty alluvial deposits. Higher elevated areas consist of gleyic brown soil, whereas lower parts towards the valley center suffer from moory influences despite of heavy drainage. Areas of differing soil moisture content, as a result of elevation, can even be discriminated within the observed fields.

3.4.1 Phenological Aspects of the Observed Fields

Winter barley was sown by the farmer on October 13th 1998. Mean durations of *germination*, *seedling growth* and *tillering* significantly vary in literature [79][108][109], because the thermal time required for each of these stages mainly depends on soil temperature and depth of sowing, rather than on the type of cultivar. Autumn sown cultivars normally complete tillering by the end of the year before they enter a quiet phase which includes the vernalization time needed by winter cultivars to trigger floral initiation.

Phenological observation of the winter barley field started in early April. *Stem elongation* marks the transition from the *vegetative* to the *generative phase* and started mid-April. *Inflorescence emergence* and *completion* are important phenological stages observed in most cereal growth studies. For the observed winter barley field, they occurred towards the end of May, followed by a five to six days period of *flowering* (*anthesis*). The time between *anthesis complete* and *harvest ripeness* is characterized by grain-fill and physical drying. During this period of about 40 days, a progressive senescence, first of

the leaves and then of the awns and glumes of the ears is visible. This *generative phase* includes the stages of *milk development* and *dough development*, where grain moisture content falls from around 45% to 20% (*hard dough*). The process of *ripening* is based on physical drying. *Harvest ripeness* of the observed winter barley field was reached 36 day after the last plants' *completion of anthesis* (July 5th 1999).

The date of spring wheat *sowing* was March 17th 1999. *Seedling growth* started three weeks later (April 9th), followed by *tillering* around mid-May. *Stem elongation* took place during the second part of May. *Inflorescence emergence* was completed by mid-June and *anthesis* was over on June 24th, well in accordance with literature [79]. *Grain fill* and *ripening* were heavily disturbed by instable weather conditions preventing the grains from proper ripening and forcing premature germination.

Tab. 3.3 and Tab. 3.4 give a detailed overview of the phenological development of the observed winter barley and spring wheat fields. Duration from *sowing* to *harvest* was 305 days for winter barley and 158 days for spring wheat. *Harvest* of both winter barley and spring wheat was heavily delayed because of bad weather conditions. Kolbe [79] indicates mean durations of 289 to 296 days for winter barley and 144 days for spring wheat. Both cultivars observed during the 1999 growing season could not be harvested at their optimal growth stage, which is at a grain moisture content of 15% (DC 92).

Comparison of the observed dates of *inflorescence emergence* and *harvest* with data from two stations of the Swiss phenological observation network (Oeschberg, Jegenstorf) was performed. The available data from the network shows considerable lacks of information, but partly dates back to the 1960s [97]. Whereas the beginning of *inflorescence emergence* of the observed winter barley and spring wheat fields lies well within one week of the network stations' annual means, observed *harvest* data of the 1999 observations differ up to three weeks from the recorded annual mean dates due to bad weather.

The length of time from the end of grain fill (achievement of maximum grain dry matter) until *harvest ripeness* is difficult to predict since grains can gain as well as lose water. In rain-free periods, moisture content declines by about 2% per day when the daily maximum temperature exceeds 20°C. Time from the end of *flowering* until *harvest ripeness* is often described as 40 days.

The observed spring wheat reached its *harvest ripeness* on July 5th 1999 (DOY 186, 275 days after *sowing*). It was severely damaged by a heavy hailstorm on the same evening, but could only be harvested on August 4th (DOY 216, 305 days after *sowing*) due to constantly instable weather conditions. It's grain moisture content was 12.5% at the date of *harvest*.

Spring wheat never reached *harvest ripeness* and was harvested on August 22nd (DOY 234, 158 day after *sowing*) at a grain moisture content of 18%.

The grains of both cultivars started sprouting before *harvest* due to prolonged rainfall and high air humidity. As a result, spring wheat could not be used for bread making, since the alpha-amylase enzyme produced under such conditions reduced grain quality for bread making to a level unacceptable for baking. It could only be used for fodder purposes. Because grain fill could not be completed, the hectoliter weight was lower than in the years before. Drying costs to make the grain tenable are at the farmer's expenses. If *harvest* is delayed past the optimum date, grain weight declines and quality deteriorates, especially if wet conditions encourage premature germination. 1999's yields of winter barley and spring wheat were worst for the last ten years when it comes to yield per area [21]. Known parameters by the farmer concerning yield are listed in Tab. 7.3 on page 129.

Table 3.3 Phenological development of the observed winter barley field.

Date	Day of Year (DOY)	Development Stage	Decimal Code (DC) [137]
13. 10. 1998	-	Sowing	00
09. 04. 1999	99	Tillering completed	29
02. 05. 1999	122	Pseudo stem erection	30
10. 05. 1999	130	Boots swollen - Flag leaf sheath opening	45-47
18. 05. 1999	138	Half of inflorescence emerged - Emergence of inflorescence completed	55-59
27. 05. 1999	147	Emergence of inflorescence completed (Beginning of anthesis)	59 (61)
01. 06. 1999	152	Beginning of anthesis	61
09. 06. 1999	160	Caryopsis water ripe (Anthesis complete)	71 (69)
16. 06. 1999	167	Medium milk	75
24. 06. 1999	175	Medium milk - Soft dough	75-85
02. 07. 1999	183	Soft dough	85
05. 07. 1999	186	Caryopsis hard (<16% water content)	92
17. 07. 1999	198	Over-ripe, straw dead and collapsing	94
04. 08. 1999	216	Harvest	

Table 3.4 Phenological development of the observed spring wheat field.

Date	Day of Year (DOY)	Development Stage	Decimal Code (DC) [137]
17. 03. 1999	76	Sowing	
09. 04. 1999	99	1st leaf unfolded	11
		(1st leaf emergence)	(10)
02. 05. 1999	122	3 leaves unfolded	13
10. 05. 1999	130	Main shoot, 1 tiller -	21-25
		Main shoot, 5 tillers	
18. 05. 1999	138	Pseudo stem erection	30
		(1st node detectable)	(31)
27. 05. 1999	147	1st node detectable	31
01. 06. 1999	152	2nd node detectable -	32-33
		3rd node detectable	
09. 06. 1999	160	Flag leaf sheath opening	47
		(Half of inflorescence emerged)	(55)
16. 06, 1999	167	Emergence of inflorescence completed	59
		(Half of inflorescence emerged,	(55, 61)
		Beginning of anthesis)	
24. 06. 1999	175	Anthesis complete	69
02. 07. 1999	183	Caryopsis water ripe	71
05. 07. 1999	186	Caryopsis water ripe - Medium milk	71-75
17. 07. 1999	198	Medium milk	75
26. 07. 1999	207	Medium milk - Soft dough	75-85
04. 08. 1999	216	Hard dough (<20% water content)	87
12. 08. 1999	224	Hard dough (<20% water content)	87
22. 08. 1999	234	Harvest	

3.4.2 Meteorological Aspects

Compared to the records of the 1995 to 2000 period of time, the year 1999 can be characterized by maximum precipitation and minimum length of sunshine period and solar flux. Tab. 3.5 shows mean annual air temperature, annual precipitation, sunshine period and solar flux as being calculated from observations performed at Bern-Liebefeld and Wynau, two stations of the automatic surface network of Meteo Swiss (ANETZ), situated closest to the observed fields in the Limpach valley.

Daily observations of air temperature values, as well as daily precipitation and sunshine period, performed at Bern-Liebefeld, are represented in Fig. 3.2, Fig. 3.3 and Fig. 3.4 for the time from March 1st 1999 (DOY 60) through August 28th 1999 (DOY 240).

Table 3.5 Observation values of annual mean temperature, precipitation, sunshine period and global flux averaged for Bern-Liebefeld and Wynau.

Year	Mean Annual Temperature [°C]	Annual Precipitation [mm]	Annual Sunshine [h]	Annual Solar Flux [kW m^{-2}]
1995	9.17	1302.75	1588.08	3.7938
1996	8.20	957.75	1530.65	3.6862
1997	9.30	897.00	1769.25	3.8569
1998	9.21	1021.10	1690.04	3.7899
1999	9.29	1324.95	1491.57	3.5967
2000	9.98	1052.75	1701.63	3.8494
1995-2000[1)]	9.05	1092.75	1628.54	3.7622

[1)] mean values of annual data

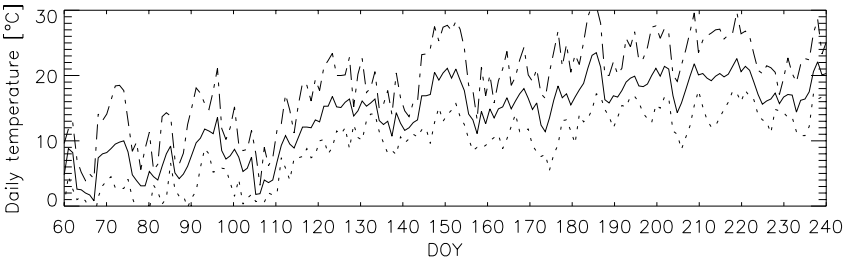

Figure 3.2 Minimum (dotted line), mean (solid line) and maximum (dashed-dotted line) daily air temperature as observed at Bern-Liebefeld for the time from March 1st through August 28th 1999.

Fig. 3.3 clearly shows the heavy rainfall on the evening of July 5th 1999 (DOY 186), which was followed by a hailstorm that severely damaged the ripe winter barley field. Frequent rain and reduced sunshine period, which made *harvest* impossible, was recorded for the following days.

The humid period of August 1999 started with heavy rainfall on August 6th (DOY 218) and lasted for almost two weeks. It prevented the spring wheat field from reaching *harvest* ripeness.

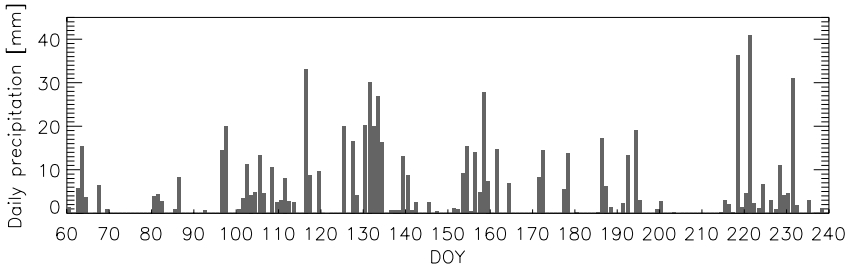

Figure 3.3 Daily precipitation as observed at Bern-Liebefeld for the time from March 1st through August 28th 1999.

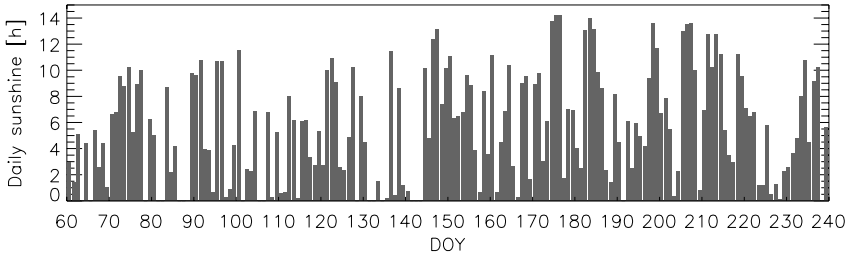

Figure 3.4 Daily sunshine period as observed at Bern-Liebefeld for the time from March 1st through August 28th 1999.

Chapter 4

Methodology of Parameter Retrieval

4.1 Introduction

Extraction of quantitative information on the state of the earth's surface from remote sensing data is based on methods that can be subdivided into three categories: empirical and semi-empirical approaches, statistical approaches, and modelling approaches [73].

Empirical approaches are based on simple relations established between a variable of interest and spectral data. Correlation of single bands or spectral indices with ground truth data is a prominent technique of empirical data extraction. Semi-empirical approaches have a physical basis. Their mathematical formulation of a parameter's state is related empirically to spectral data. Clevers' WDVI concept for estimating LAI of a green canopy [27][28] is an example of a semi-empirical reflectance model.

Statistical approaches determine parameter characteristics statistically, i.e., the choice of wavelengths for data extraction is not predetermined. Spectral mixture analysis, that reduces spectral information into independent sources of variability, called endmembers, and multiple stepwise regression analysis are two methods of quantitative information retrieval based on statistics of a calibration set of samples.

Modelling or analytical approaches offer a formal representation of the processes involved in light interaction with remotely sensed surfaces. These physically based models encapsulate the actual knowledge about the system under study. Verstraete [130] emphasizes that physically based models can be truly validated, because they can be inverted, whereas validation of empirical models cannot be done a priori because any polynomial or other function with enough adjustable parameters can be made to fit any data set. As a consequence, empirical approaches can only be considered validated if the values of the parameters retrieved by a validation set match the values of these parameters as measured or observed.

4.2 Determination of LAI

As stated in Chapter 2.7.3, the optical properties of a vegetation canopy are influenced by various factors, one of them being soil background. Its spectral contribution to reflectance of the canopy strongly varies during the growing season, being a problem in multitemporal analysis. At low plant cover, soil reflectance contributes strongly to the composite canopy-soil reflectance. Furthermore, soil moisture content is not constant during the season and differences in soil moisture content influence soil reflectance. A correction for soil background is necessary when ascertaining the relation between reflectance and crop characteristics such as LAI. Various vegetation indices have been developed in order to enhance the spectral contribution of green vegetation while minimizing those from background and senesced vegetation [67]. Richardson and Wiegand [103] introduced the *perpendicular vegetation index* (PVI), using the soil line, a linear relation between the reflectances of soil at two different wavelength positions. Huete [68] introduced a *soil adjusted vegetation index* (SAVI). Baret and Guyot [8] improved the SAVI by taking into account the soil line for definition of the *transformed soil adjusted vegetation index* (TSAVI). All these vegetation indices are based on ratios of single wavelength bands of the visible and near-infrared region. Low transmittance of a green leaf in the visible region implies that only reflectance of the upper layer of leaves determines the contribution of the canopy to the total measured reflectance. Increased transmittance of a green leaf in the near-infrared region allows canopy layers underneath the upper layer to contribute significantly to the total measured reflectance. This multiple reflectance indicates that the near-infrared reflectance is a suitable estimator of LAI. However, the lower layers' contribution strongly decreases with increasing depth in the canopy, making indices insensitive to changes in leaf area from LAI 6-8 onwards.

The drawback of the abovementioned indices is their incomplete physical basis. As a consequence, a simplified reflectance model for estimating LAI, introduced by Clevers [27][28], is chosen for this work. The model calculates a corrected near-infrared reflectance, known as *weighted difference vegetation index* (WDVI), by subtracting the contribution of the soil from the measured reflectance. It is assumed that the ratio between the reflectances of bare soil in different spectral bands is constant for a given soil background and independent of soil moisture content. This enables to calculate the corrected near-infrared reflectance without knowing soil reflectances. The WDVI is then used for estimation of LAI according to the inverse of an exponential function.

The following section, leading to the derivation of Eq. 4.11 for LAI determination from WDVI is based on Clevers [27][28]. The measured reflectance of a canopy-soil composite from nadir can be expressed as:

$$\rho = \rho_v \cdot B + \rho_s \cdot (1 - B) \tag{4.1}$$

where

ρ	total measured reflectance of the canopy-soil composite,
ρ_v	reflectance of the canopy,
ρ_s	reflectance of the soil,
B	fraction of plant cover [0-1].

Eq. 4.1 can be written in a manner, that $\rho_s \cdot (1 - B)$, which is the soil's contribution to the total measured reflectance ρ, is subtracted, to express the soil-corrected reflectance ρ' of the canopy:

$$\rho' = \rho - \rho_s \cdot (1 - B) \tag{4.2}$$

where $\rho' = \rho_v \cdot B$.

The terms ρ' and $\rho_s \cdot (1 - B)$ are unknown. It is obvious, that ρ' is closely related to LAI, because of the presence of B and the dependence of ρ_v from LAI (Chapter 2.7.3)

Calculation of WDVI is performed from measured red and near-infrared reflectances of the canopy-soil composite. Therefore, Eq. 4.2 can be written as (Eq. 4.3, Eq. 4.4):

$$\rho'(\lambda_{RED}) = \rho(\lambda_{RED}) - \rho_s(\lambda_{RED}) \cdot (1 - B) \tag{4.3}$$

$$\rho'(\lambda_{NIR}) = \rho(\lambda_{NIR}) - \rho_s(\lambda_{NIR}) \cdot (1 - B) \tag{4.4}$$

where

$\rho'(\lambda_{RED})$	red reflectance of the canopy,
$\rho'(\lambda_{NIR})$	near-infrared reflectance of the canopy.

WDVI determination requires a coefficient C for correction of the canopy-soil composite for soil background. C is soil-type dependent. Reflectance of a soil changes with varying moisture content. The ratio of the reflectance in two spectral bands can be assumed as constant and independent of soil moisture content. The existence of a soil line in red and near-infrared wavelength space is widely accepted in literature [33][68]. Therefore, C is being calculated as (Eq. 4.5):

$$C = \frac{\rho_s(\lambda_{NIR})}{\rho_s(\lambda_{RED})} \tag{4.5}$$

where

$\rho_s(\lambda_{NIR})$ near-infrared reflectance of the soil,
$\rho_s(\lambda_{RED})$ red reflectance of the soil.

The expression $\rho_s(\lambda_{NIR})$ from Eq. 4.4 is being replaced by $C \cdot \rho_s(\lambda_{RED})$ from Eq. 4.5. The value of C is considered to be known from empirical data of bare soil.

$$\rho'(\lambda_{NIR}) = \rho(\lambda_{NIR}) - (C \cdot \rho_s(\lambda_{RED}) \cdot (1 - B)) \tag{4.6}$$

Eq. 4.6 is solved for $\rho_s(\lambda_{RED}) \cdot (1 - B)$, resulting in:

$$\rho_s(\lambda_{RED}) \cdot (1 - B) = \frac{\rho(\lambda_{NIR}) - \rho'(\lambda_{NIR})}{C} \tag{4.7}$$

The result of Eq. 4.7 is used to replace the term $\rho_s(\lambda_{RED}) \cdot (1 - B)$ in Eq. 4.3, as done in (Eq. 4.8):

$$\rho'(\lambda_{RED}) = \rho(\lambda_{RED}) - \frac{\rho(\lambda_{NIR}) \cdot \rho'(\lambda_{NIR})}{C} \tag{4.8}$$

Eq. 4.8 can be written in a manner that known $(\rho(\lambda_{RED}), \rho(\lambda_{NIR}), C)$ and unknown terms $(\rho'(\lambda_{RED}), \rho'(\lambda_{NIR}))$ are separated on each side:

$$\rho(\lambda_{NIR}) - (C \cdot \rho(\lambda_{RED})) = \rho'(\lambda_{NIR}) - (C \cdot \rho'(\lambda_{RED})) \tag{4.9}$$

The reflectance of the canopy, expressed as $\rho'(\lambda_{NIR}) - (C \cdot \rho'(\lambda_{RED}))$, can be determined from Eq. 4.9. Since $C \cdot \rho'(\lambda_{RED}) \ll \rho'(\lambda_{NIR})$ by a factor between five and ten, the term $C \cdot \rho'(\lambda_{RED})$ can be neglected. As a consequence, the equation for the corrected near-infrared reflectance of the canopy can be written as follows:

$$WDVI = \rho'(\lambda_{NIR}) \approx \rho(\lambda_{NIR}) - (C \cdot \rho(\lambda_{RED})) \tag{4.10}$$

Eq. 4.10 represents the near-infrared reflectance of the vegetation canopy as corrected for soil background. It is called *weighted difference vegetation index*.

Based on Bunnik [23], this WDVI is now used for estimating LAI according to the inverse of an exponential function (Eq. 4.11):

$$LAI = -\frac{1}{\alpha} \cdot \ln\left(1 - \frac{WDVI}{\rho_{\infty}(\lambda_{NIR})}\right) \tag{4.11}$$

where α and $\rho_{\infty}(\lambda_{NIR})$ have to be determined empirically from a ground truth data set. Eq. 4.10 and Eq. 4.11 form a semi-empirical reflectance model for estimation of LAI.

4.3 Determination of FAPAR

Based on the definition of absorbed photosynthetically active radiation, given in Chapter 2.8, APAR can be written as [58]:

$$APAR = I_{PAR,\,i} - I_{PAR,\,r} - (I_{PAR,\,t} - I_{PAR,\,s}) \tag{4.12}$$

where

$I_{PAR,\,i}$ incoming radiation intensity [W m^{-2} nm^{-1}] at the top of the canopy,

$I_{PAR,\,r}$ upward radiation intensity [W m^{-2} nm^{-1}] at the top of the canopy (reflected by plants and soil),

$I_{PAR,\,t}$ downward radiation intensity [W m^{-2} nm^{-1}] at the canopy bottom (transmitted),

$I_{PAR,\,s}$ radiation intensity [W m^{-2} nm^{-1}] reflected at soil surface.

The term $I_{PAR,\,t} - I_{PAR,\,s}$ represents the radiation absorbed by the soil. As a consequence, Eq. 4.12 describes the amount of PAR radiation that is absorbed by the canopy and thus available for photosynthesis by taking into account both the radiation reflected by the canopy-soil composite and the amount absorbed by the soil. The requisite field measurement strategy for APAR assessment based on Eq. 4.12 is presented in Chapter 5.2.1.2.

The fraction of absorbed photosynthetically active radiation (FAPAR) is given by:

$$FAPAR = \frac{APAR}{I_{PAR,\,i}} \tag{4.13}$$

Combination of Eq. 4.12 and Eq. 4.13 leads to the following representation of FAPAR:

$$FAPAR = 1 - \frac{I_{PAR,\,r} + (I_{PAR,\,t} - I_{PAR,\,s})}{I_{PAR,\,i}} \tag{4.14}$$

The seasonal behavior of FAPAR has been related to LAI empirically using an exponential function [64][8]. The relation used in this work is given as follows:

$$FAPAR = b_0 \cdot (1 - (b_1 \cdot \exp(-b_2 \cdot LAI))) \tag{4.15}$$

The parameters b_0, b_1 and b_2 have to be determined on a training data set. Baret and Guyot [8] propose to set $b_1 = 1$.

4.4 Determination of Chlorophyll Content

Chlorophylls and carotenoids, the primary pigments of plant biomass production, are responsible for photosynthesis and resulting crop yield. Remote sensing can contribute to characterize crop condition from detection of concentrations of photosynthetic pigments. Concentration of chlorophyll a is reported to be approximately three times higher than in the case of chlorophyll b [85]. In general, the ratio chl_a/chl_b depends on the amount of sun exposure of the leaves, fertilization treatment, the plant's phenological stage and the type of species [56][66][95]. Nitrogen, which is closely related to chlorophyll, is an essential element in the formation of primary plant pigments and acts as a limiting factor. Management of nitrogen treatment is a driving force in using remotely sensed spectral data for agricultural purposes.

An inverse relation between the reflectance of light in the red region of the solar spectrum and leaf chlorophyll concentration has been demonstrated by Thomas and Gausman [126]. The main chlorophyll a absorption region near 675 nm has been shown to become saturated at medium to high chlorophyll contents. Horler et al. [66] found red edge shifts that can be related to leaf chlorophyll content for a variety of species, including wheat and barley. For a pile of leaves, the inflection point of the red edge, λ_{re}, defined as the wavelength of maximum slope, was found to be unaffected by its background, even for incomplete cover. They concluded that field application measurements in the red edge region are unaffected by ground cover. The

effect of leaf stacking, however, caused spectral shifts of λ_{re} towards longer wavelengths, as observed for increased chlorophyll contents of single leaves.

Several studies have linked chlorophyll content to the position of λ_{re} [26][51]. The red edge inflection point of plant spectra, whose LAI and chlorophyll contents were progressively increasing, was found to be a good estimator of both LAI and chlorophyll content at canopy level. Horler et al. [66] and Boochs et al. [20] attributed spectral shifts of λ_{re} to changes in the chemical and physiological status or vitality of plants. They found chlorophyll content along with canopy scattering properties, which are linked to total biomass, responsible for the shape of the red edge and the position of its inflection point. Nevertheless, Filella and Peñuelas [51] stated that it was difficult to separate the two effects in order to find a good estimate for each one, in case of low correlations between LAI and chlorophyll content.

Since the red edge characterizes the boundary between chlorophyll absorption in the red wavelength range and the increased multiple scattering of radiation in the near-infrared, chlorophyll determination by a remote sensor is influenced by canopy effects as stated in Chapter 2.7.3. It therefore differs from laboratory studies performed on single leaves. Increased LAI values lead to a deepening and widening of the main chlorophyll a absorption feature around 675 nm and a spectral shift of λ_{re} towards longer wavelengths. An investigation by Yoder and Pettigrew-Cosby [136] demonstrated that it was difficult to separate leaf chlorophyll from LAI when using remote sensing data. As a consequence, Baret and Weiss [133] proposed to focus on the canopy integrated chlorophyll content, which is the product between leaf chlorophyll content and LAI. Retrieval of chlorophyll concentration per unit area (expressed as [µg m^{-2}]) is reported to correlate better with spectral data than concentration per unit mass (expressed as [µg g^{-1}]).

Considerable effort has been undertaken in the search for simple ratios of spectral data for remote estimation of chlorophyll content of leaves [26][39][56], but none of the methods was applied to measured spectral data of agricultural crop stand canopies, so far. Blackburn [18] applied several narrow-band reflectance indices for chlorophyll retrieval, like the *pigment specific simple ratio algorithm* (PSSR) [17] and the *ratio of reflectance spectra algorithm* (RARS) [26], which was developed for soybean leaves, to a canopy of bracken throughout a growing season. He found that both PSSR and RARS indices have a strong correlation with their respective pigments per unit area and an exponential function best describes these relations. PSSR is reported to correlate best with canopy chlorophyll concentrations of bracken. Nevertheless, it remains to be tested whether the method is transferable to cereals undergoing fundamental changes both on canopy level and plant

physiology within a phenological cycle. This is a question which is addressed in this work.

Based on the *chlorophyll absorption in reflectance index* (CARI) [76], which corrects for the influence of non-photosynthetic materials, Daughtry et al. [41] presented the *modified chlorophyll absorption in reflectance index* (MCARI), being reported as responsive to chlorophyll variation and resistant to non-photosynthetic material effects. They concluded that the combined use of MCARI and an *optimized soil-adjusted-vegetation index* (OSAVI) [107] was linearly related to leaf chlorophyll concentration over a wide range of LAI and background reflectance. Their investigations were carried out based on simulated spectral data of a corn canopy using the SAIL model [128]. In simulations with the PROSPECT [71] and SAIL models, Haboudane et al. [61] found MCARI still sensitive to LAI and non-photosynthetic element effects, and proposed to use the *transformed chlorophyll absorption in reflectance index* (TCARI) in a ratio with OSAVI. Application of the method for chlorophyll estimation of corn plants was performed on an imaging spectroscopy data set and reported being successful. However, the method was not tested to track chlorophyll of different phenological stages. Verification should include early growth stages with low LAI, when information on leaf chlorophyll content and coupled leaf nitrogen concentration is most critical for agricultural management.

In this work, PSSR and the ratio TCARI/OSAVI are applied to the spectral data and laboratory chlorophyll measurements of the winter barley and spring wheat field over the cropping cycle observed, because they represent the most promising spectral indices for chlorophyll estimation of agricultural crop stands.

The PSSR ratios for chlorophyll a and b determination, as used in this work, involve optimal individual wavebands in the red and near-infrared region.

$PSSR_a$ and $PSSR_b$ are determined as:

$$PSSR_a = \frac{\rho_{800}}{\rho_{680}} \tag{4.16}$$

$$PSSR_b = \frac{\rho_{800}}{\rho_{635}} \tag{4.17}$$

The ratio TCARI/OSAVI is defined as follows:

$$\frac{TCARI}{OSAVI} = \frac{3 \cdot [(\rho_{700} - \rho_{670}) - (0.2 \cdot (\rho_{700} - \rho_{550}) \cdot (\rho_{700} / \rho_{670}))]}{((1 + 0.16) \cdot (\rho_{800} - \rho_{670})) / (\rho_{800} + \rho_{680} + 0.16)} \quad (4.18)$$

Multiple stepwise linear regression, as described in the following chapter for water content retrieval, is not performed for chlorophyll determination in this work. The method is reported successful in the case of laboratory determination of chlorophyll content from single leaves [37], but the relation between canopy reflectance and leaf chlorophyll content is mainly dominated by canopy structural effects (LAI), as will be discussed in Chapter 6.4. As a consequence, linear relations between leaf chlorophyll and corresponding reflectance values, as mentioned earlier in this section, do no longer apply to spectroradiometric data of a vegetation canopy.

4.5 Determination of Water Content

Although the spectral reflectance properties of vegetation canopies are determined primarily by the absorption and scattering processes within the plant material and the stand's architecture, there are superimposed effects of absorption by water and other biochemical constituents. Since the internal leaf- and canopy structure changes during plant development, the ability to predict leaf- or plant water status from reflectance measurements is complicated by these variations. Early studies by Gates et al. [53], Sinclair et al. [116] and Gausman [55] showed that in the near- and shortwave-infrared region, an inverse relation between leaf water content and leaf reflectance can be found. Negative linear relations of leaf reflectance at selected wavelengths in this region are reported with relative leaf water content (RWC, expressed as [%]) and specific water density (SWD, expressed as [mg cm^{-2}]) [24][125]. The measurements were performed in the laboratory on a limited number of wavelengths located at maxima and minima positions of a leaf's reflectance curve.

As mentioned in Chapter 2.7, incoming radiation in the near-infrared region of the electromagnetic spectrum penetrates deeper into the canopy, since foliage absorption is low. High transmittance causes multiple scattering. Therefore, reflectance of a vegetation canopy in the near-infrared region is highly influenced by canopy characteristics, making reflectance a mixture of contributions from plant biochemicals, canopy structure and soil background contribution. Variations in leaf- and canopy structure during the stand's phenological stages affect the relations between water content and reflectance mainly in the 700-1300 nm region [38]. Since water content and green

biomass are positively correlated, observed high positive correlations between canopy water content and reflectance values in this region [106] are basically caused by biomass and not by water itself. Nevertheless, this relation bears the potential for canopy water estimation from a remote sensor in the near-infrared region. As a consequence, determination of water content as performed in this work mainly focuses on canopy- or plant water content, to track the phenological development of the cereal stands under investigation. Estimation of grain water content during the *reproductive phase* is done by relating grain water content to plant water content, since L_S, the total radiance received by the sensor, does not result from specific plant parts, but from the canopy as a whole.

As spectroscopy data bears the potential of continuous spectral information over a certain wavelength range, methods other than simple ratios of spectral bands can be applied for plant water retrieval. Stepwise multiple linear regression, being a statistical approach, is chosen to retrieve plant water content. Several studies have shown the feasibility of stepwise, multiple linear regression to quantify leaf biochemicals, both from dried and fresh leaves [35][36][60][72]. Danson et al. [38] correlated specific water density of single leaves with spectroradiometric data, while Rollin et al. [106] investigated the bandwise correlation of a high spectral resolution data set with canopy water content for grassland [106]. Thenkabail et al. [124] presented an optimum multiple narrow band reflectance (OMNBR) predictor for multiple linear regression with a fixed number of regressor wavelengths. None of the approaches to be found in literature deals with multiple linear regression of spectroscopy data from a whole vegetation period.

In this work, determination of predictive spectral wavebands of water content is performed by correlation of measured water content and corresponding spectral data in all channels for all phenological stages available. This produces a Pearson product moment correlation coefficient *r*, being a measure of the linear relation between water content and spectral reflectance.

The next step, designed for data reduction, selects maxima and minima of *r* over the wavelength range. This is done by first derivative analysis of the wavelength dependent correlation coefficient *r*. Wavelengths selected in this manner are assumed to represent positions in the spectrum, where the correlation between the biochemical variable under investigation and spectral data is at its maximum or minimum, compared to the neighboring wavelength channels. Therefore, these wavelengths are most promising to reduce data and inter-channel correlation. The selected wavelengths are then sorted in a descending order following their corresponding correlation coefficient *r*.

Stepwise multiple linear regression, which is selected to make use of the information content of a number of wavelengths, is applied to the selected data set. It fits the observed dependent data set (plant water content *c*) to a linear combination of independent variables (measured reflectances $\rho(\lambda_i)$ of the regressor wavelengths). The linear equation determined by the regression has the form as shown in Eq. 4.19:

$$c = a_0 + \sum_{i=1}^{n} a_i \cdot \rho(\lambda_i) \tag{4.19}$$

where

c	plant water content,
n	number of wavelengths λ_i used in the regression model,
a_0	regression constant,
$a_{i=1,n}$	coefficients of the selected regressor wavelengths λ_i,
$\rho(\lambda_i)$	reflectance data of the selected regressor wavelengths λ_i.

Regression analysis is both performed on absolute reflectance data and on continuum removed and band normalized spectral data, as proposed by Kokaly and Clark [78]. They successfully used this method in the laboratory to estimate the concentrations of a number of leaf biochemicals, based on dried and ground leaves.

The regression model is established on a calibration data set. A maximum of $n-1$ regressor wavelengths selected by correlation analysis are added to the model in a stepwise manner, starting with the wavelength of highest correlation. Overfitting is a critical problem in stepwise multiple regression because an appropriate number of coefficients can fit a function to any given data set. As a consequence, the optimal number of chosen regressor wavelengths is determined by two criteria:

- The multiple coefficient of determination R^2 of the calibration data must be maximal.
- The root mean square error (*rms error*) of the verification data must be minimal.

In this way, the possibility of overfitting a calibration data set, leading to high values of R^2, is reduced by the verification set's necessity to be satisfactorily modelled by the regression model, expressed as small rms error values.

The described method of parameter retrieval from stepwise multiple linear regression can basically be applied to any linear relation between a variable of

interest and spectroradiometric data. Both the number of selected regressors and their wavelength positions are dependent on the data set. As a consequence, the regression models derived for spring wheat and winter barley both differ in the number and the spectral positions of the selected wavelengths.

Chapter 5

Data Basis

5.1 Introduction

A standardized methodology for acquisition of field- and laboratory data using various techniques and instruments is a prerequisite for successful data collection. A detailed measurement plan is presented in the first part of this chapter. It is followed by a presentation of the acquired data sets of this work in the second part.

Sample size considerations are important when performing field measurements of statistical relevance. An empirical approach of sample size determination that can be applied prior to data acquisition at any phenological stage, is presented in the third part of this chapter.

5.2 Data Acquisition

Both the spectral characterization of an agricultural stand's phenology and the retrieval of quantitative information on plant parameters from spectral data describing the stand's vitality status depend on accurate measurements. A measurement plan that incorporates spectral data takes and acquisition of plant vitality parameters must contain a sampling strategy adapted to field measurements which is designed to track the main development stages during the vegetation period. It is based on temporal and spatial requirements as well as sample size considerations. The realization of an ideal measurement plan remains an unfulfilled task since the acquisition of field and laboratory measurements is often time consuming, dependent on meteorological conditions and on the availability of measurement equipment and manpower. Nevertheless, a standardized measurement plan to be applied on a potential day of data acquisition and following laboratory sample analysis was developed. The measurement and collection plan for field data consists of the various activities performed in the field with their temporal arrangement, data acquisition strategies and sample size considerations. The laboratory analysis concept describes a standardized approach for analytical determination of selected biochemical variables in the laboratory.

5.2.1 Field Measurement Plan

5.2.1.1 Sampling Strategy Considerations

a) Temporal Sampling

To assess the biophysical and biochemical variations that an agricultural crop stand passess through during a growing season, data acquisition must take place at the major phenological stages. Mean durations of the phenological stages and their mean dates of first appearance are found in literature for many cultivars (Chapter 3.3 and Chapter 3.4). As a result, a temporal sampling interval of eight to ten days is chosen to be reasonable to track the main stages of winter barley and summer wheat development for all stages except for the periods of *booting* (DC 40-49), *inflorescence emergence* (DC 50-59) and *anthesis* (DC 60-69). These stages are generally completed within four to six days. In reality, these optimal intervals of data collection are subject to meteorological influences. Rain and overcast or instable atmospheric conditions can prevent from collecting data at a certain phenological stage. In addition, wet crop conditions that affect spectroradiometric measurements, as well as prolonged or reduced durations of stages due to unusual meteorological conditions require permanent adaptation of the data acquisition schedule.

Beside the temporal sampling over a whole vegetation period, the temporal aspect of an ideal day of data acquisition, as explained in Chapter 5.2.1.2 is of importance to perform each data take at its most promising time of day. The temporal measurement plan of Tab. 5.1, as performed on a typical measurement day is based on time requirements and optimal timing within the day (see Chapter 5.2.1.2) for acquisition of the parameters under investigation.

Table 5.1 Temporal measurement plan for the investigated spring wheat and winter barley field.

Time, cultivar	11.00 - 12.00	12.00 - 12.30	12.30 - 13.30	13.30 - 14.30	14.30 - 15.00	15.00 - 16.30	15.30 - 16.30	16.30 - 17.00
Spring wheat	LAI	FAPAR	Spectra					Sample collection, photos, field characterization
Winter barley				Spectra	FAPAR	Sample collection, photos, field characterization	LAI	

b) Spatial Sampling

Assessing the spatial variability of an agricultural plot requires many measurements. Schaepman [110] states that a spatial sampling strategy is composed of two major factors defining the representativeness of the samples: the sampling scheme and the sample size.

For this work, the measurements carried out in the field (reflectance measurements, LAI- and FAPAR measurements) were performed using stratified random sampling accross a transect along the diagonal of one half part of the fields under investigation. Congalton [34] proposes stratified random sampling when one wants to know specific information about certain subpopulations. In this method, a priori knowledge about a population is used to divide or stratify the population into nonoverlapping subpopulations. The subpopulations defined in this work are based on optical density criteria of the crop stand during data take. They include dense, medium and sparse vegetation coverage, being a result of soil fertility and moisture content, which are caused by soil type and topography variations. Sampling across a transect helps to count for such variations.

As far as the required sample size to adequately describe the variations of a population is concerned, recommendations can be found in literature [6]. On the one hand, large sample sizes represent a population more accurately. On the other hand, time and money constraints often reduce the statistical validity

of both the sample size and sampling scheme. The larger the variance of an observed variable, the larger the sample size should be. In general, statistically representative sample sizes consist of 30-40 measurements [6][62]. These sample sizes are found to be adequate to assess infield variations of crops spectroradiometrically [110]. The assessment of phenological stages of crop stands by means of spectroradiometric measurements and the determination of biophysical and biochemical parameters, both from field- and laboratory measurements within a given timeframe, most often prevents from collecting samples of the desired sample sizes. In this case, assessment of the variations, as performed in Chapter 5.3 can help to characterize the data basis available. A comprehensive method of sample size determination is presented in Chapter 5.4.

5.2.1.2 Performing the Field Measurements

A detailed description of the various field measurements performed on a typical day of data acquisition is given in this section. The factory specifications of the instruments used, both in the field and in the laboratory, can be found in the appendix.

a) Spectroradiometric Measurements

Reflectance measurements of the vegetation canopies under investigation were performed using an ASD FieldSpec Pro FR spectroradiometer [3][4] (subsequently referred to as ASD Spectrometer) covering the wavelength range between 350 and 2500 nm. All measurements were taken from nadir direction, holding the fiber optic's pistol grip approximately 1 m above the canopy. Using the common 25° field of view probe end, the area covered by one measurement is defined by a circle of nearly 45 cm in diameter, which is ideal for monitoring crop stand characteristics rather than single leaves. The spectral range of the ASD Spectrometer is covered by three detectors, that can be regarded as independent spectrometers. They all have a corresponding number of separate fiber optic bundles, each with slightly different sample views. Discontinuities in reflectance data between spectral regions are a common problem of multi-region spectromter models with fiber optic technology. To avoid such spectral discontinuities in the data, ASD's recommendation of slightly altering the probe's field of view was applied during data acquisition. For each of the two cultivars investigated, between 50 to 60 reflectance measurements were recorded randomly along a transect and characterized as representing a dense, medium or sparse vegetation coverage. Depending on the atmospheric stability, the reflectance calibration of the spectroradiometric measurements against a Spectralon reference standard

panel was performed every five to ten measurements. The spectroradiometric measurements were performed around solar noon to minimize mutual shading of the crop stand.

b) Measurements of Leaf Area Index

Leaf area index of the crop stands' different phenological stages was measured using a LI-COR LAI-2000 Plant Canopy Analyzer [86]. This instrument for indirect measurement of canopy architecture is widely accepted and commonly used in the agricultural community. Direct measurements of canopy structure, which plays a fundamental role in canopy processes and interaction between vegetation and its environment, are most often labour intensive and tedious. Indirect techniques base on the close coupling between radiation penetration and canopy structure. They provide an alternative to direct measurements of LAI, foliage density, leaf angle distribution and leaf inclination angle. The absolute accuracy of LAI-2000 measurements is reported as within 15% of directly determined LAI [131]. The instrument's optical sensor uses a fish-eye lens with a hemispheric FOV to project radiation onto the detector. This assures that LAI calculations are based on a large sample of canopy. The detector consists of five separate silicon detectors arranged in concentric rings. Each detector records radiation in a different range of angles, ranging from 0° (nadir view) to 74° off-nadir view. The LAI-2000 meter is designed to discriminate foliage against the brighter sky. Therefore, the sensor contains an optical filter to restrict incoming radiation to wavelengths below 490 nm, in order to minimize the contribution of radiation that has been scattered by foliage. As a result, the foliage appears 'black' against the brighter sky [86][131].

The measurement procedure combines a measurement of incident radiation above the canopy with a second measurement taken within the canopy with the sensor looking skywards. It is then assumed that the ratio of each ring's signal from below and above is equivalent to the canopy's gap fraction at that ring's viewing angle. The gap fraction of a canopy is defined as the fraction of view in some direction from within a canopy that is not blocked by foliage. The instrument is judged the most powerful and practical tool available for indirect sensing of canopy structure [86]. LAI and other canopy structural parameters are obtained from gap fraction data by the use of inversion methods based on the following assumptions [131]:

- Only sky radiation is seen by the sensor beneath the canopy, since leaf reflectance and transmittance are assumed to be minimal.
- Foliage is randomly positioned in the canopy.
- Foliage elements are small.

- Foliage may be inclined with any distribution of angles, but is randomly oriented with respect to azimuth.

Since the measurements of canopy gap fractions and resulting estimates of LAI are based on a radiation interception method, not only leaf area, but all opaque objects such as stems, ears and grain in the direct path of incoming radiation prevent it from reaching the bottom of the canopy. In addition, the sensor cannot distinguish between living and dead tissue. Therefore, it is not possible to separate photosynthetically active LAI from standing litter material. Welles and Norman [131] conclude that the term foliage area index is a better description of what is measured by the LAI-2000 meter than (green) leaf area index.

Acquisition of LAI data in this work using the LAI-2000 meter was performed at low solar zenith angles, preferably at the beginning or towards the end of a day of data takes. However, the absence of direct sun during LAI measurements is best. As a consequence, measurements should be performed under cloudy skies, when the contribution of scattered radiation is low. Direct sunlight, that hits the canopy, significantly increases scattered radiation, which itself increases the below-canopy readings, resulting in underestimates of LAI. The necessity of direct incoming solar radiation for spectroradiometric measurements on the one hand, and obscured sun for LAI readings on the other hand, are most often incongruous demands. Therefore, view caps for the lens were used to mask the portion of the sky that contains the sun.

Each LAI data take consisted of one above- and five below-canopy readings to achieve a suitable spatial average for the specific measurement site. Around 20 LAI measurements per cultivar and observation day were taken randomly along a transect and described as being of dense, medium or sparse vegetation coverage. The direction of the sun was chosen as being in the observer's back, so that both the sun and the observer could be masked by using a 270° view cap installed on the optical sensor's lens.

c) Measurements of Fraction of Absorbed Photosynthetically Active Radiation

As indicated in Chapter 2.8, integrated APAR over a certain interval of time is particularly interesting for plant growth monitoring and requires both incident PAR and FAPAR. FAPAR, which can be estimated from a remote sensing platform is best being measured around solar noon [40]. Like spectroradiometric measurements, FAPAR must be measured under clear sky conditions and at high solar zenith angles, forcing the observer in the field to efficiently allocate time to both measurements.

Determination of APAR was performed using a Sunfleck Ceptometer [44] which captures the total solar flux of the 400-700 nm wavelength range,

known as the region of photosynthetically active radiation of the solar spectrum. The instrument has 80 light sensors placed at 1 cm intervals along a probe. The determination of FAPAR is based on single PAR readings above and below the canopy. The measurement strategy, as illustrated in Fig. 5.1 is based on Eq. 4.14 in Chapter 4.3.

First, one measurement of incoming radiation intensity at the top of the canopy ($I_{PAR,i}$) is performed by placing the probe above the plant stand. Second, the probe is placed on the canopy bottom, to perform data takes of the transmitted radiation at the bottom ($I_{PAR,t}$). The third step of measuring $I_{PAR,r}$, the upward radiation at the top of the canopy, which is reflected by the plants and the soil, is performed by turning the ceptometer's sensors downward. Finally, measuring $I_{PAR,s}$, the radiation reflected at soil surface, is carried out at the bottom of the canopy with the sensor probe's top turned towards the soil surface. Measurements of $I_{PAR,t}$, $I_{PAR,r}$ and $I_{PAR,s}$ are averaged values of 10 single measurements that should be performed within a few centimeters of the same part of the canopy investigated, to achieve accurate readings. Approximately 20 FAPAR values were recorded for each of the two agricultural stands per measurement day. The data was acquired randomly along a transect, and characterized as being of dense, medium or sparse vegetation coverage.

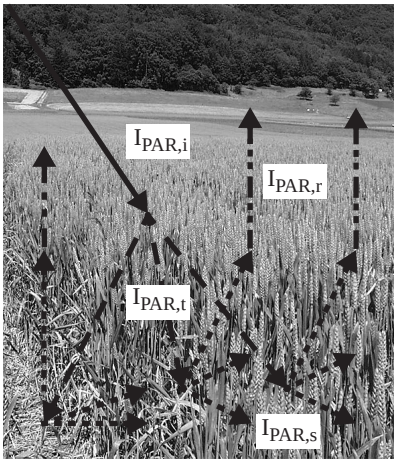

Figure 5.1 Components of the radiation present in a crop stand. The determination of FAPAR is based on the single measurement of each of the four components needed in Eq. 4.14.

5.2.1.3 Sample Collection for Laboratory Measurements

a) Collection of Samples for Chlorophyll Content Determination

Determination of leaf chlorophyll content is based on leaf samples collected in the field and immediately placed in plastic bags to prevent them from dehydration. The amount of samples to be taken for laboratory extraction of chlorophyll is limited by the time needed to perform the extraction and measurements of chlorophyll content in the laboratory. Normally, five sets of leaves were gathered per measurement day, both for spring wheat and winter barley. Each set itself consisted of five leaves brought together in one bag. Once chlorophyll was no longer present in the winter barley leaves, the amount of samples of spring wheat was doubled to ten bags. Collection of single leaves was based on the following considerations:

- Selected plants must be representative for the field.
- The same leaf must be collected from each plant. As a consequence, the last leaf unfolded on the plant's main shoot was chosen, since it reflects the plant's vitality and therefore its phenology.

A chlorophyll meter reading of each of the collected leaf samples was performed in the field using a handheld Minolta chlorophyll meter SPAD-502 [118]. Leaf greenness or the amount of chlorophyll per unit leaf area is a good indicator of the overall condition of the plant. Leaf greenness is affected by a number of factors like the plant's physiological status, reflected by its phenology or the nitrogen status of the plant. The majority of leaf nitrogen is contained in chlorophyll molecules. Therefore, available nitrogen and leaf chlorophyll can be correlated, making the SPAD-502 a widely used tool to improve nitrogen management by detecting nitrogen deficiency and determining the need for additional nitrogen fertilizer. The meter has two diodes active at 650 nm and 940 nm, which emit light onto the upper surface of a leaf. Arbitrary units of chlorophyll content are calculated as a ratio of leaf transmittance at 650 nm, which is affected by leaf chlorophyll content, and transmittance of light at 940 nm, which is not sensitive to chlorophyll content and therefore serves as a reference. The amount of light reaching the photodiode detector is inversely proportional to the amount of chlorophyll in the light path. Since the SPAD-502 meter readings are only in arbitrary units, laboratory extracted chlorophyll concentrations of the observed leaves were correlated to the readings to calibrate the SPAD-502 for winter barley and spring wheat chlorophyll determination over a cropping cycle. The relation between the SPAD-502 meter values and leaf chlorophyll concentration is reported as nonlinear. Markwell et al. [94] were able to fit both a second order polynomial function and an exponential function to the data. The regression

coefficients, obtained for spring wheat and winter barley, are given in Chapter 6.4.4.

b) Collection of Samples for Water Content Determination

Water content was determined for samples of single leaves and whole plants. From the phenological stage of *caryopsis water ripe* (DC 71) until *havest*, grain water content was measured additionally. A measurement day's sample size for leaf water determination amounted to ten independent sets of leaves, each consisting of ten single leaves. Twenty complete plants were collected for plant water determination. For grain water content determination, twenty ears were collected. All samples were immediately placed in a plastic bag to avoid dehydration. Only samples that were representative for the main part of the observed fields were collected. Leaf samples consisted of the last leaf unfolded on the plant's main shoot, as in the case of chlorophyll determination.

5.2.2 Laboratory Measurement Plan

5.2.2.1 Determination of Chlorophyll Content

Leaf chlorophyll was extracted in the laboratory with 100% acetone (pure solvent). Using the equations given by Lichtenthaler [85] for the simultaneous determination of chlorophyll a and b in pigment extract solution, the absorbance (extinction) of the solvent at specified wavelengths was determined using a CADAS-100 Spectrophotometer [83]. Chlorophyll determination consisted of four main steps to be accomplished:

1) *Measurement of the total leaf area of all leaves present in a plastic bag of field samples using a LI-COR LI-3100 Area Meter [88].* The samples are placed between the guides of a conveyor belt allowing them to pass through the LI-3100 Area Meter. As a sample travels under a fluorescent light source, the accumulated leaf area is recorded.
2) *Extraction of chlorophyll from finely cut material.* To facilitate pounding with a mortar, the cuttings were freeze-dried with liquid nitrogen. The material is homogenized and macerated by adding up to a total of 10 cl of 100% acetone. Filtration of pigment extract solution using this amount of acetone results in colorless filtrate and washings with all chlorophyll being extracted.
3) *Quantitative determination of chloropyll a and b.* This step should be carried out immediately after preparation of the extract, since chlorophylls are extremely light-sensitive. A cuvette filled with pigment extract solution is entered into the spectrophotometer for the determination of

absorbance *A* at the wavelengths positions given in Eq. 5.1, Eq. 5.2 and Eq. 5.3.

4) *Calculation of total chlorophyll a, b and a+b of the pigment extract solution.* This step is performed using the equations of Lichtenthaler:

$$C_a = 11.24 \cdot A_{661.6} - 2.04 \cdot A_{644.8} \quad (5.1)$$

$$C_b = 20.13 \cdot A_{644.8} - 4.19 \cdot A_{661.6} \quad (5.2)$$

$$C_{a+b} = 7.05 \cdot A_{661.6} + 18.09 \cdot A_{644.8} \quad (5.3)$$

where

A	measured absorbance value [µg ml^{-1}] of plant extract solution at the designated wavelength positions,
C_a	chlorophyll a concentration [µg ml^{-1}],
C_b	chlorophyll b concentration [µg ml^{-1}],
C_{a+b}	chlorophyll a+b concentration [µg ml^{-1}].

These equations allow the determination of chlorophyll in the whole solvent (10 cl) and per unit leaf area, since total leaf area was measured prior to pounding of the leaves. Determination of chlorophyll content in the described manner takes approximately 30 minutes per sample.

5.2.2.2 Determination of Water Content

Water content of the collected samples was determined from oven drying of the samples at 85°C for 48 hours until the material reached weight constancy. Water content determination consisted of three main steps to be accomplished:

1) *Weighting of the collected vegetation samples*. Weight determination must be performed with the samples inside their plastic bags to avoid losses of moisture that evaporated in the time from sample collection until weighting. For leaf water determination, the leaf size is measured using a LI-COR LI-3100 Area Meter [88]. Grain water content determination is performed on grains that are separated from the surrounding ear material.
2) *Drying of the samples in a drying oven at 85°C for 48 hours.* This time is sufficient for the plant material to lose its moisture and to reach weight constancy.
3) *Re-weighting of the dried samples.* The difference in weight allows for leaf-, plant- and grain water content determination. Whereas leaf-, plant- and grain water content are specified per unit mass (expressed as [g g^{-1}]), leaf water content can equally be computed per unit leaf area ([g cm^{-2}]).

5.3 Acquired Data Sets

The acquisition of both spectral data and biophysical and -chemical parameters at distinct growth stages allows to track a crop stand's vitality during its phenological development. The data set, acquired following the field and laboratory measurement plan described in Chapter 5.2, is presented in this section. The measured spectral data, LAI and FAPAR readings, as well as water content and chlorophyll concentration values of the observed spring wheat and winter barley field form the basis of this work's main objective to evaluate the potential of spectroscopy data for the retrieval of the abovementioned parameters to track a crop stand's main phenological stages.

5.3.1 Ground Spectroradiometric Data

Spectral data takes of the spring wheat canopy cover the main phenological stages between the stages of *first leaf unfolded* (DC 11) and *hard dough* (DC 87). The data was collected on 14 measurement days, given in Fig. 5.2. For winter barley, spectral data was collected on 13 measurement days between the phenological stages of *tillering completed* (DC 29) and *grains over-ripe* (DC 94), given in Fig. 5.3. To assess the spectral variability of the observed canopies, each plot shows the mean reflectance of approximately 50 individual reflectance measurements (see Chapter 5.2.1.2) and the reflectance of ± 1 standard deviation of the data from the mean reflectance.

The percent deviation of ± 1 standard deviation from mean reflectance, as given in Fig. 5.4 and Fig. 5.5, shows spectral variations of up to 20% or more for the visible and near-infrared part of the canopies' spectra on a single measurement day. Especially when more than one phenological stage is currently present in a field, the deviations of single spectra from a mean value increase. Maximum deviations in the visible range can be found around the chlorophyll a absorption region (675 nm) and the wavelength region where the near-infrared shoulder is first reached (760 nm). Minimum deviations are present around the green peak (550 nm) and the red edge inflection point (730 nm), making them relatively stable features of a certain phenological stage.

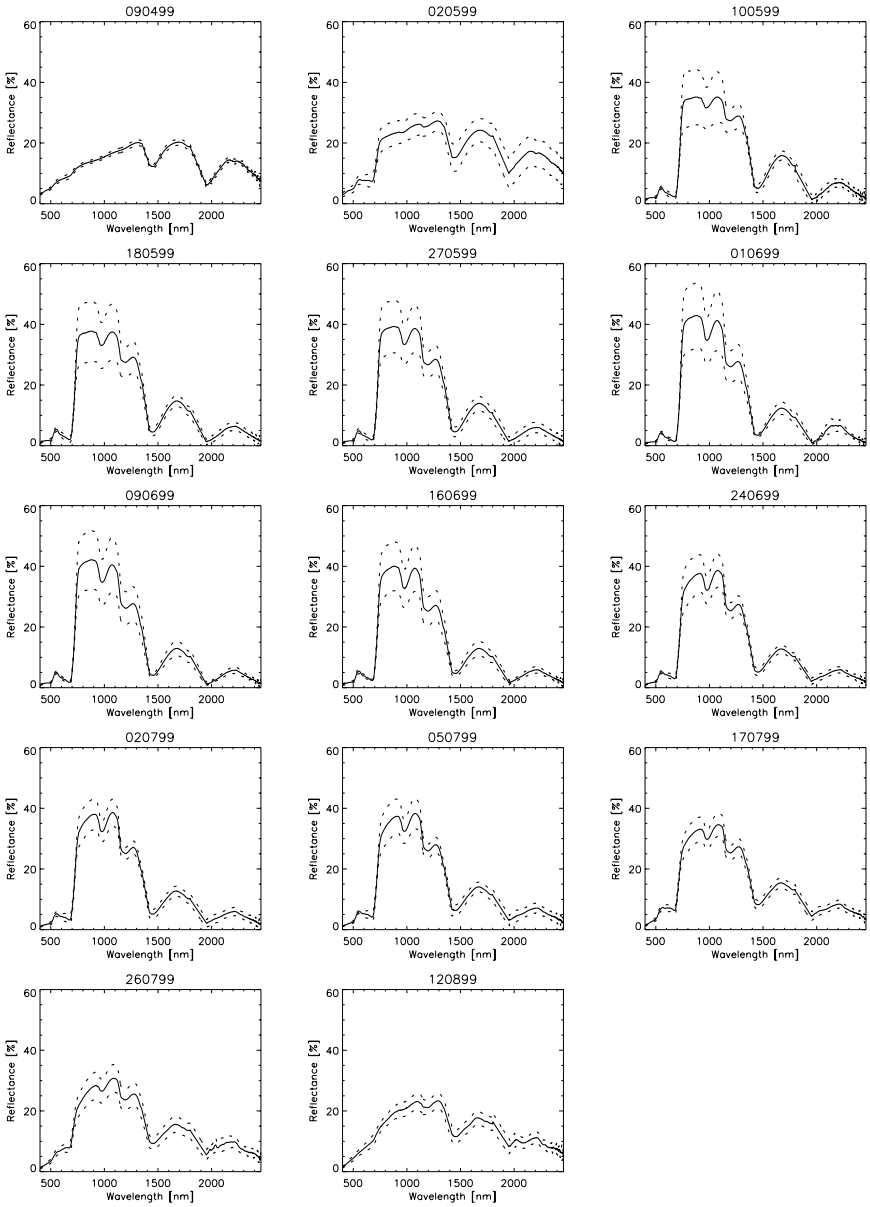

Figure 5.2 Spectral data of the observed spring wheat field for the main phenological stages between *first leaf unfolded* (DC 11) and *hard dough* (DC 87). The mean reflectance (solid line) of approximately 50 data takes and the reflectance of ± 1 standard deviation of the data from mean (dashed lines) is shown for each measurement day, given by its date in the plot title.

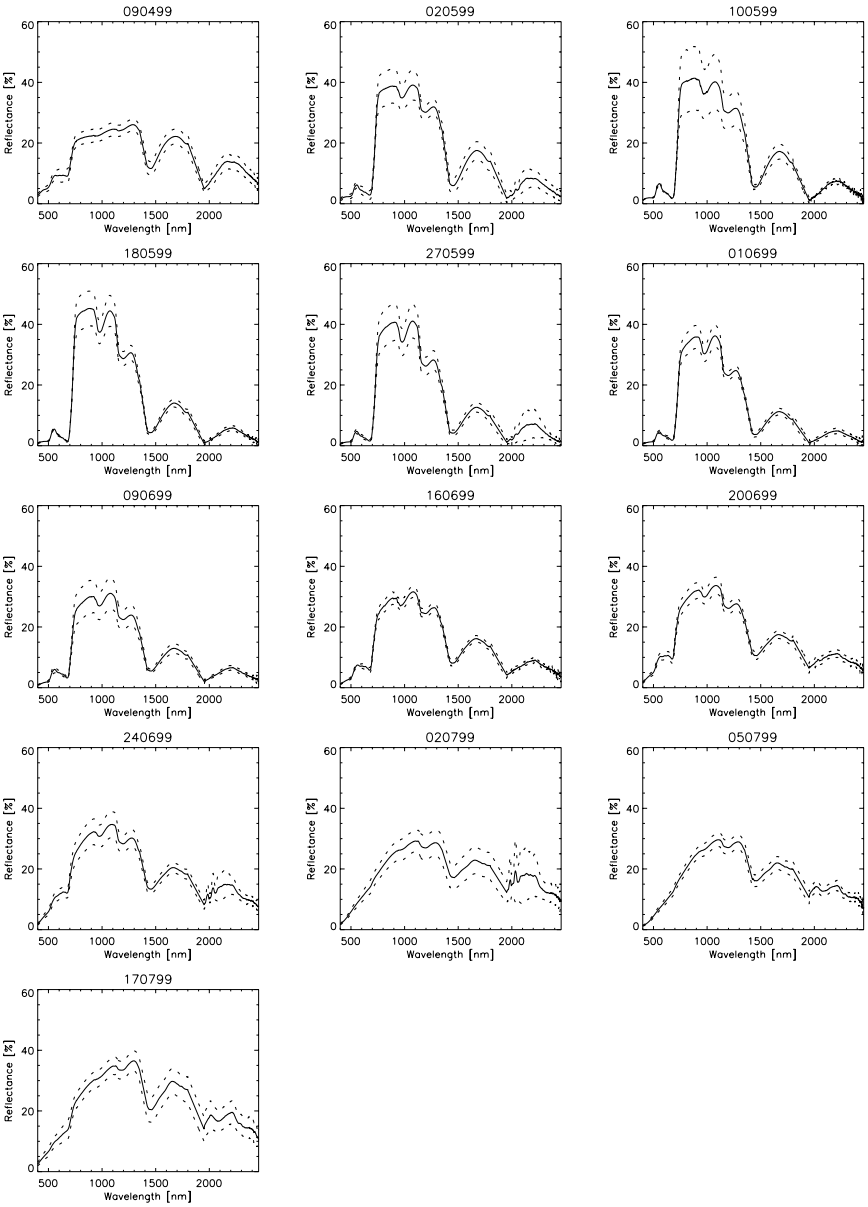

Figure 5.3 Spectral data of the observed winter barley field for the main phenological stages between *tillering completed* (DC 29) and *grains over-ripe* (DC 94). The mean reflectance (solid line) of approximately 50 data takes and the reflectance of ± 1 standard deviation of the data from mean (dashed lines) is shown for each measurement day, given by its date in the plot title.

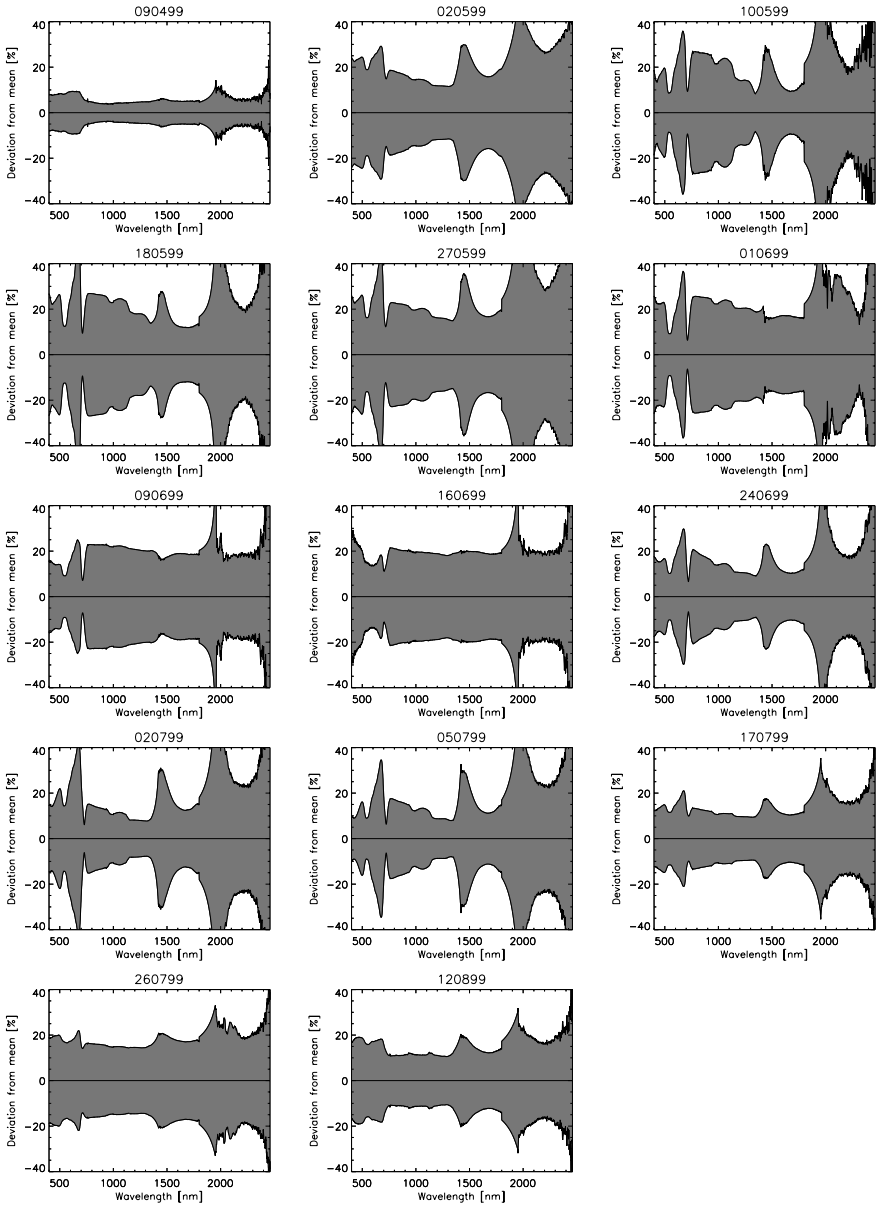

Figure 5.4 Percent deviation from mean reflectance of ± 1 standard deviation for spring wheat data in Fig. 5.2. The spectral data between 1350-1420 nm and 1800-1950 nm is linearly interpolated because spectroradiometric data takes in these regions are heavily influenced by the variation of atmospheric water vapor.

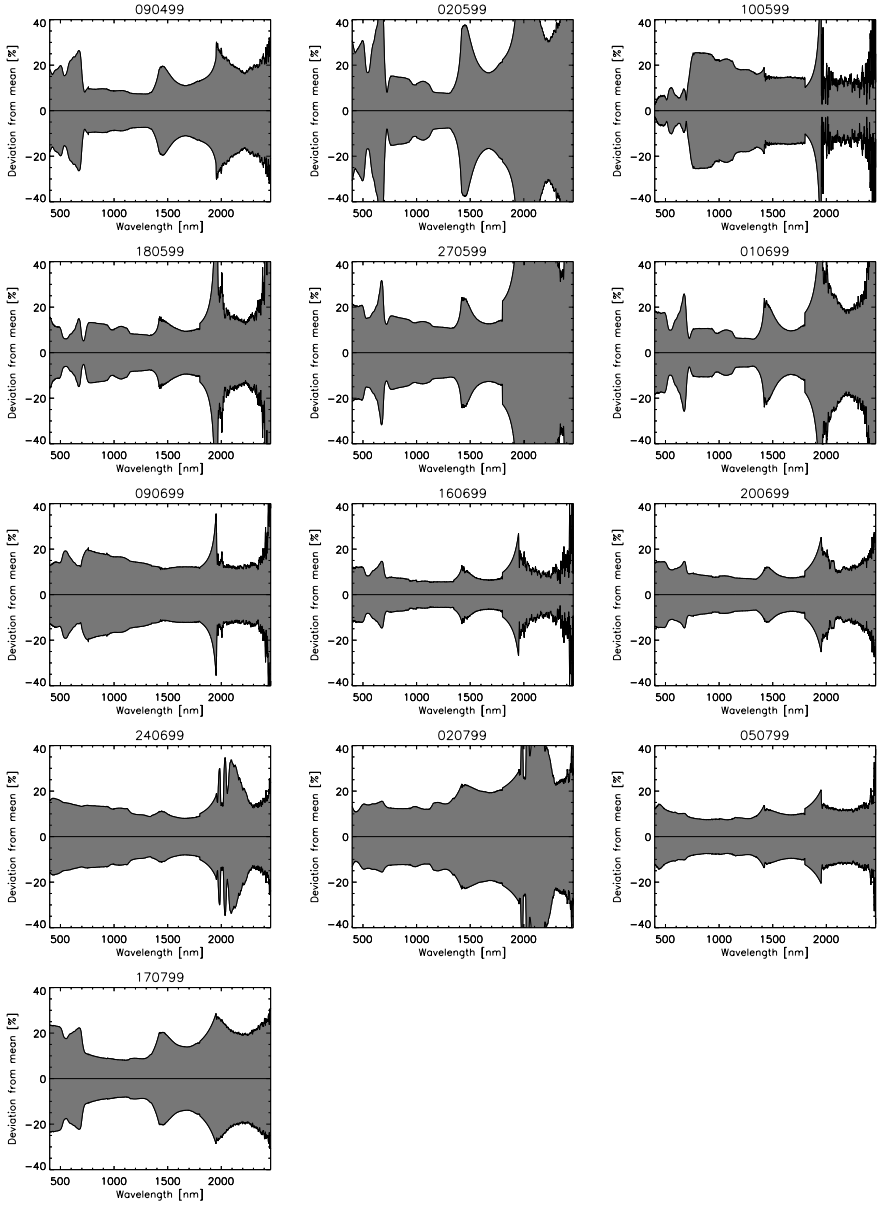

Figure 5.5 Percent deviation from mean reflectance of ± 1 standard deviation for winter barley data in Fig. 5.3. The spectral data between 1350-1420 nm and 1800-1950 nm is linearly interpolated because spectroradiometric data takes in these regions are heavily influenced by the variation of atmospheric water vapor.

The spectral regions between 1350-1420 nm and 1800-1950 nm, where major absorptions by atmospheric water vapor occur, are subject to low signal-to-noise ratios. As a consequence, the spectral data of this regions is linearly interpolated. This data is not not used in the applied methods of parameter retrieval in Chapter 6.5.

As can be seen in Fig. 5.4 and Fig. 5.5, the low signal-to-noise (SNR) ratio of the third spectrometer of the ASD FieldSpec Pro FR spectroradiometer, covering the wavelength range from 1700-2500 nm, causes noisy spectral data mainly above 2000 nm. This range is excluded from further analysis, too.

5.3.2 LAI Data

Leaf area index values of spring wheat were recorded on twelve measurement days between the stages of *three leaves unfolded* (DC 13) until *hard dough* (DC 87). LAI of winter barley was acquired on nine days of data take, ranging from the stage of *pseudo stem erection* (DC 30) to the stage of *soft dough* (DC 85). The mean LAI values of approximately 20 data takes and the deviations of ± 1 standard deviation of the data from the mean is given in Fig. 5.6 and Fig. 5.7.

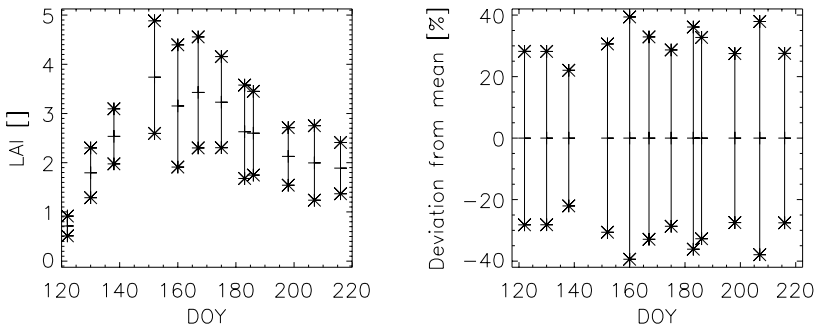

Figure 5.6 Left: LAI values of the observed spring wheat field for the main phenological stages between *three leaves unfolded* (DC 13) and *hard dough* (DC 87), given as mean values of approximately 20 data takes and ± 1 standard deviation of the data from mean. Right: Percent deviation from mean of ± 1 standard deviation of the LAI data for spring wheat.

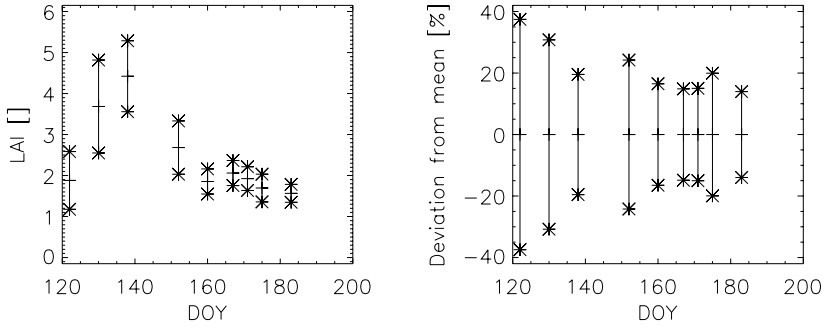

Figure 5.7 Left: LAI values of the observed winter barley field for the main phenological stages between *pseudo stem erection* (DC 30) and *soft dough* (DC 85), given as mean values of approximately 20 data takes and ± 1 standard deviation of the data from mean. Right: Percent deviation from mean of ± 1 standard deviation of the LAI data for winter barley.

Spring wheat reached its maximum LAI values at the stages of *2nd and 3rd node detectable* (DC 32-33) and kept high LAI values until *completion of anthesis* (DC 69). Highest LAI values in the winter barley field were observed at the stages of *half of inflorescence emerged* to *emergence of inflorescence completed* (DC 55-59). A time lack of 14 days due to unstable weather conditions made further LAI observations impossible until *beginning of anthesis* (DC 61), when a much lower LAI was measured. Contrary to spring wheat, a considerable amount of leaves of winter barley became yellowish before *anthesis*, diminishing the area of leaves detectable by a leaf area meter.

The percent deviations of ± 1 standard deviation of LAI data from the mean value are considerably high during the whole season, both for spring wheat and winter barley. They lie between 20-40%. Infield variations are mainly caused by topography, soil properties, nutrient and water availability, which affect phenology. Deviations become smaller for winter barley towards the end of the cropping cycle, a fact which can be seen also in the spectral deviations of winter barley in Fig. 5.5. Considering LAI and spectral data of both spring wheat and winter barley, the winter barley field appears to be more homogeneous, especially during the *reproductive phase*.

5.3.3 FAPAR Data

Measurements of the fraction of absorbed photosynthetically active radiation, given in Fig. 5.8 for spring wheat and in Fig. 5.9 for winter barley, can be characterized by a long period of high, relatively constant FAPAR values.

FAPAR data of spring wheat was recorded on ten measurement days between the phenological stages of *first leaf unfolded* (DC 11) and *medium milk* to *soft dough* (DC 75-85). FAPAR data of winter barley ranges from *tillering completed* (DC 29) to *caryopsis hard* (DC 92), acquired on eight days of data take. A set of about 20 individual readings was recorded per measurement day for each of the two cultivars.

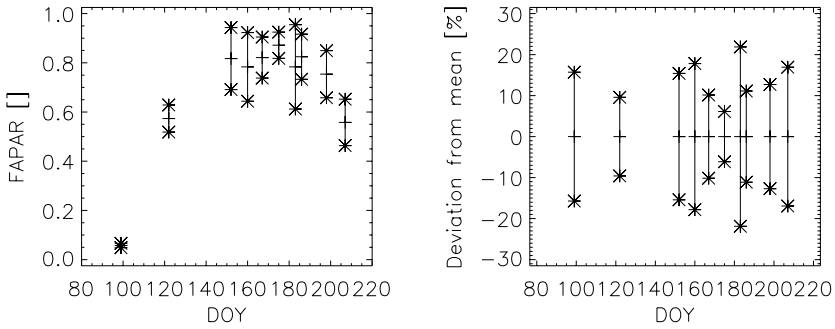

Figure 5.8 Left: FAPAR values of the observed spring wheat field for the main phenological stages between *first leaf unfolded* (DC 11) and *medium milk* to *soft dough* (DC 75-85), given as mean values of approximately 20 data takes and ± 1 standard deviation of the data from mean. Right: Percent deviation from mean of ± 1 standard deviation of the FAPAR data for spring wheat.

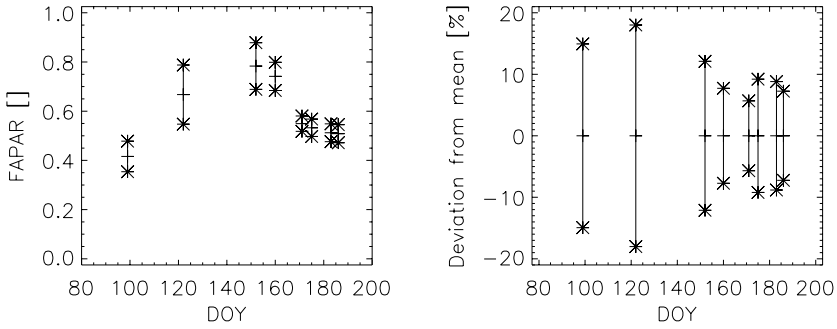

Figure 5.9 Left: FAPAR values of the observed winter barley field for the main phenological stages between *tillering completed* (DC 29) and *caryopsis hard* (DC 92), given as mean values of approximately 20 data takes and ± 1 standard deviation of the data from mean. Right: Percent deviation from mean of ± 1 standard deviation of the FAPAR data for winter barley.

The percent deviations of ± 1 standard deviation of FAPAR data from the mean value range up to 20%. Deviations for spring wheat remain constantly high during r*ipening*, whereas the deviations for winter barley fall below ± 10%, indicating a more homogeneous canopy in the *reproductive phase*.

The fact that both FAPAR readings from a ceptometer and LAI readings from an LAI-2000 Plant Canopy Analyzer remain high even when most parts of a crop canopy have turned yellow, is addressed in Chapter 6.2.4.

5.3.4 Chlorophyll Content Data

Chlorophyll a and b content per unit leaf area of the last unfolded leaf on the plant's main shoot is found to decrease during the whole phenological phase. The ratio chl_a/chl_b changes during the vegetation period in favour of chlorophyll b. Leaf chlorophyll content was determined from at least five individual sets of leaves, each made up of five single leaves, (Chapter 5.2.1.2) on twelve measurement days for spring wheat and on seven measurement days for winter barley, respectively. The data of spring wheat covers the stages from *three leaves unfolded* (DC 13) until *medium milk* to *soft dough* (DC 75-85), chlorophyll measurements of winter barley were performed during *pseudo stem erection* (DC 30) and s*oft dough* (DC 85). The concentrations of both chlorophyll a and b per unit leaf area are given in Fig. 5.10 for spring wheat and winter barley.

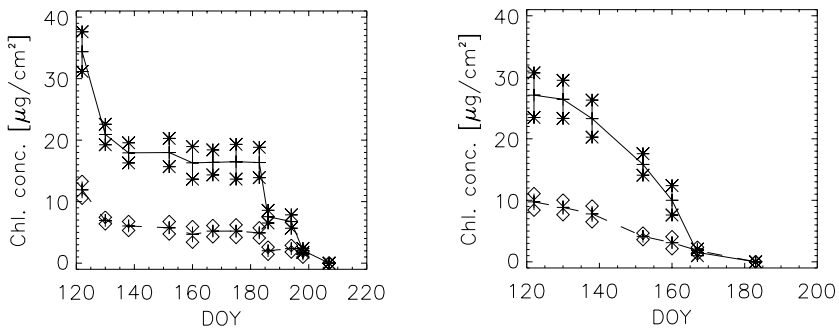

Figure 5.10 Left: Chlorophyll a (solid line) and chlorophyll b (dashed line) content per unit leaf area and ± 1 standard deviation of the data from mean for spring wheat between the phenological stages of *three leaves unfolded* (DC 13) and *medium milk* to *soft dough* (DC 75-85). Right: Chlorophyll a (solid line) and chlorophyll b (dashed line) content per unit leaf area and ± 1 standard deviation of the data from mean for winter barley between the phenological stages of *pseudo stem erection* (DC 30) and *soft dough* (DC 85).

In general, the percent deviations from mean of ± 1 standard deviation of leaf chlorophyll a and b per unit area lie between 10-20%, with slightly increased values during the *reproductive phase*.

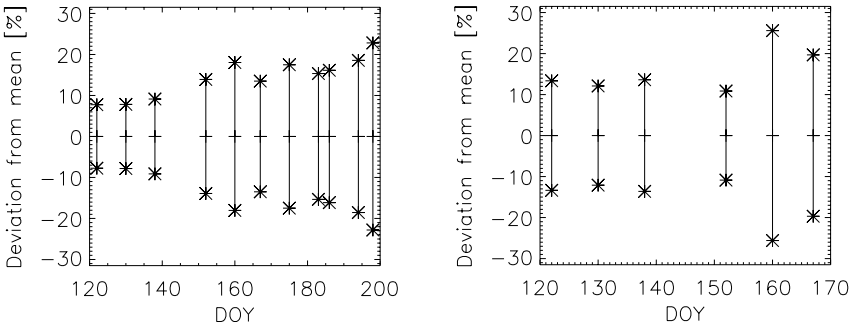

Figure 5.11 Percent deviation from mean of ± 1 standard deviation of leaf chlorophyll a and b per unit leaf area for spring wheat (left) and winter barley (right).

The SPAD-502 meter readings collected in the field to calibrate the instrument with the total chlorophyll a and b concentrations determined in the laboratory are discussed in Chapter 6.4.4.

5.3.5 Water Content Data

Percent leaf and plant water content, together with percent grain water content was determined for spring wheat and winter barley as given in Fig. 5.12. Leaf water content was derived from ten independent sets of last unfolded leaves, each consisting of ten single leaves on 14 measurement days for spring wheat and eight measurement days for winter barley. The phenological stages covered for spring wheat lie between *three leaves unfolded* (DC 13) and *hard dough* (DC87), those for winter barley lie between *pseudo stem erection* (DC30) and *soft dough* (DC 85). Plant water content was determined between the stages of *main shoot and one through five tillers* (DC 21-25) and *hard dough* (DC 87) for spring wheat and between *boots swollen* to *flag leaf sheath opening* (DC 45-47) and *grains over-ripe* (DC 94) for winter barley. Plant water determination was performed from a total of 20 plants on eleven measurement days for both cultivars. Grain water content was determined from 20 individual ears per cultivar during the *reproductive phase*, starting at *caryopsis water ripe* (DC 71) and covering seven measurement days for spring wheat and nine for winter barley, respectively.

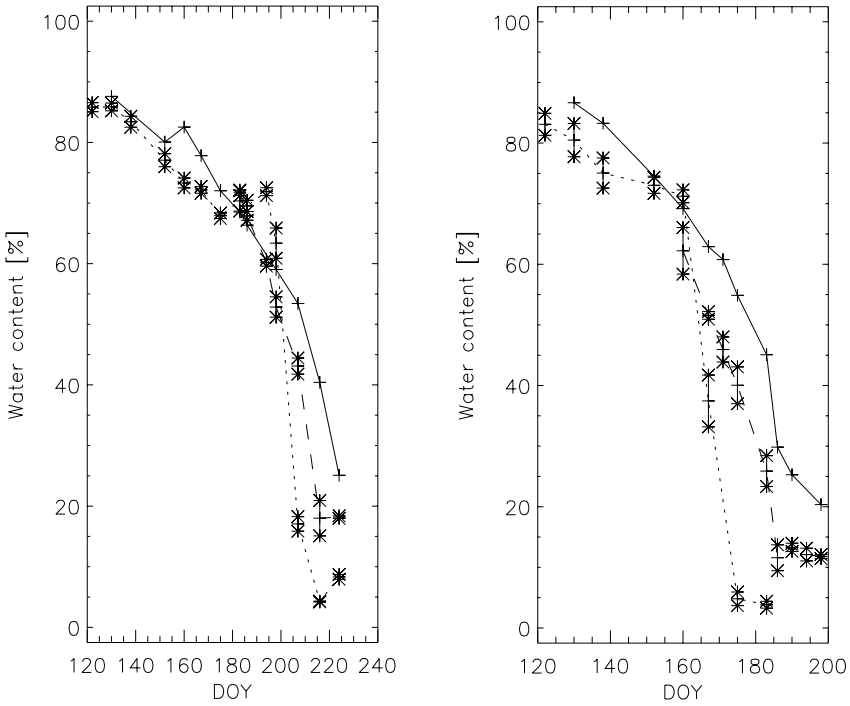

Figure 5.12 Percent plant water content (solid line), percent leaf water content (dotted line) with ± 1 standard deviation of the data from mean, and percent grain water content (dashed line) with ± 1 standard deviation of the data from mean for spring wheat (left) and winter barley (right) over the observed time periods.

As can be seen in Fig. 5.13 (left) and Fig. 5.14 (left), the percent deviations of ± 1 standard deviation of leaf water content from the mean value remain below ± 5% until the phenological stage of *medium milk* (DC 75) is reached. During the reproductive phase, water content of the last unfolded leaves becomes less uniform, both for spring wheat and winter barley. Grain water content variations range below ± 5% for spring wheat (Fig. 5.13, right) and below ± 10% for winter barley (Fig. 5.14, right) except for the stages of *hard dough* (DC 87) in spring wheat and *caryopsis hard* (DC 92) in winter barley. While the increased deviations from the mean value of spring wheat grain water content can be explained by precipitation on the day before, no rain is recorded in the case of winter barley. It can be assumed, that the winter barley field contained considerable amounts of plants at the stages of both, *hard dough* (DC 87, grain water content < 20%), and *caryopsis har*d (DC 92, grain

water content < 16%).

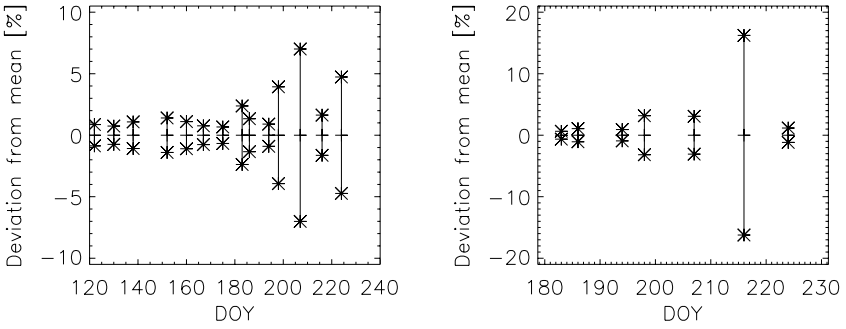

Figure 5.13 Percent deviation from mean of ± 1 standard deviation of leaf water content (left) and grain water content (right) for spring wheat over the observed period.

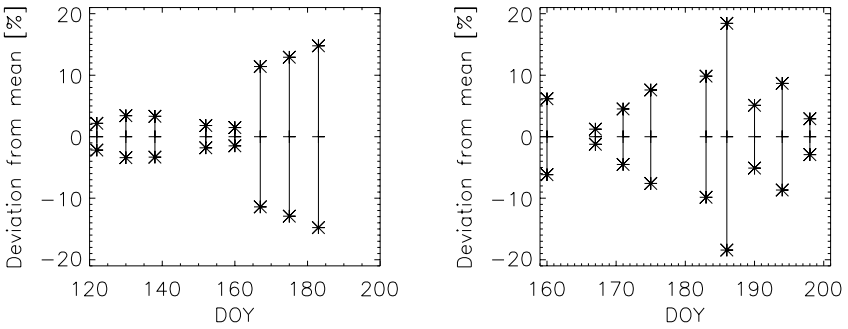

Figure 5.14 Percent deviation from mean of ± 1 standard deviation of leaf water content (left) and grain water content (right) for winter barley over the observed period.

5.3.5.1 Summary of Acquired Field- and Laboratory Data of the 1999 Field Campaign

Tab. 5.2 summarizes the data sets acquired during the field campaign from April to August 1999, which was performed to track the phenological development of the observed spring wheat and winter barley field, and to collect ground truth of the biophysical and biochemical parameters under investigation. A graphical summary of the collected data sets, together with meteorological data observed at Bern-Liebefeld during the observed phenological cycle, is given in Fig. 5.15 for spring wheat.

Table 5.2 Date, day of year (DOY), decimal code (DC) and data sets acquired during the 1999 field campaign to cover the phenological development of a spring wheat and a winter barley cultivar.

Date	DOY	DC		Spectral Data		LAI Data		FAPAR Data		Chlorophyll Content Data		Water Content Data	
		Spring wheat	Winter barley	Spring wheat	Winter barley	Spring wheat	Winter barley	Spring wheat	Winter barley	Spring wheat	Winter barley	Spring wheat	Winter barley
09.04.	99	11 (10)	29	√	√			√	√				
02.05.	122	13	30	√	√	√	√	√	√	√	√	√[1)]	√
10.05.	130	21-25	45-47	√	√	√	√			√	√	√√[2)]	√√
18.05.	138	30	55-59	√	√	√	√			√	√	√	√√
27.05.	147	31	59 (61)	√	√								
01.06.	152	32-33	61	√	√	√	√	√	√	√	√	√√	√√
09.06.	160	47 (55)	71 (69)	√	√	√	√	√	√	√	√	√√	√√√
16.06.	167	55-61	75	√	√	√	√	√		√	√	√√	√√√
20.06.	171		75		√		√		√				√√
24.06.	175	69	75-85	√	√	√	√	√	√	√		√√	√√√
02.07.	183	71	85	√	√	√	√	√	√	√	√	√√√[3)]	√√√
05.07.	186	71-75	92	√	√	√		√	√	√		√√√	√√
09.07.	190		92										√√
13.07.	194	71-75								√		√√	√
17.07.	198	75	94	√	√	√		√		√		√√√	√√
26.07.	207	75-85		√		√		√		√		√√√	
04.08.	216	87				√						√√√	
12.08.	224	87		√								√√√	

[1)] √ leaf water content
[2)] √ plant water content
[3)] √ grain water content

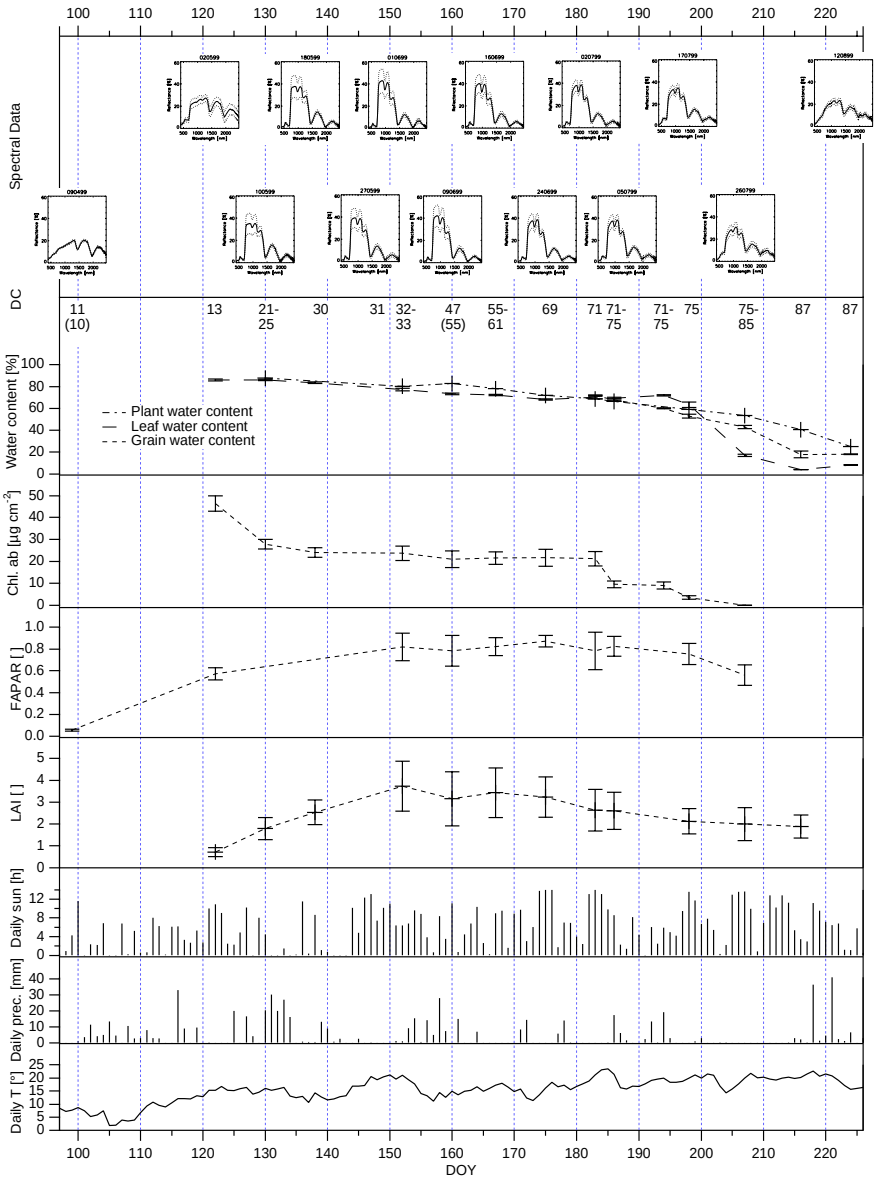

Figure 5.15 Graphical summary of the collected data sets for spring wheat, and meteorological data observed at Bern-Liebefeld during the 1999 phenological ground truth campaign.

5.3.5.2 HyMap Data Take

The observed spring wheat and winter barley fields were covered by the HyMap imaging spectrometer on July 16th 1999, one day prior to harvest of winter barley. Spring wheat was at the phenological stage of *medium milk* (DC 75) whereas winter barley was *over-ripe* (DC 94). Flight altitude was 3.2 km a.s.l., resulting in a spatial sampling of 5 m pixel size. At the time of data take (10.30 UTC), parts of the Limpach valley were covered by scattered clouds, but the two test fields were unaffected by both clouds and shadows (c.f., Figure 6.26 on page 120 (left)). The two fields under investigation are situated between 4.5°-11.5° off nadir relative to the flight line. Atmospheric correction was performed using ATCOR4 [104].

The HyMap sensor's spectral range lies between 450-2500 nm, being covered by 128 image channels. It's system, calibration and performance is described by Cocks et al. [31]. A description and quality assessment of HyMap data is given by Schaepman and Kneubühler [112], as a contribution to the Pro*Smart* Initiative of DaimlerChrysler Aerospace. In this study, the radiometric performance of HyMap is reported to be significantly better than in the case of any other hyperspectral imager operated in Europe in the past.

5.4 Determination of Sample Size

The question of how many data takes of a variable to be measured on a day of data acquisition are necessary to include the true, but unknown mean with a probability Q within a certain confidence interval is of great importance in terms of trade off between the duration of data acquisition and statistical relevance. An approach of minimum sample size determination from a set of measurements is presented in this chapter and applied both, to spectral data and LAI readings of spring wheat for all phenological stages observed, and an extensive collection of LAI data of winter wheat performed on a single measurement day in June 2001 [87][120].

5.4.1 Theoretical Background

Given a random sample x_i of size n, drawn from a normal population with mean μ and standard deviation σ, the sample mean be $\bar{x}$ and the sample standard deviation be s. Then the quantity

$$t = \frac{\bar{x} - \mu}{s / \sqrt{n}} \tag{5.4}$$

has a *t*-distribution with $n-1$ degrees of freedom, where

$$s_{\bar{x}} = \frac{s}{\sqrt{n}} = \sqrt{\frac{\sum_{i=1}^{n} (x_i - \bar{x})^2}{n \cdot (n-1)}} \tag{5.5}$$

is called standard error. The sample mean $\bar{x}$ can be written as:

$$\bar{x} = \frac{1}{n} \sum_{i=1}^{n} x_i \tag{5.6}$$

The population mean μ is situated with a probability value Q within a confidence interval. The confidence level of a confidence interval is often expressed as a percentage, dependent on a significance level α:

$$Q = 1 - \alpha \tag{5.7}$$

A population with mean μ lies with a probability Q within a confidence interval given by:

$$[\bar{x} - t_\alpha \cdot s_{\bar{x}}, \bar{x} + t_\alpha \cdot s_{\bar{x}}], \tag{5.8}$$

where t_α is the critical value of the *t*-distribution at a specified degree of freedom $\nu = n-1$ and a significance level $\alpha = 1 - Q$.

For a specific value of uncertainty δ, the confidence interval can equally be written as:

$$[\bar{x} - \bar{x} \cdot \delta, \bar{x} + \bar{x} \cdot \delta] \tag{5.9}$$

The uncertainty δ can be expressed from Eq. 5.5, Eq. 5.8 and Eq. 5.9 as:

$$\delta = \frac{t_\alpha \cdot s_{\bar{x}}}{\bar{x}} = \frac{t_\alpha \cdot s}{\bar{x} \cdot \sqrt{n}} \tag{5.10}$$

The critical value t_α at a certain significance level α can be fitted to the curve given in Eq. 5.11, for a varying number *n* of samples:

$$t_\alpha = \frac{1}{a + b \cdot n} + c \tag{5.11}$$

The fit parameters *a*, *b* and *c*, determined for the two tailed probabilities $Q = 0.9$ and $Q = 0.8$ and an uncertainty $\delta = 0.05$ are given in Tab. 5.3.

Table 5.3 Fit parameters of the curve for t_α, given in Eq. 5.11, determined for the probabilities $Q = 0.9$ and $Q = 0.8$ (two tailed) and an uncertainty of $\delta = 0.05$.

Fit Parameters	$Q = 0.9, \delta = 0.05$	$Q = 0.8, \delta = 0.05$
a	-1.145	-1.858
b	0.642	1.169
c	1.644	1.281

Substituting Eq. 5.11 into Eq. 5.10 and solving for *n* samples is reported as [87]:

$$n = \frac{-B + \sqrt{B^2 - 4 \cdot b \cdot C}}{2 \cdot b} \tag{5.12}$$

where the parameters B and C are:

$$B = a - b \cdot c \cdot \left(\frac{\sigma}{\bar{x} \cdot \delta}\right)^2 \tag{5.13}$$

$$C = -(1 + a \cdot c) \cdot \left(\frac{\sigma}{\bar{x} \cdot \delta}\right)^2 \tag{5.14}$$

5.4.2 Application to Field Data

5.4.2.1 Spring Wheat of the 1999 Cropping Cycle

Based on Eq. 5.12, the minimum sample size necessary is determined for the acquired spectral data and LAI data of spring wheat at all phenological stages observed. As a basic assumption, the data takes were performed randomly and include all variations present in the field during data acquisition.

Tab. 5.4 shows the minimum number of spectral measurements and LAI data takes to be performed to meet the demand, that the field's unknown mean values μ at distinct phenological stages lie at probabilities of $Q = 0.9$ and $Q = 0.8$ (two tailed) within a confidence interval of an uncertainty of $\delta = 0.05$ (Eq. 5.9). The range of the spectral data used is limited to 550-1350 nm in order to exclude the regions affected by major water vapor absorption. It is obvious from Tab. 5.4, that the number of spectral samples needed to meet the statistical requirements is less than the number of data takes actually performed, both for the probability of $Q = 0.9$ and $Q = 0.8$. However, the

number of samples required varies during the phenological development. A maximum number of samples is required during the growth stages of *tillering*, *stem elongation*, *booting* and *inflorescence emergence* (Tab. 7.4). The spectral response becomes more uniform during the *reproductive phase*. The transition from *medium milk* (DC 75) to *soft dough* (DC 85), clearly visible in heavy losses of leaf water content within a few days (Fig. 5.12), results in a larger number of spectral- and LAI samples (DOY 207) required.

The deviations of ± 1 standard deviation of the LAI data from its mean, as given in Fig. 5.6, lies between 20-40% for all phenological stages observed. These large variations within a field require a larger number of sample data to be measured in order to meet the statistical requirements of Tab. 5.4. In case of a probability of $Q = 0.9$, a larger number of LAI measurements are required, than were actually performed during the 1999 field campaign. Apart of *flag leaf sheath opening* (DOY 160) and the transition from *medium milk* to *soft dough* (DOY 207), no distinct growth stages of maximum variations in LAI are visible.

As far as the spectral data and LAI values of winter barley are concerned, it can be concluded from Fig. 5.3, Fig. 5.5 and Fig. 5.7, that the percent deviations of ± 1 standard deviation from the mean is less than in the case of spring wheat. These smaller infield variations result in smaller optimum samples size for spectral- and LAI data takes in case of winter barley.

The results of Tab. 5.4 confirm, that the sample size recommended by Schaepman [110] for spectroradiometric assessment of infield variations of crops is adequate to meet common accuracy requirements (Chapter 5.2.1). However, it is dependent on infield phenology. LAI readings are found to be more inhomogeneous, forcing larger sample sizes to be collected.

Table 5.4 Number of data takes performed and required at probabilities of $Q = 0.9$ and $Q = 0.8$ (two tailed) based on an uncertainty of $\delta = 0.05$. The values are given for spectral data (550-1350 nm) and LAI data of spring wheat at all phenological stages observed.

	Spectral Data (550-1350 nm)			LAI Data		
DOY	Number of data takes performed	Data takes required at $Q = 0.9$	Data takes required at $Q = 0.8$	Number of data takes performed	Data takes required at $Q = 0.9$	Data takes required at $Q = 0.8$
99	16	3	2	-	-	-
122	70	17	4	21	54	11
130	54	31	7	23	54	11
138	61	36	8	20	33	8

Table 5.4 Number of data takes performed and required at probabilities of $Q = 0.9$ and $Q = 0.8$ (two tailed) based on an uncertainty of $\delta = 0.05$. The values are given for spectral data (550-1350 nm) and LAI data of spring wheat at all phenological stages observed.

	Spectral Data (550-1350 nm)			LAI Data		
DOY	Number of data takes performed	Data takes required at $Q = 0.9$	Data takes required at $Q = 0.8$	Number of data takes performed	Data takes required at $Q = 0.9$	Data takes required at $Q = 0.8$
147	65	27	6	-	-	-
152	50	36	8	15	63	13
160	56	32	7	22	103	21
167	45	26	6	21	73	15
175	56	15	4	18	55	12
183	84	11	3	18	87	18
186	61	13	4	18	72	15
198	59	10	3	15	51	11
207	74	17	4	19	96	20
224	24	11	3	20	51	11

5.4.2.2 Winter Wheat of June 21st 2001

On June 21st 2001, a total of 237 LAI measurements of winter wheat was collected in a time two and a half hours prior and after solar noon (09.00-15.00 UTC). Data collection was carried out using an LAI-2000 meter and was aimed to represent all variations of LAI present. The agricultural field was located in the Limpach valley and at the phenological stage of *anthesis complete* (DC 69). Infield variations were lower than in the case of 1999's spring wheat field, the percent deviation of ± 1 standard deviation from the mean being only 17.1%, compared to values between 20-40% for the case of spring wheat.

In an experiment, thinning out of the data set is performed. 236 data sets of randomly selected LAI values are generated by iteratively reducing the number of LAI values by one. Based on Eq. 5.10, the critical value t_α of the *t*- distribution at a specified degree of freedom $\nu = n - 1$, a significance level $\alpha = 1 - Q$ and an uncertainty of δ, is calculated for each individual set of LAI data. An exponential function given in Eq. 5.15 can be fitted to the relation between sample size n and calculated t_α values, as presented in Fig. 5.16.

$$t_\alpha = a_0 + a_1 \cdot \exp(-a_2 \cdot n) + a_3 \cdot \exp(-a_4 \cdot n) \tag{5.15}$$

Fig. 5.17, which is a subset of the graph in Fig. 5.16, allows the determination of the number n of samples needed to statistically represent the variations of LAI in the field, based on the assumptions made for the probability Q and the uncertainty δ. Therefore, around 14 samples of LAI are needed at a two tailed probability of $Q = 0.8$ (dotted line), 22 samples at $Q = 0.9$ (dashed line) and 29 samples at $Q = 0.95$ (dashed-dotted line).

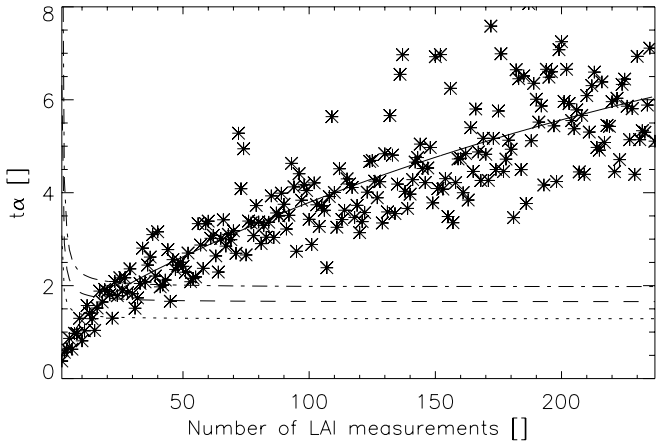

Figure 5.16 t_α values of a subsequently, but randomly thinned out set of LAI measurements. The dotted line represents a *t*-distribution with $\nu = n - 1$ degrees of freedom for a two tailed probability of $Q = 0.8$, the dashed line for $Q = 0.9$, and the dashed-dotted line for $Q = 0.95$. The uncertainty is set to $\delta = 0.05$.

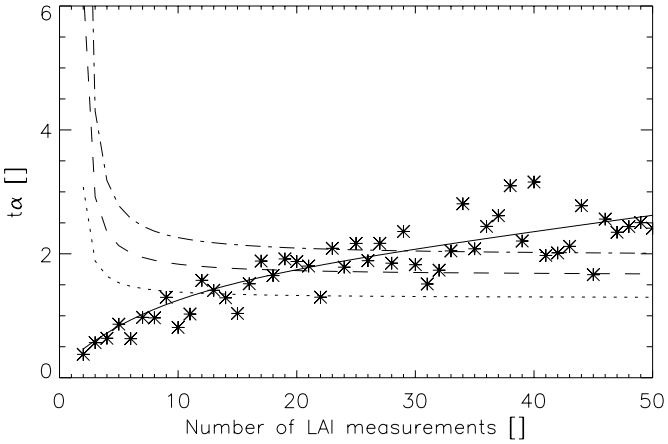

Figure 5.17 Subset of the relation between t_α values and number n of LAI measurements, as given in Fig. 5.16. The optimum number of data takes can be determined for different probabilities: $Q = 0.8$ (dotted line), $Q = 0.9$ (dashed line) and $Q = 0.95$ (dashed-dotted line) at an uncertainty of $\delta = 0.05$.

A comparison of the results of optimum sample size determination for LAI characterization of the 1999 phenological observations and the 2001 data set clearly shows the influence of infield variability on the number of samples required for adequate statistical representation of the field's unknown mean value μ. Less samples are needed in the case of a more homogeneous field.

To assess the true number of samples to be acquired, it is advised to collect a test data set including the thinnest and densest part of a canopy prior to each data take. This allows to calculate the optimum sample size needed, based on Eq. 5.12 [87]. Infield variations are caused by topography, soil properties, nutrient and water availability and phenology. Phenology itself is affected by these factors, too.

Chapter 6

Results

6.1 Introduction

This work's goal is to track the main stages of development of two observed cultivars by means of vegetation parameters retrieved from spectroscopy data. The underlying data sets of this work, that are presented in Chapter 5, were acquired following the field- and laboratory measurement plan described in the same chapter. The applied methods of parameter retrieval are presented in Chapter 4. The results of the retrieval of the four investigated parameters (LAI, FAPAR, chlorophyll content and water content) from spectroscopy data over a phenological phase, are presented in this chapter, followed by accuracy considerations.

The availability of a HyMap hyperspectral data set of July 16th 1999, that includes the two test fields, allows the application of selected parameter retrieval methods to imaging spectroscopy data.

6.2 Results of LAI Determination

The simplified reflectance model used in this work for estimating LAI is introduced by Clevers [27][28] and described in detail in Chapter 4.2. It is based on an inverse exponential relation between the *weighted difference vegetation index* (WDVI) and LAI. The WDVI requires a soil-type specific parameter C. In this chapter, the determination of C, as a prerequisite for WDVI calculation, and the determination of LAI of winter barley and spring wheat over the vegetation period observed, are discussed.

6.2.1 Determination of Soil Parameter C

As stated in Chapter 4.2, the WDVI is a near-infrared reflectance of the canopy-soil composite, which is corrected for soil background influences according to Eq. 4.10. The soil parameter C, being the ratio of soil reflectance in a near-infrared (870 nm) and a red (670 nm) wavelength channel, is assumed to be constant and independent of soil moisture content for a given soil type. C ranges from 1.0-2.0, depending on the soil type. As a consequence, C is determined both for the spring wheat and winter barley

field, based on spectral measurements of bare soil at the beginning of the phenological observations of the two fields under investigation (April 9th). The absence of surrounding vegetation is important when determining C, since radiation from nearby vegetation strongly influences the shape of a soil spectrum due to adjacency effects. This is the case mainly in the visible and near-infrared region of the electromagnetic spectrum [101].

The C values determined from measured spectroradiometric data, that are used for WDVI calculation and LAI estimation in this work are $C = 1.54$ for spring wheat and $C = 1.93$ for winter barley. The differing values for the two fields can be explained by soil type differences of the fields and possible adjacency effects of winter barley plants, being at the phenological stage of *tillering completed* (DC 29) at the time when the soil spectra were taken. Especially the lower parts of the spring wheat field suffered from moory influences, whereas the winter barley field consisted of more homogeneous gleyic brown soil.

Two additional C values for spring wheat, determined from soil spectra that were measured at the phenological stages of *pseudo stem erection* (DC 31) and *emergence of inflorescence completed* (DC 59), showed increased values in comparison to the one determined from spectral data of April 9th, due to the influence of surrounding vegetation. The application of these soil parameters for WDVI and subsequent LAI calculation resulted in small differences, compared to the results obtained when using the C values determined at the beginning of the phenological observations (April 9th). Maximum differences using soil parameters from different phenological stages occured at the beginning and the end of the cropping cycle, when soil influence was high. Minimum differences were found for maximum plant cover. The mean percent deviation between calculated LAI values from WDVI based on C values of April 9th and C values of the two later stages did not exceed 3.5%. Nevertheless, it is important to measure soil spectral data for C determination under absence of adjacent vegetation scattering influence, since variations in C strongest influence LAI estimation at low vegetation cover. Therefore, reliable soil parameter values are important especially during the early and late growth stages.

6.2.2 Determination of LAI from WDVI

Although the concept of estimating LAI from WDVI was developed for green vegetation, it is reported to be likewise applicable to the phenological stages of *anthesis*, *milk* and *dough development* and *ripening* [29], when LAI and photosynthetic activity decrease. In this work, the growth stages of the *vegetative phase* and the *generative phase* until the *beginning of anthesis*

(flowering) are subsequently referred to as *growing phase*, the stages of *anthesis complete* and the following *reproductive phase* are referred to as *senescing phase*. The mathematical relation between the WDVI of a crop canopy in the *senescing phase* and LAI can be described by a similar equation as for the *growing phase*, but with different parameter estimates (see Eq. 4.11 on page 43).

A number of different data sets to determine the regression coefficients of the exponential relation between WDVI and LAI, given in Tab. 6.1, was generated to test whether spectral data and LAI data from both the *growing* and *senescing phase* could be used as a whole for LAI estimation. Determination of the relative rms error [%] was performed, both for spring wheat and winter barley over the wohle cropping cycle.

Table 6.1 Use of different data sets to determine the regression coefficients for the exponential relation between WDVI and LAI over the whole cropping cycle, both for spring wheat and winter barley, and the resulting rms errors [%] for LAI estimation.

Data Base Investigated	Regression Coefficients' Data Set	Rel. rms error [%]
Spring wheat all phases	Spring wheat all phases	18.6
(DC 10-DC 87)	Spring wheat, winter barley all phases	19.0
Winter barley all phases	Winter barley all phases	101.5
(DC 29-DC 85)	Spring wheat, winter barley all phases	81.7

Tab. 6.1 shows that LAI estimation from WDVI is possible for spring wheat of all observed phenological stages at a mean relative rms error of less than 20%, when using regression coefficients from a joint data set of the *growing* and *senescing phases* of spring wheat and even from a combined data set of spring wheat and winter barley. As far as winter barley is concerned, LAI estimation based on regression coefficients of a joint data set of the *growing* and *senescing phase* is not successful, neither for winter barley itself (rms error: 101.5%), nor for the combined data sets of both winter barley and spring wheat (rms error: 81.7%). Possible reasons are discussed later in this chapter.

As a consequence, a compilation of different data sets to determine the fitted regression coefficients of the exponential relation between WDVI and LAI of spring wheat and winter barley for separate *growing* and *senescing phases* and the resulting relative rms errors for LAI estimation are given in Tab. 6.2 and Tab. 6.3, respectively. They illustrate the data sets with the most promising correlation coefficients for LAI estimation during the *growing* and *senescing phases* for the two cultivars.

Table 6.2 Compilation of different data sets to determine the regression coefficients of the exponential relation between WDVI and LAI of spring wheat for separate *growing* and *senescing phases,* and the resulting rms errors [%] for LAI estimation.

Data Base Investigated	Regression Coefficients' Data Set	Rel.rms error [%]
Spring wheat growing phase (DC 10-DC 61)	Spring wheat all phases	20.2
	Spring wheat growing phase	20.4
	Spring wheat senescing phase	24.2
	Spring wheat, winter barley all phases	20.2
	Spring wheat, winter barley growing phases	20.9
	Spring wheat, winter barley senescing phases	21.6
	Winter barley all phases	20.4
	Winter barley growing phase	21.4
	Winter barley senescing phase	20.7
Spring wheat senescing phase (DC 69-DC 87)	Spring wheat all phases	16.2
	Spring wheat growing phase	21.1
	Spring wheat senescing phase	13.2
	Spring wheat, winter barley all phases	17.4
	Spring wheat, winter barley growing phases	23.3
	Spring wheat, winter barley senescing phases	13.1
	Winter barley all phases	20.4
	Winter barley growing phase	25.6
	Winter barley senescing phase	14.3

Table 6.3 Compilation of different data sets to determine the regression coefficients of the exponential relation between WDVI and LAI of winter barley for separate *growing* and *senescing phases,* and the resulting rms errors [%] for LAI estimation.

Data Base Investigated	Regression Coefficients' Data Set	Rel. rms error [%]
Winter barley growing phase (DC 29-DC 61)	Spring wheat all phases	23.1
	Spring wheat growing phase	23.1
	Spring wheat senescing phase	24.2
	Spring wheat, winter barley all phases	23.0
	Spring wheat, winter barley growing phases	23.3
	Spring wheat, winter barley senescing phases	24.1
	Winter barley all phases	23.1
	Winter barley growing phase	23.6
	Winter barley senescing phase	23.5

Table 6.3 Compilation of different data sets to determine the regression coefficients of the exponential relation between WDVI and LAI of winter barley for separate *growing* and *senescing phases,* and the resulting rms errors [%] for LAI estimation.

Data Base Investigated	Regression Coefficients' Data Set	Rel. rms error [%]
Winter barley senescing phase (DC 69- DC 85)	Spring wheat all phases	132.6
	Spring wheat growing phase	154.0
	Spring wheat senescing phase	116.9
	Spring wheat, winter barley all phases	132.6
	Spring wheat, winter barley growing phases	162.4
	Spring wheat, winter barley senescing phases	110.6
	Winter barley all phases	150.3
	Winter barley growing phase	172.6
	Winter barley senescing phase	118.7

LAI estimation during the *growing phase* of spring wheat is possible at relative rms errors around 20% (Tab. 6.2). During the *senescing phase*, rms errors range between 13.1% and 25.6%, depending on the type of data set used to determine the regression coefficients of the exponential relation between WDVI and LAI. A relative rms error around 23% is calculated for LAI estimation of winter barley for a range of data sets in order to determine the regression coefficients (Tab. 6.3). However, LAI estimation of winter barley in the *senescing phase* is not successful for any data set. The high rms errors for LAI estimation of winter barley over the whole cropping cycle, as listed in Tab. 6.1, are therefore caused by the data of the *senescing phase*. Two main reasons for the failure of LAI estimation of winter barley during the *senescing phase* can be addressed:

- Winter barley, which was treated in an extensive manner that forbids the use of herbicides, suffers from heavy weed infestation during ripening.
- The LAI-2000 meter's measurement design, which is based on a radiation interception method involving all elements of a vegetation canopy's architecture (Chapter 5.2.1.2), such as green leaves, litter, ears and beards, tends to overestimate LAI of a crop stand mainly towards the end of a vegetation period [131]. The canopy closure of winter barley is denser than the one of spring wheat with no beards.

As a consequence, LAI readings of winter barley taken in the field towards the end of the phenological cycle, stay more or less constant around a value of LAI = 2, despite the plants' progressing senescence.

It can be seen from Tab. 6.2 and Tab. 6.3 that the *growing phase* of both spring wheat and winter barley is best described by a joint data set of both cultivars over the whole cropping cycle. Its regression coefficients for LAI

estimation can be used for both cultivars. The *senescing phase* of both spring wheat and winter barley is best described by a joint data set of both cultivars over the *senescing phase*. Especially LAI estimates in the *senescing phase* are more accurate under the absence of data from the *growing phase*.

The fitted relations between WDVI values and measured LAI values are given in Fig. 6.1 for spring wheat (left) and winter barley (right), both for the growing and the senescing phase. They are based on the best suited data sets for the determination of the regression coefficients, as listed in Tab. 6.2 and Tab. 6.3. The regression coefficients used by Eq. 4.11 are given in Tab. 6.4.

Table 6.4 Fitted regression coefficients used by Eq. 4.11 for LAI estimation of spring wheat and winter barley during the *growing* and *senescing phase*, as derived from the best suited data sets for regression coefficient determination, given in Tab. 6.2 and Tab. 6.3.

Cultivars of LAI Estimation	α	$\rho_\infty(\lambda_{NIR})$
Spring wheat growing phase Winter barley growing phase	0.106	127.193
Spring wheat senescing phase Winter barley senescing phase	0.082	141.224

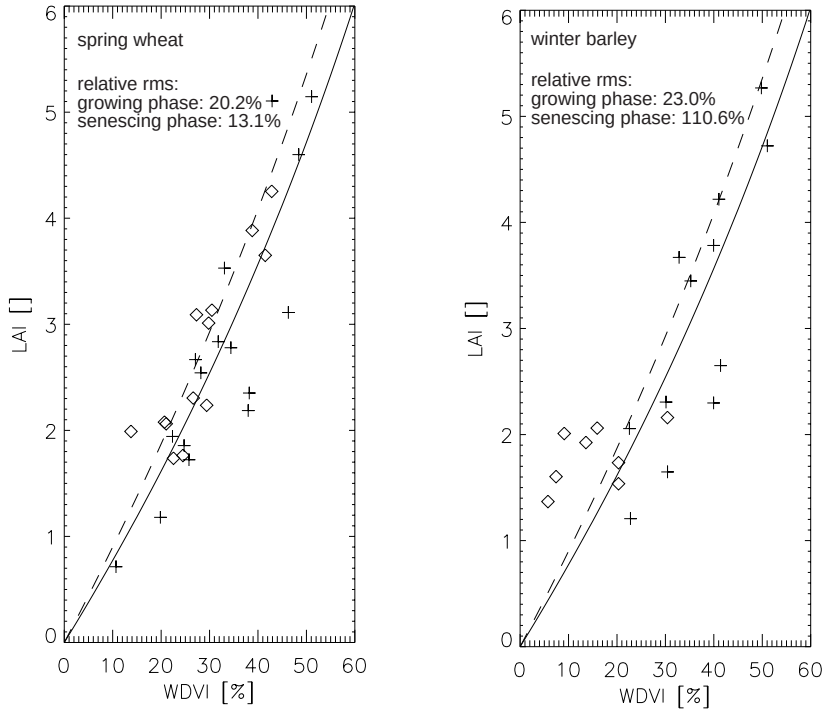

Figure 6.1 Fitted relations between WDVI and LAI for spring wheat (left) and winter barley (right). The solid line represents the exponential fit for the *growing phase*, the dashed line for the *senescing phase*. Crosses denote WDVI values and corresponding measured LAI of the *growing phase*, rhombs WDVI values and measured LAI of the *senescing phase*.

The correlation analysis between measured and calculated LAI values, as given in Fig. 6.2 results in a a correlation coefficient of $r = 0.83$ for the *growing phase* of both spring wheat and winter barley. The correlation coefficient for the *senescing phase* is $r = 0.92$ for spring wheat and $r = 0.5$ for winter barley. The analysis is performed using the LAI data of Fig. 6.1.

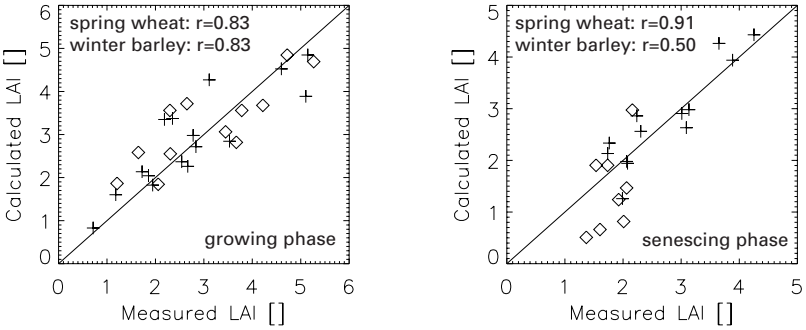

Figure 6.2 Correlation analysis between measured and calculated LAI values of spring wheat (crosses) and winter barley (rhombs) for the *growing* (left) and *senescing phase* (right) of both cultivars.

The calculated LAI values from mean spectral data of the observed phenological stages can be seen in Fig. 6.3. The calculations are based on the regression coefficients of Tab. 6.4. The figure shows mean values of LAI data derived from all available spectral data per measurement day (Chapter 5.2). Therefore, the calculated LAI data represents a mean LAI per cultivar and day of observation.

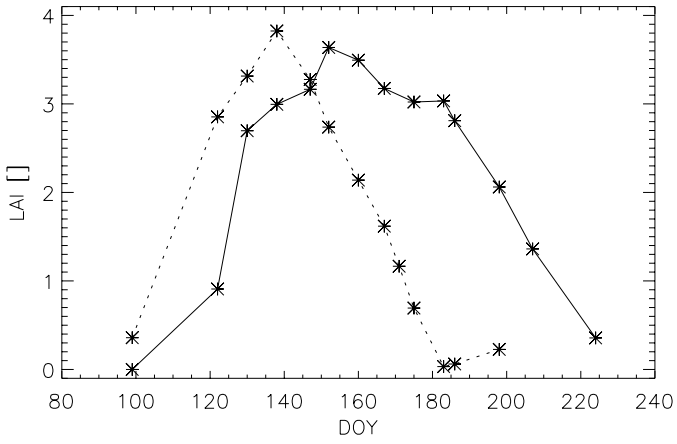

Figure 6.3 Mean calculated LAI of spring wheat (solid line) and winter barley (dotted line) over the observed phenological period. Since the calculation is based on mean spectral data per measurement day, the LAI data represents mean values per cultivar and measurement day.

As mentioned earlier in this chapter, the best results for LAI estimation during the *growing phase* of both cultivars are obtained using a joint data set of both crops over the whole cropping cycle in order to determine the regression coefficients of Tab. 6.4. The LAI determination in the *senescing phase*, however, is best performed using the regression coefficients calculated only for the *senescing phase* of both cultivars. The variations in LAI estimation to be expected when applying the regression coefficients determined from data of the whole cropping cycle to the *senescing phase* on the one hand, and the regression coefficients of the *senescing phase* to the data of the *growing phase*, on the other hand, can be seen in Fig. 6.4.

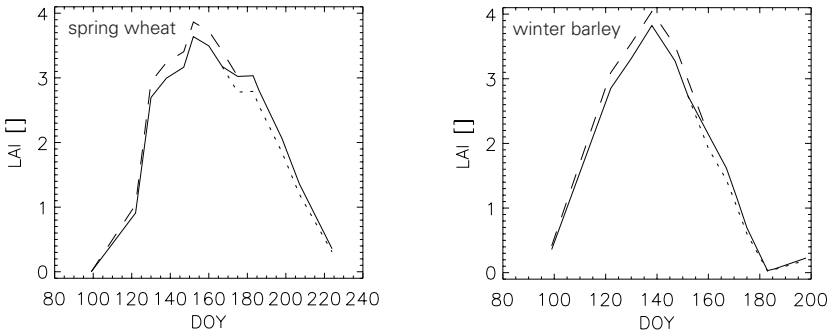

Figure 6.4 Variations of LAI estimations to be expected when applying the regression coefficients of the whole cropping cycle to the *senescing phase* (dotted line), and the ones of the *senescing phase* to the *growing phase* (dashed line) for spring wheat (left) and winter barley (right). The solid line represents the optimal use of the determined regression coefficients in Tab. 6.4.

6.2.3 Comparison of the WDVI Approach to the Use of Uncorrected NIR Data

The *weighted difference vegetation index* (WDVI) is reported to successfully correct for soil background influences mainly during the early and late stages of plant development, when canopy closure is low. To assess the errors to be expected when correlating LAI values to near-infrared reflectances (870 nm) without applying the WDVI correction, both an inverse exponential and a linear relation are fitted to a joint data set of spring wheat and winter barley during the *growing phase*. These results are given in Fig. 6.5, together with the fitted relation for LAI calculation from WDVI, based on the regression coefficients of Tab. 6.4. Contrary to the case of WDVI (left), where the regression curve passes through the origin, an offset a_0 is assumed in the case of the inverse exponential function for LAI calculation from near-infared reflectances (middle). By definition, WDVI = 0 denotes the absence of any

vegetation, whereas in the case of LAI calculation from near-infrared reflectances, an LAI value of zero does not require a NIR reflectance value of zero, because of the influence of the non-corrected background signal.

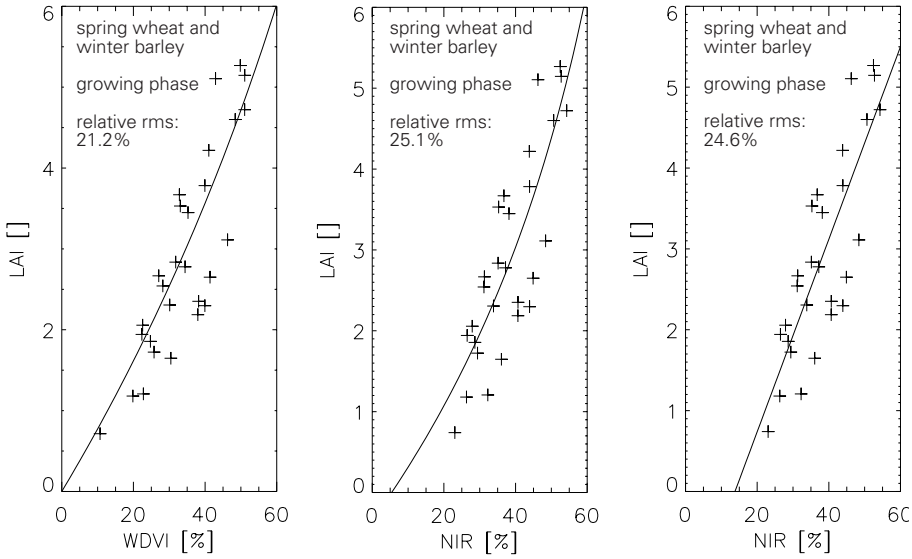

Figure 6.5 Fitted relation between WDVI and LAI, based on the inverse exponential function of Eq. 4.11 and the best found regression coefficients of Tab. 6.4 (left), between an uncorrected NIR reflectance and LAI, based on an inverse exponential function with offset (middle) and between an uncorrected NIR reflectance and LAI, based on a linear assumption (right), for a joint data set of spring wheat and winter barley during the growing phase.

Determination of LAI, as presented in Fig. 6.5, results in lowest relative rms errors when performed on WDVI data. The rms errors of both the inverse exponential and the linear approach for LAI determination from uncorrected NIR data are 3-4% higher, confirming the necessity of a background correction to be applied to low closure canopy data.

6.2.4 Comments on the Use of an LAI-2000 Plant Canopy Analyzer

The technical design of the LAI-2000 Plant Canopy Analyzer, that was used in this work for LAI determination of the observed cultivars, is addressed in Chapter 5.2.1.2. The fact, that the instrument determines LAI from canopy gap

fraction measurements performed by detectors arranged in five concentric rings that record radiation below 490 nm in a different range of angles, has the following main implications on the resulting LAI value:

- Direct sunlight increases canopy scattering processes and, as a consequence, below canopy readings of incident radiation. Readings which are performed on vegetation that is directly illuminated, can result in a 10-50% reduction of LAI [131]. However, the acquisition of a number of additional vegetation parameters and spectral data depends on direct solar irradiation. As a consequence, performing LAI measurements at low solar zenith angles is most often the compromise chosen on a typical measurement day.
- LAI readings vary significantly during the day, due to changes in solar zenith and the relative azimuth angle between the sun and the crop rows' direction. These variations are much larger than the ones caused by leaf angle changes of the plant during the day. Fig. 6.6 shows the variations in LAI, measured in an experiment on June 21st 2001, on a winter barley field. Sky conditions were clear. A set of five individual LAI measurements, acquired every 30 minutes at a predefined location within the field, is averaged for a time of five hours prior and four hours after solar noon (08.30-15.30 UTC). First, it can be seen that LAI values strongly decrease towards solar noon and increase again, afterwards. Second, the influence of rows is clearly visible. Minimum LAI is not measured around solar noon, but approximately half an hour later, when the solar azimuth and the azimuth of the crop rows coincide and maximum direct radiation reaches the canopy floor. Comparable LAI measurements under clear sky conditions should therefore be acquired at low zenith angles and equal sun-row geometry, preferably at large relative azimuth angles between the sun's and the rows' direction. The use of a sensor view cap to prevent possible reflections of the sun, is recommended.

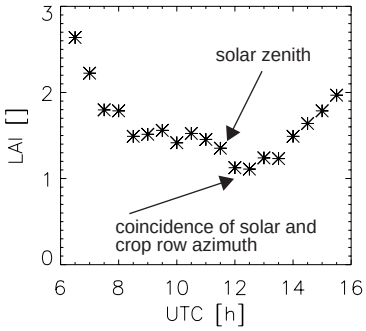

Figure 6.6 LAI readings performed every 30 minutes on a winter barley field at a predefined location in the field. They differ significantly with solar- and crop row geometry.

- The amount of canopy gap fraction measured by an LAI-2000 meter is not only determined by green leaves, but also by standing litter material, stems and ears. Light interception by non-photosynthetic components of a canopy increases during the *reproductive phase*. As a consequence, the green leaf area index, most often referred to as an indicator of forthcoming crop yield and vitality, becomes more and more a foliage index or a non-photosynthetic vegetation index (NPVI). As far as the green LAI during *senescence* is concerned, it is most likely overestimated when using an LAI-2000 meter. Studies performed by Clevers [29] result in curves describing the inverse exponential relation between WDVI and LAI (Chapter 6.2.2) during the *senescing phase*, that lie 'below' the curves of the *growing phase*, which is contrary to the findings of this work (Fig. 6.1). This can be explained by the fact that Clevers determined LAI by harvesting the plants of a small section and separating the whole sample into green and yellow leaves, stems and ears. Only the area of the green leaves was then measured by using an optically scanning area meter. Unless the readings of an LAI-2000 meter are understood as a foliage index or, to be more precise, a mixture of leaf- and non-photosynthetic vegetation index (NPVI), a correction of the data should be applied during the *senescing phase* in order to receive green LAI. However, it would be necessary to determine the parameters of a correction function from empirical data gathered for the main phenological stages.
  Effects of plant canopy architecture, as well as sun and row geometry equally apply to ceptometer readings for FAPAR acquisition, to be

performed under clear sky conditions. Standing litter material is believed to cause the constantly high FAPAR values of the *senescing phase* by preventing incoming radiation from reaching the canopy floor (Fig. 5.8, Fig. 5.9).

6.2.5 Conclusions on LAI Determination

Determination of LAI performs best when treating *growing* and *senescing phase* separately. During the *growing phase*, LAI determination can be performed at relative rms errors around 20% for both spring wheat and winter barley. High rms errors can occurr during *senescence*, due to weed infestation and the LAI-2000 meter's measurement design. Using the semi-empirical approach proposed by Clevers [27][28], that applies a background correction to the reflectance of the combined canopy-soil composite results in lower rms errors, compared to approaches with uncorrected data. LAI data, which shows large variations over a cropping cycle, is a key parameter to track phenology, especially during the *vegetative* and *generative phase*.

6.3 Results of FAPAR Determination

An exponential relation relating LAI values to FAPAR, as described in Chapter 4.3 on page 43, is used to determine the regression coefficients of Eq. 4.15. The regression curves between calculated LAI values (Chapter 6.2) and measured FAPAR values are given in Fig. 6.7 for spring wheat, winter barley and a joint data set of the two cultivars. The FAPAR reading of 0.41, in combination with a calculated LAI of 0.1 for winter barley, situated at the left border of Fig. 6.7, was not used for regression calculation, since it is not representative due to heavy weed infestation during the *ripening* stages of winter barley. FAPAR estimation from calculated LAI values can be performed at a mean relative rms error of 8.2% for spring wheat, 5.0% for winter barley and 8.2% for a joint data set of spring wheat and winter barley.

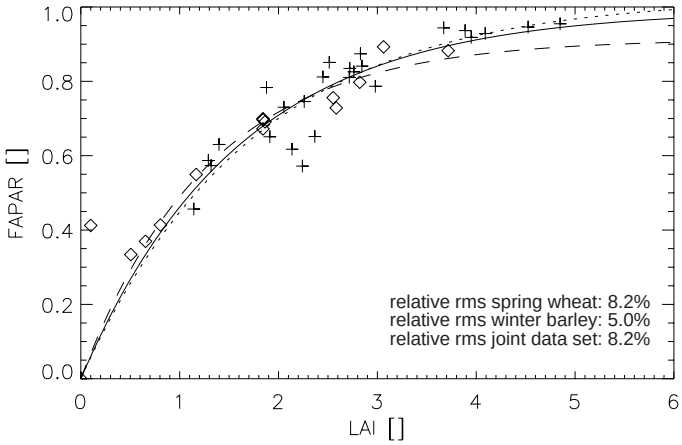

Figure 6.7 Fitted relations between calculated LAI values and measured FAPAR values for spring wheat (crosses, dotted line), winter barley (rhombs, dashed line) and a joint data set of both cultivars (solid line).

The fitted regression coefficients for Eq. 4.15 are given in Tab. 6.5.

Table 6.5 Fitted regression coefficients used by Eq. 4.15 for FAPAR estimation of spring wheat, winter barley and a joint data set of the two cultivars, based on calculated LAI values of Fig. 6.1 and measured FAPAR data. The parameter b_1 is kept constant [8].

Cultivar of FAPAR Estimation	b_0	b_1	b_2
Spring wheat	0.574	1.0	1.026
Winter barley	0.768	1.0	0.914
Spring wheat and winter barley	0.626	1.0	0.993

The correlation coefficients between measured and calculated FAPAR data are $r = 0.96$ for spring wheat, $r = 0.99$ for winter barley and $r = 0.96$ for the joint data set of both crops. Fig. 6.8 illustrates the correlation analysis for the case of FAPAR calculation based on the regression coefficients of the joint data set.

Mean values of FAPAR, both for spring wheat and winter barley, are calculated from mean spectral data of the observed phenological stages and illustrated in Fig. 6.9. The calculations are based on the crop stands' respective regression coefficients of Tab. 6.5.

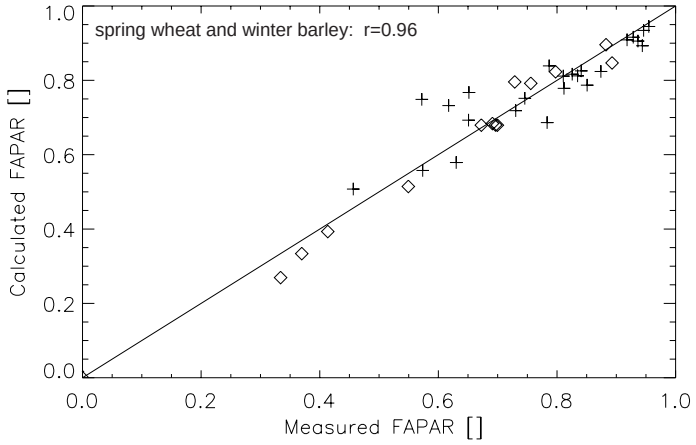

Figure 6.8 Correlation analysis between measured and calculated FAPAR values of spring wheat (crosses) and winter barley (rhombs) based on the regression coefficients of the joint data set of both cultivars.

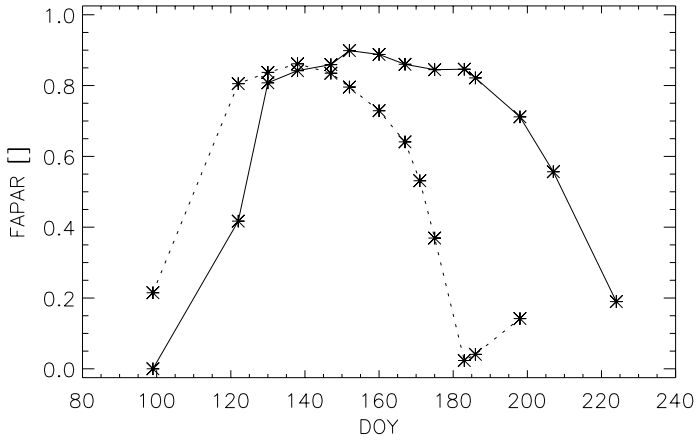

Figure 6.9 Mean calculated FAPAR of spring wheat (solid line) and winter barley (dotted line) over the observed phenological period. Since the calculation is based on mean spectral data per measurement day, the FAPAR data represents mean values per cultivar and measurement day. The data is calculated using the crop stands' respective regression coefficients of Tab. 6.5.

Since FAPAR calculation is based on previously determined LAI values derived from spectral data, variations in LAI, as a result of the use of non-optimal regression coefficients, as illustrated in Fig. 6.4, have an impact on FAPAR determination. Fig. 6.10 illustrates the variations of FAPAR, when regression coefficients of the whole cropping cycle are applied to the *senescing phase*, and coefficients of the *senescing phase* are applied to the *growing phase*, respectively, to calculate LAI.

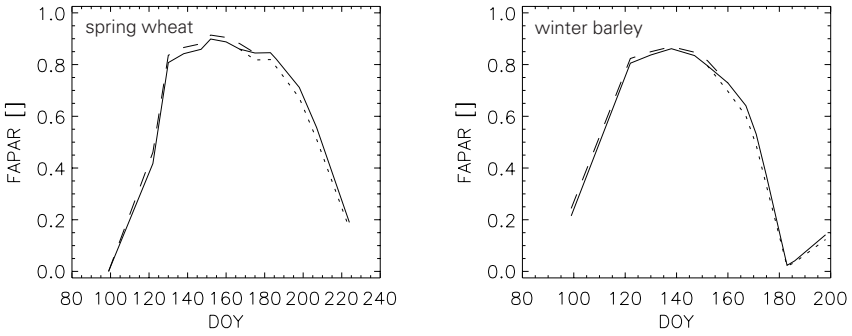

Figure 6.10 Variations of FAPAR values to be expected when estimating FAPAR from calculated LAI data using non-optimal regression coefficients for the *growing* (dashed line) and *senescing phase* (dotted line), as illustrated in Fig. 6.4. The solid line shows FAPAR values based on LAI data calculated by using the optimal regression coefficients for the *growing* and *senescing phases*, given in Tab. 6.4.

6.3.1 Conclusions on FAPAR Determination

Determination of FAPAR from LAI can be performed at a relative rms error around 8% for a joint cultivar of spring wheat and winter barley over a cropping cycle. During the senescing phase, FAPAR values are slightly overestimated due to the ceptometer's measurement design. FAPAR variations during a vegetation period allow phenological tracking of the observed cultivars. Since FAPAR is derived from LAI data, the two vegetation parameters contain highly correlated information.

6.4 Results of Chlorophyll Content Determination

The methods applied in this work for leaf chlorophyll estimation of spring wheat and winter barley from spectral data of the crop stands during the phenological stages observed are the *pigment specific simple ratio algorithm* (PSSR) and a ratio of TCARI and OSAVI, both explained in detail in Chapter 4.4. Originally, these methods were either applied to uniform canopies of bracken (PSSR), tested on simulated spectral data (ratio TCARI/OSAVI) or applied to spectral data of distinct phenological stages in order to detect chlorophyll variations within a field, but not from one phenological stage to another (ratio TCARI/OSAVI). The results of applying the two methods to spectral data of the observed spring wheat and winter barley fields, in order to track their leaf chlorophyll content during a whole cropping cycle, are discussed in this chapter.

6.4.1 Application of PSSR

The application of PSSR to the data of the observed crop fields shows strong variations of PSSR values with chlorophyll a and b content per unit leaf area. Nevertheless, the strong exponential relation between the reflectance ratios and chlorophyll concentrations, as described in literature [18], can not be found (Fig. 6.11). However, the curve's shape can be divided into two main parts, the first half belonging roughly to the *growing phase* with increasing PSSR values, and the second half dominated by the *senescing phase* with decreasing ratio values. This overall trend is clearly evident for winter barley (Fig. 6.11, right), whereas spring wheat shows small variations of chlorophyll a and b content from the stages of *pseudo stem erection* (DC 30) through *caryopsis water ripe* (DC 71), but large changes in PSSR values for the same period (Fig. 6.11, left).

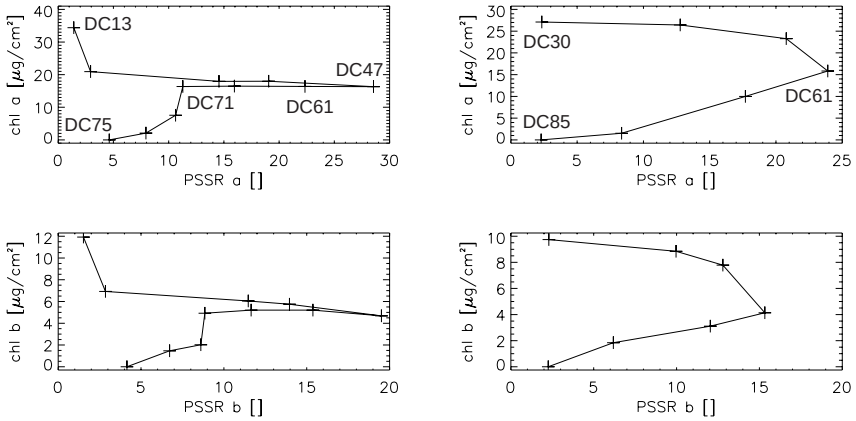

Figure 6.11 PSSR values and corresponding chlorophyll measurements per unit leaf area [µg cm^{-2}] for spring wheat (left) and winter barley (right) over the observed 1999 cropping cycle.

6.4.2 Application of the Ratio TCARI/OSAVI

The most consistent fits of the ratio TCARI/OSAVI and laboratory measured chlorophyll content reported in literature are obtained using logarithmic functions [61]. These results apply to data collected within fields of the same phenological stage. Application of the method to the data of the observed spring wheat and winter barley fields, as performed in Fig. 6.12, shows that the expected logarithmic functions can not be applied to the data of a whole vegetation period. At least for the data of the *senescing phase*, a trend towards a logarithmic relation between the spectral ratio and chlorophyll content may be assumed, since variations in plant physiology, that have a strong impact on canopy architecture, become weaker.

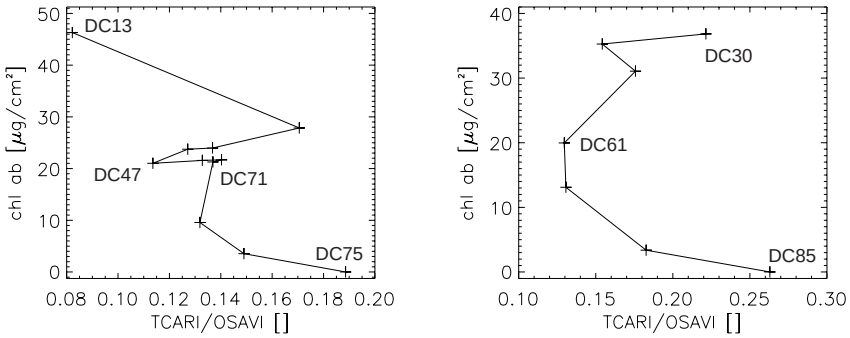

Figure 6.12 Values of the ratio TCARI/OSAVI and corresponding chlorophyll measurements per unit leaf area [µg cm^{-2}] for spring wheat (left) and winter barley (right) over the observed 1999 cropping cycle.

6.4.3 Investigation of the Main Chlorophyll a Absorption Feature

The use of PSSR and the ratio TCARI/OSAVI to track leaf chlorophyll content of spring wheat and winter barley over a wide range of phenological stages is not successful, as could be demonstrated in the preceding chapters. Both methods involve spectral data of the transitional region between the visible and the near-infrared part of the electromagnetic spectrum, where multiple scattering within the canopy becomes an important factor affecting reflectance. The main chlorophyll a absorption feature, located in this region around 675 nm, represents a reflectance minimum, above which the strong increase in reflectance, known as the red edge, occurs.

Scattering properties, that are linked to biomass (LAI), are reported to enhance a leaf-level signal [20][66]. However, beside the leaf chlorophyll content, multiple scattering within the canopy is responsible for a deepening and widening of the chlorophyll absorption feature, and the position of λ_{re}, the red edge inflection point (see Chapter 2.7.3 and Chapter 4.4).

An investigation of the width and the depth of the 675 nm chlorophyll a absorption feature is performed for mean spectra of all phenological stages observed, both for spring wheat (Fig. 6.13) and winter barley (Fig. 6.14). The analysis bases on the determination of the wavelength position of the maximum feature depth, which is calculated from continuum removal of the chlorophyll a absorption feature. It is then followed by the calculation of the feature width at the positions of the FWHM on both sides of the maximum absorption feature depth. As the abovementioned figures demonstrate, both feature width and feature depth increase during the *growing phase* of the two

cultivars, and decrease during the *senescing phase*.

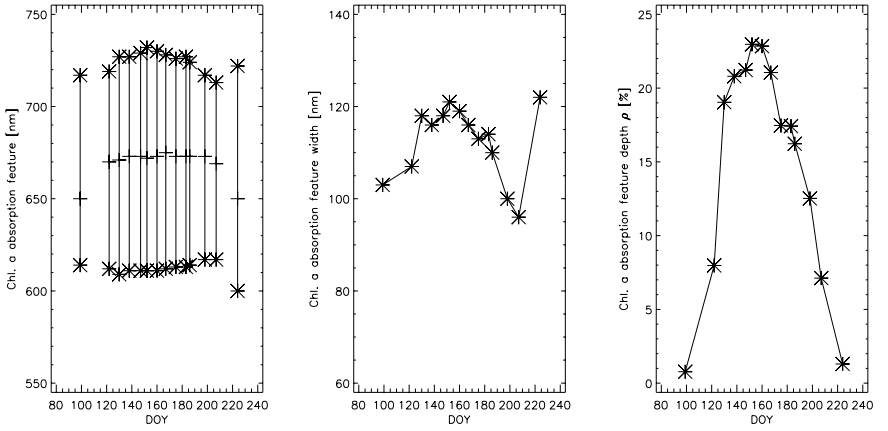

Figure 6.13 Range of chlorophyll a absorption feature (left), absorption feature width (middle) and absorption feature depth reflectance ρ (right) for spring wheat over the phenological stages observed. The feature width is defined by the wavelength positions of the FWHM on both sides of the wavelength of maximum absorption feature depth.

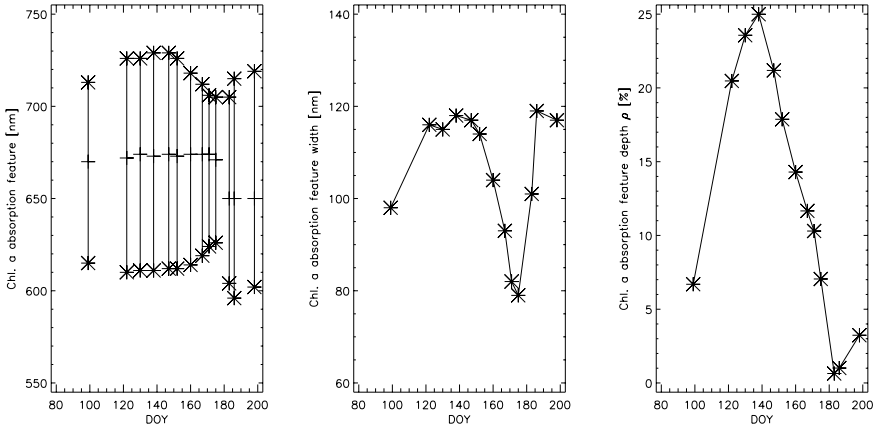

Figure 6.14 Range of chlorophyll a absorption feature (left), absorption feature width (middle) and absorption feature depth reflectance ρ (right) for winter barley over the phenological stages observed.

A comparison between the chlorophyll a absorption feature depth and the calculated LAI of each phenological stage (Chapter 6.2) is given in Fig. 6.15

for spring wheat and in Fig. 6.16 for winter barley. It can be seen that feature depth and LAI highly correlate throughout the season ($r = 0.98$ for spring wheat, $r = 0.99$ for winter barley). In addition, the curves of measured leaf chlorophyll values are shown in the abovementioned figures. Laboratory determined chlorophyll content per unit leaf area decreases from the early phenological stages, and does not follow the development of the chlorophyll a feature's absorption depth. While the position of maximum chlorophyll a absorption, the feature depth and the feature width all follow the shape of the LAI curve during the cropping cycle, the data values of measured leaf chlorophyll content follow a different trend. Therefore, it can be concluded, that the spectral response of a vegetation canopy around the main chlorophyll a absorption region, as seen by a remote sensing device, is predominantly driven by green biomass (green LAI), not chlorophyll. Since the observed crop stands undergo fundamental physiological changes within a whole vegetation period from *seedling growth* until *harvest*, chlorophyll estimation from remote sensing data using the transitional region between visible and near-infrared wavelengths is not successful. This fact confirms results by Filella and Peñuelas [51] and Yoder and Pettigrew-Cosby [136], who found it difficult to separate the effects of leaf chlorophyll and LAI on spectral data, when using remote sensing data. Methods of chlorophyll estimation from a remote sensing device, including the ones applied to the data of this work, may either work on canopy spectral data of a more or less uniform LAI or, in case the LAI and the canopy structure are not changing, when applied to plants over a range of phenological stages.

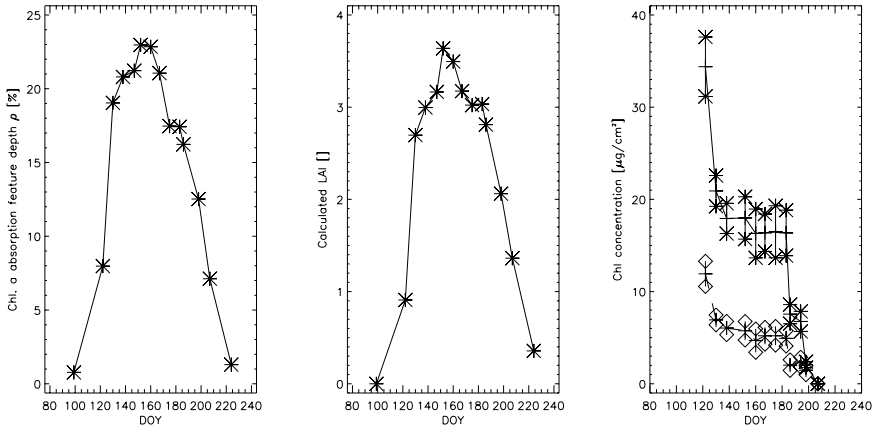

Figure 6.15 Chlorophyll a absorption feature depth ρ (left), calculated LAI (middle) and laboratory determined chlorophyll concentrations per unit leaf area [µg cm^{-2}].

(right) for spring wheat over the phenological stages observed.

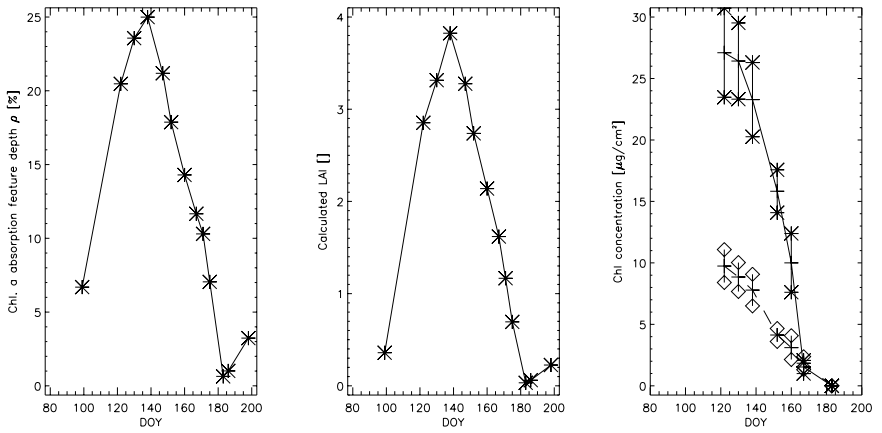

Figure 6.16 Chlorophyll a absorption feature depth ρ (left), calculated LAI (middle) and laboratory determined chlorophyll concentrations per unit leaf area [µg cm^{-2}] (right) for winter barley over the phenological stages observed.

6.4.4 Calibration of a SPAD-502 Leaf Chlorophyll Meter

Since the laboratory determination of leaf chlorophyll content is (a) time consuming, (b) not instantaneous, (c) destructive and (d) dependent on a range of equipment and techniques of organic extraction and spectrophotometric analysis, as described in Chapter 5.2.2, the use of a handheld chlorophyll meter bears the potential of fast determination of leaf chlorophyll content from a large number of individual measurements (c.f., Chapter 5.2.1.3). However, the optical properties of a leaf are dependent on its morphology (Chapter 2.7), making it necessary to relate the arbitrary units of the chlorophyll meter to laboratory measured leaf chlorophyll concentrations for individual cultivars. Wheat and barley both belong to the tribe *Triticae* of the family *Poaceae*. Therefore, their leaf optical properties are comparable. In the case of the observed spring wheat and winter barley fields of this work, a joint data set of both cultivars was used for the calibration of the SPAD-502 meter. As can be seen in Fig. 6.17, leaf chlorophyll concentration can be correlated to SPAD readings using an exponential or a second order polynomial relation, as proposed in literature. The regression coefficients of the two mathematical functions are given in Tab. 6.6. Correlation coefficients between measured

and calculated SPAD readings of $r = 0.93$ are found for both relations, being slightly weaker than the ones reported by Markwell et al. [94] for soybean and corn.

However, the average error to be expected when estimating leaf chlorophyll content from SPAD readings, expressed as relative rms error, is of greater interest for practical applications [37]. The rms errors calculated in this work are considerably high, being 58.5% for the exponential relation and 37.3% for the polynomial fit. No rms errors are reported by Markwell et al. [94] for their calibration functions.

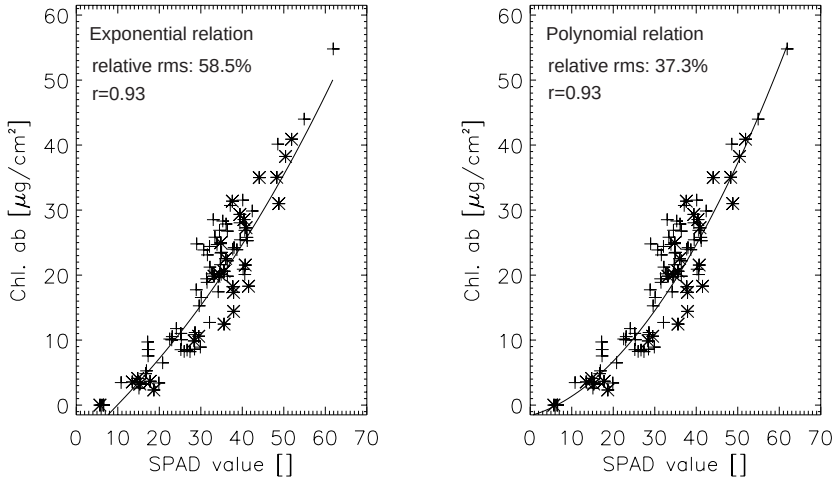

Figure 6.17 Exponential (left) and polynomial (right) relation (Tab. 6.6) between measured SPAD-502 meter values and laboratory determined chlorophyll a,b concentrations per unit leaf area for a joint data set of spring wheat (crosses) and winter barley (stars) over the phenological stages observed.

It is obvious from Fig. 6.17, that the SPAD measurements are relatively insensitive to variations in total leaf chlorophyll content between approximately 10-30 µg cm^{-2}, both for spring wheat and winter barley. Therefore, the high rms errors mainly apply to the *generative phase* of crop

development, when SPAD readings lie between values of 30 and 40.

Table 6.6 Fitted regression coefficients for the exponential relation (middle) and the polynomial relation (right) between SPAD-502 meter values and laboratory determined chlorophyll a,b concentrations per unit leaf area for a joint data set of spring wheat and winter barley over the phenological stages observed.

Regression Coefficient	Exponential Relation $y = a_0 + \exp(x^{a_1})$	Polynomial Relation $y = a_0 + a_1 \cdot x + a_2 \cdot x^2$
a_0	-8.878	-1.637
a_1	0.341	0.180
a_2	-	0.012

6.4.5 Conclusions on Chlorophyll Content Determination

The use of wavelengths ratios involving the visible and near-infrared spectral region is not successful in tracking leaf chlorophyll content over a cropping cycle. Canopy structural effects dominate a vegetation spectrum in the investigated spectral regions. The maximum chlorophyll a absorption feature depth of a vegetation canopy spectrum around 675 nm highly correlates with LAI, when analyzed throughout the season. As a consequence, leaf chlorophyll content can not be used to track plant phenology using the applied methods.

6.5 Results of Water Content Determination

As pointed out in Chapter 2.7.3 and Chapter 4.5, the spectral response of a vegetation canopy is strongly influenced by structural effects of the crop stand. Therefore, methods of water content determination developed on single leaves under laboratory conditions do not necessarily work in case they are scaled up to whole canopies. Many techniques described in literature work on the leaf scale, others were applied to canopies at distinct phenological stages to retrieve variations in canopy water content. In this work, stepwise multiple linear regression, which is reported as successful for laboratory determination of chemical compounds of leaves, is applied to spectroradiometric data of the observed spring wheat and winter barley fields to evaluate its potential for tracking canopy water content over a whole phenological cycle.

6.5.1 Plant Water Content

Stepwise multiple linear regression is performed based on the resolution and center wavelength positions of the HyMap imaging spectrometer [31], as operated in 1999, to assess the suitability of a commonly operated airborne hyperspectral device for canopy water retrieval. Calculation of the bandwise correlation coefficient *r*, followed by first derivative analysis of *r*, as described in Chapter 4.5, is done for plant water content data of the phenological stages observed. The optimal number of wavelengths, the wavelength positions and the relative rms errors to be expected, are determined for spring wheat, winter barley and a joint data set of both cultivars. The results are compared to those of stepwise multiple linear regression performed on leaf water content data.

Fig. 6.18 (left) shows the bandwise correlation coefficient *r* between measured plant water content and field-measured mean spectral data at HyMap resolution for a joint data set of spring wheat and winter barley over the observed phenological stages. It is obvious, that the curve's shape strongly resembles a spectrum of green vegetation, thus emphasizing the potential of plant water as a main indicator of plant vitality. However, it must be considered, that not all wavelengths of high correlation coefficients are casually related to water content, but indirectly to other biochemical or biophysical variables like chlorophyll or, on the canopy level, canopy greenness, which themselves are an indicator of plant vitality. Nevertheless, these indirectly related wavelengths also bear the potential of parameter estimation [37]. First derivative analysis of the correlation coefficient *r*, as given in Fig. 6.18 (right), calculates zero-crossing wavelengths. They are then sorted by their corresponding correlation value *r* for subsequent use by multiple regression analysis (Tab. 6.7). Wavelengths above 1800 nm are excluded from regression analysis because of distortion by occurring broad atmospheric water vapor absorption bands and low at-sensor radiances in this part of the electromagnetic spectrum.

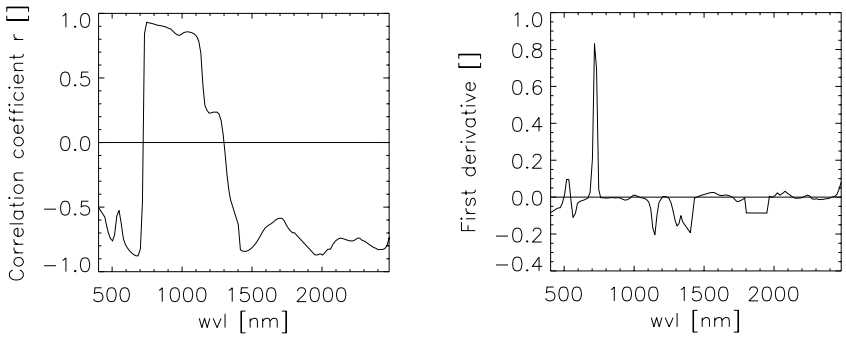

Figure 6.18 Bandwise correlation coefficient *r* between measured plant water content and mean spectral data at HyMap resolution for a joint data set of spring wheat and winter barley over a whole vegetation period (left) and first derivative analysis of the correlation coefficient *r* for the same data set (right).

It can be seen in Tab. 6.7 from ground spectroradiometric data being convolved to HyMap resolution, that predictive wavebands determined by first derivative analysis are either located (a) in the green region of the electromagnetic spectrum, (b) around the red edge or at its inflection point or (c) in a number of regions associated with leaf water absorption, as discussed in Chapter 2.7.2. Some wavelengths can be found in the first derivative analysis of all three data sets (e.g. 1444.0 nm, requiring an accurate atmospheric correction of imaging spectrometer data), others differ slightly in the band position of the sensor, but still denote the same feature within a certain wavelength range (e.g. chlorophyll a absorption region, red edge, 975 nm and 1175 nm water absorption range). Regardless of whether the selected wavelengths are casually or indirectly related to plant water content, they are entered into stepwise multiple linear regression analysis, as given by Eq. 4.19, according to the descending order of Tab. 6.7.

Table 6.7 Zero-crossing wavelengths at HyMap resolution, determined by first derivative analysis of spectral data and plant water content, and their corresponding correlation coefficients *r* for spring wheat, winter barley and a joint data set of both cultivars over the observed phenological stages.

Spring Wheat		Winter Barley		Spring Wheat, Winter Barley	
Wavelength [nm]	Correlation coefficent r []	Wavelength [nm]	Correlation coefficient r []	Wavelength [nm]	Correlation coefficient r []
791.900[b1)]	0.97	777.400[b]	0.94	746.575[b]	0.93
746.575[b]	0.97	670.800[b]	-0.91	685.419[b]	-0.88
777.400[b]	0.97	1444.900[c]	-0.91	1043.500[c]	0.86
670.800[b]	-0.96	1058.510[c]	0.86	1444.900[c]	-0.84
996.300[c2)]	0.96	996.300[c]	0.79	965.394[c]	0.83
918.400[c]	0.96	502.800[a]	-0.78	502.800[a]	-0.76
1118.900[c]	0.95	1706.390[c]	-0.65	1694.200[c]	-0.59
1444.900[c]	-0.94	533.406[a]	-0.56	533.406[a]	-0.57
1073.510[c]	0.94	1235.700[c]	0.16	1235.700[c]	0.24
486.800[a3)]	-0.89	1207.000[c]	0.15	1207.000[c]	0.23
1694.200[c]	-0.77				
533.406[a]	-0.72				

1) Wavelength around the red edge or at its inflection point
2) Wavelength associated with a leaf water absorption region
3) Wavelength in the green region of the electromagnetic spectrum

The resulting number n of selected regressor wavelengths λ_i, together with their coefficients a_i are given in Tab. 6.8. The relative rms error of the verification data set as calculated is 7.7% for spring wheat, 3.1% for winter barley and 6.7% for the joint data set of both cultivars.

Table 6.8 Number n of selected regressor wavelengths $\lambda_{i=1,n}$ and corresponding regression coefficients $a_{i=0,n}$ of the stepwise multiple linear regression of spectral data and plant water content of spring wheat, winter barley and a joint data set of both cultivars over the phenological stages observed.

Spring Wheat n=3		Winter Barley n=4		Spring Wheat, Winter Barley n=3	
$\lambda_{i=1,n}$	$a_{i=0,n}$	$\lambda_{i=1,n}$	$a_{i=0,n}$	$\lambda_{i=1,n}$	$a_{i=0,n}$
	-59.801		78.548		37.676
791.900	701.556	777.400	498.663	746.575	433.958
746.575	316.164	670.800	200.645	685.419	-141.029
777.400	-623.393	1444.900	-282.846	1043.500	-250.372
		1058.510	-444.271		

Measured and calculated plant water content values, based on the equation parameters of spring wheat and winter barley of Tab. 6.8 are given in Fig. 6.19. The relative rms error indicated is calculated from a verification data set of randomly selected plant water content data that is not used for calibration of the regression model.

Contrary to winter barley, the regressor wavelengths of spring wheat, determined for plant water content calculation, lie within a very small spectral range. As a consequence, the inter-correlation between the three HyMap wavebands is high. An investigation using simple linear regression based on the highest correlating wavelength of spring wheat in Tab. 6.8 (791.9 nm) resulted in an rms error of 7.9%, being only slightly higher than in the case of using three regressor wavelengths. Therefore, plant water determination of spring wheat over the observed phenological stages could well be performed using simple linear regression with $\lambda_1 = 791.9\,\text{nm}$, $a_0 = -44.0396$ and $a_1 = 312.996$.

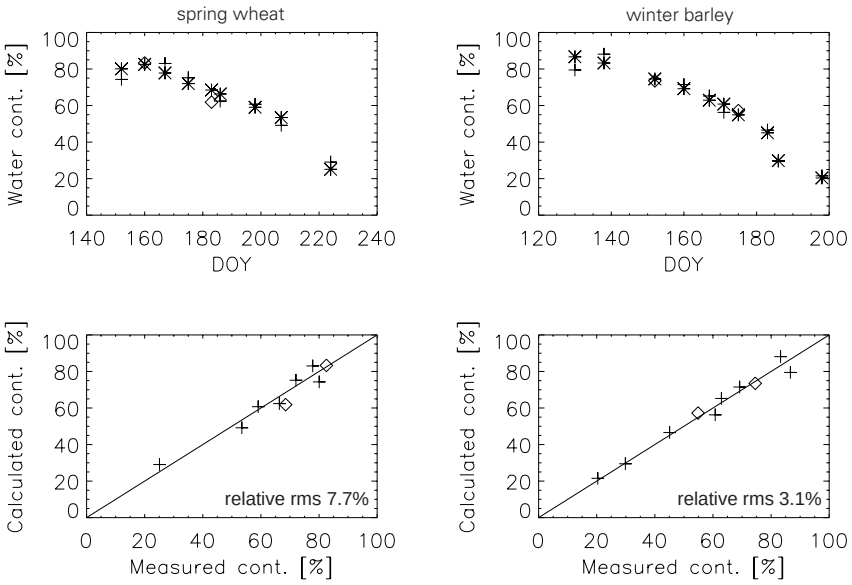

Figure 6.19 Determination of plant water content of spring wheat (left) and winter barley (right) using stepwise multiple linear regression. Asterisks denote plant water content as measured in the laboratory, crosses are calculated water content values from the calibration set of the multiple regression and rhombs are water content values calculated for validation of the regression equation.

A relative rms error of 6.7% is calculated for the verification data when a joint data set of spring wheat and winter barley is used to determine the

number n of wavelengths and the coefficients a_i of the multiple linear regression over the vegetation period observed. As demonstrated by Fig. 6.20, it is possible to use the same regression model (Tab. 6.8, right) for plant water content determination of both spring wheat and winter barley.

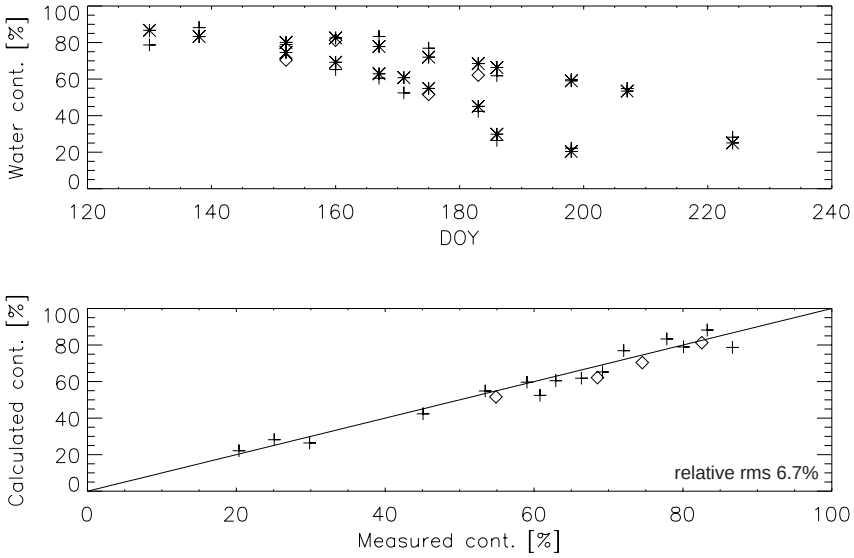

Figure 6.20 Determination of plant water content of a joint data set of spring wheat and winter barley using stepwise multiple linear regression. Asterisks denote plant water content as measured in the laboratory, crosses are calculated water content values from the calibration set of the multiple regression and rhombs are water content values calculated for validation of the regression equation.

The application of stepwise multiple linear regression to normalized band depths calculated from continuum removed, band normalized reflectance spectra, as proposed by Kokaly and Clark [78], calculates plant water content at rms errors almost similar to the ones obtained by regression analysis with absolute reflectance data. They are 7.6% for spring wheat, 3.5% for winter barley and 6.5% for a joint data set of both cultivars. Stepwise multiple linear regression selects an optimal number of two regressor wavelengths for spring wheat, and three regressor wavelengths for both winter barley and the joint data set.

Fig. 6.21 demonstrates continuum removal for a mean spectrum of spring wheat, measured in the field on May 2nd 1999. The spectral region between the green peak (around 550 nm) and the reflectance maximum around 1700 nm of the electromagnetic spectrum is used at HyMap resolution. The

continuum is a convex hull being fitted to the top of the spectrum. Normalized band depths are calculated from feature depth reflectance by dividing the band depth of each wavelength band by the band depth at the corresponding band center. The center is defined as the maximum feature depth of the continuum removed absorption feature.

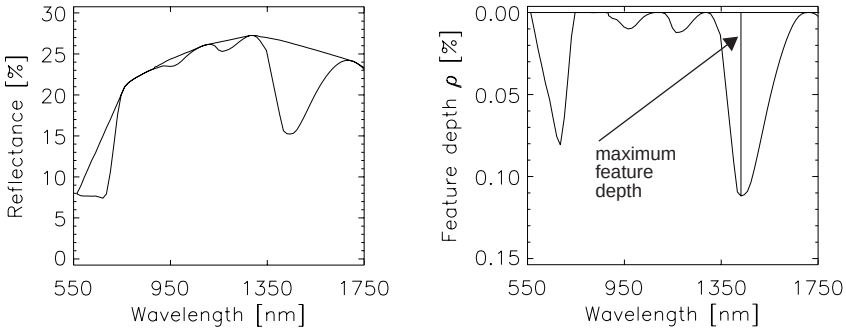

Figure 6.21 Calculation of feature depth reflectance (right), which is used for band depth normalization, as performed for an example of mean spectral data (HyMap resolution) of spring wheat of May 2nd 1999 (left).

The fact, that stepwise multiple linear regression using absolute reflectance data on the one hand, and continuum removed, band normalized data on the other hand, lead to almost similar accuracies, as shown in this chapter, favourites the use of the simpler approach based on absolute reflectance data as input to multiple linear regression for plant water retrieval.

6.5.2 Leaf Water Content

A comparison of the accuracies of both plant water content and leaf water content determination from absolute reflectance data shows considerably higher rms errors for the case of leaf water retrieval. Canopy structural effects are the dominating factor of a crop stand's spectral response, as measured by a remote sensing device. Thus, the optical properties of a vegetation canopy differ from those of single leaves. The rms errors obtained for leaf water retrieval from absolute reflectance data are 17.7% for spring wheat (using one wavelength), 56.4% for winter barley (using one wavelength) and 15.4% for the joint data set (using five wavelengths). The large rms error calculated in the case of winter barley is the result of this crop stand's architecture: from the beginning of the *reproductive phase* of winter barley, no leaves are visible any more from nadir view. The canopy closure is dense because of the ears and

beards which tend to incline towards a horizontal orientation, unlike the ears of spring wheat, which are smaller, unbearded and vertically aligned, allowing the leaves to be seen from nadir during the whole phenological cycle. Hence, correlations between spectral data and water content of winter barley represent mainly plant and grain water status, not leaf water. The use of a joint data set of both cultivars, which significantly improves the accuracy of the regression, reduces the spectral dominance of the winter barley canopy (especially ears and beards) within the data set, because the spectral data of spring wheat still contains leaf level information visible to the sensor.

6.5.3 Grain Water Content

Grain water content is an important parameter in agronomy, since the main stages of the *reproductive phase* are defined by the mean moisture content of the grain. In addition, a grain water content of 15% is ideal for harvest, as the grain needs no further artificial drying to make it tenable. Therefore, the determination of grain moisture from a remote sensing device is of practical use and relevance. After maximum grain-fill, at which grain moisture content is approximately 45%, ripening (physical drying) is no longer controlled by the potential evapotranspiration rate (PET), as it applies to a free water surface, but by the equilibration of the osmotic potential of the grain with the relative humidity of the atmosphere [109]. Precipitation leads to an increase in the moisture content of the grain. The amount of water to be lost from the grains is reported to be rather less than one day's PET. As a consequence, measurements of grain water content and the potential day of harvest are affected by rainfall on the previous day.

Fig. 6.22 shows the relation between plant water and grain water content for spring wheat and winter barley during the *reproductive phase*, consisting of *milk* and *dough development* (DC 70-79 and DC 80-89), and *ripening* (DC 90-99), as presented in Tab. 7.4. A strong linear relation between plant and grain water content is visible for spring wheat between *caryospsis water ripe* (DC 71) and *hard dough* (DC 87) and for winter barley between *caryopsis water ripe* (DC 71) and *caryopsis hard* (DC 92), when grain moisture content is ideal for harvest (<16%). Nevertheless, the linear relation is heavily disturbed in case of precipitation on the day before moisture content determination. The linear correlation coefficients r in Fig. 6.22, the equations for grain moisture content determination from plant water, and the corresponding rms errors are calculated from the part of the data, where the linear relation applies, because no rainfall was recorded on the days before.

Fig. 6.23 demonstrates, that grain water content of spring wheat and winter barley must be calculated separately. A joint use of the data would result in an

rms error of 33.1%. The drying process of the larger, bearded winter barley ears is slower than in the case of spring wheat.

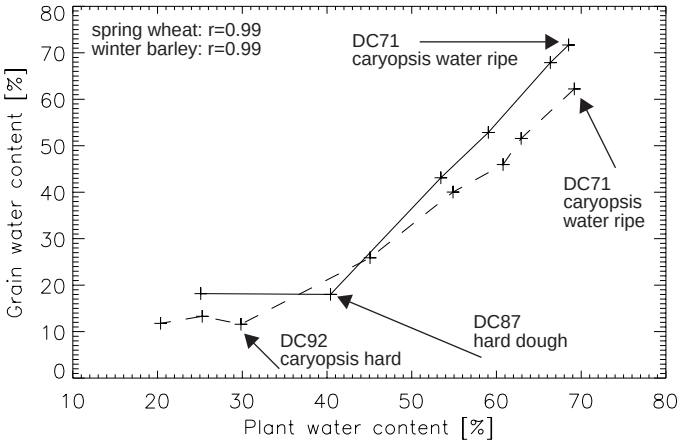

Figure 6.22 The relation between plant water content and grain water content of spring wheat (solid line) and winter barley (dashed line) during the reproductive phase is strongly linear under the absence of precipitation.

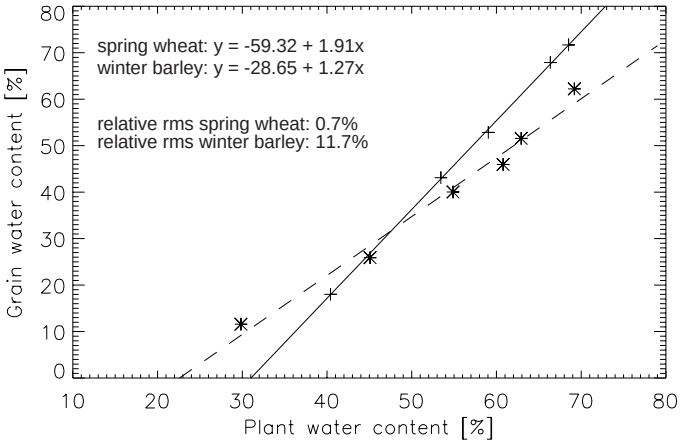

Figure 6.23 Linear regression between plant water content and grain water content for spring wheat (solid line) and winter barley (dashed line) during the reproductive phase. Grain water content determination of both cultivars must be performed separately.

6.5.4 Conclusions on Water Content Determination

Plant water content retrieval over a phenological cycle can be performed at relative rms errors between 3% and 8% for both separate and joint data sets of spring wheat and winter barley by using stepwise multiple linear regression analysis. Determination of leaf water content is less accurate due to different optical properties of a vegetation canopy, as seen by a remote sensing device, and a single leaf. Strong linear relations are found between plant and grain water content during the phenological stages of *caryopsis water ripe* (DC 71) and *caryopsis hard* (DC 92). Plant water content is considered the most promising vegetation parameter to be used for phenological studies.

6.6 Application to Imaging Spectroscopy Data

6.6.1 Context

Image based hyperspectral remote sensing data bears the potential of providing spatially distributed, timely information of a certain regional extent. In agricultural management, the timeliness of availability of key canopy characteristics is of great importance. As a consequence, the derivation of biophysical and biochemical parameters from hyperspectral imaging data favorites the use of remote sensing data, instead of conventional field sampling techniques (Chapter 1.2, Chapter 2.3).

One of the main goals of the field measurement campaign, that was carried out during the 1999 cropping cycle is the investigation of the potential of retrieving key vegetation parameters, that can be related to vitality and therefore phenological stages, from imaging spectroscopy data (Chapter 1.1). The feasibility and accuracies of the retrieval methods applied are discussed extensively, earlier in this chapter.

The semi-empirical approaches for LAI and FAPAR determination, as well as the statistical method of plant water retrieval from spectroscopy data (Chapter 4) are applied to the imaging spectroscopy data of the observed spring wheat and winter barley fields, acquired on July 16th 1999 by the HyMap airborne hyperspectral scanner. Since the tracking of chlorophyll over the plants' phenological development was not successful for the two cultivars (Chapter 6.4), no chlorophyll determination from the imaging data is performed. In addition, the method of plant water retrieval is applied to a subset of the HyMap [31] data set to demonstrate the potential of parameter retrieval at regional scale. The sensor covers the spectral range between 450-2500 nm and consists of 128 image channels.

6.6.2 HyMap Data of July 16th 1999

As mentioned in Chapter 5.3.5.2, the HyMap data take of July 16th 1999 took place one day prior to harvest of winter barley, which was *over-ripe* (DC 94). Spring wheat was at the phenological stage of *medium milk* (DC 75). Although parts of the Limpach valley were covered by scattered clouds at the time of data take (10.30 UTC), the two test fields were unaffected by both clouds and shadows. Determination of LAI, FAPAR and plant water content present in the two fields at the time of data take is performed as follows:

- LAI is calculated from spectral data based on the fitted regression coefficients α and $\rho_{\infty}(\lambda_{NIR})$ of the *senescing phase* of both cultivars, as given in Tab. 6.4.
- FAPAR is calculated from LAI based on the fitted regression coefficients b_0, b_1 and b_2 of a joint data set of both cultivars, as given in Tab. 6.5.
- Plant water content is calculated based on the regressor wavelengths $\lambda_{i = 1, n}$ and the corresponding regression coefficients $\lambda_{i = 0, n}$ determined by stepwise multiple linear regression for spring wheat and winter barley, as given in Tab. 6.8.

Fig. 6.24 and Fig. 6.25 show the spatial distribution of LAI, FAPAR and plant water content, as determined for winter barley and spring wheat during the overflight. In the case of spring wheat, the field can clearly be divided into a lower part of stronger variations of the observed parameters and a slightly elevated part which is much more uniform. These differences are in correspondence with soil variations within the field, as explained in Chapter 3.4. For both spring wheat and winter barley, the field's patterns of LAI and FAPAR are very much comparable since FAPAR is derived from LAI using an exponential relation. However, the pattern of plant water content shows the same trends in vitality, as can be found in the case of LAI and FAPAR, too. Hence, it can be concluded, that the applied methods of determination of both LAI (or FAPAR) and plant water content from spectral data lead to similar information on infield variations of vitality.

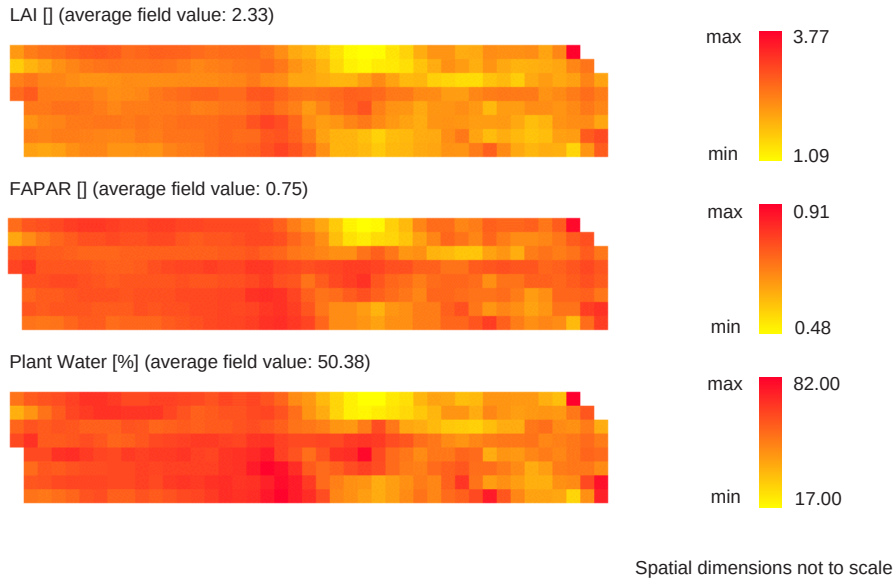

Figure 6.24 Determination of LAI, FAPAR and plant water content from HyMap data of July 16th 1999 for the spring wheat field.

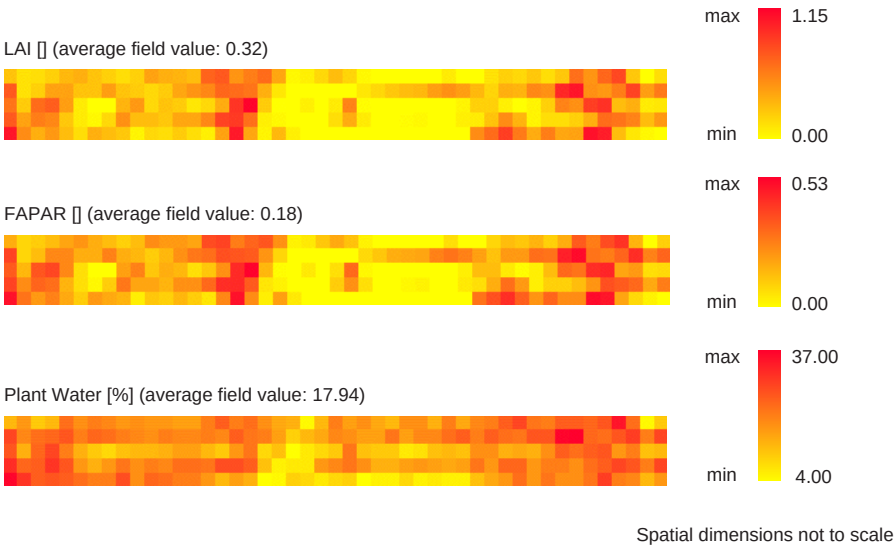

Figure 6.25 Determination of LAI, FAPAR and plant water content from HyMap data of July 16th 1999 for the winter barley field.

Mean field values of the three parameters, that are determined from imaging data, together with measured mean values acquired in the field one day after the overflight, are given in Tab. 6.9.

The comparison of spectral data acquired in the field and from an air- or spaceborne remote sensing device is not trivial. Insufficient correction of atmospheric effects due to limited knowledge on the atmosphere's actual state, view angle dependency of spectral data acquired by wide field-of-view sensors and scale dependency of objects under investigation [25] are the main reasons for differences between spectral data from field measurements and remotely sensed data. The correction of bidirectional effects in imaging spectrometer data has been addressed by Beisl [15]. The correction of such effects is important for a more accurate quantitative analysis of wide field-of-view hyperspectral data. It enables the comparison of data from different illumination- and viewing geometry.

In the case of the observed spring wheat and winter barley fields in the Limpach valley, no correction of bidirectional effects is applied to the data, since (a) the fields are situated close to nadir view, (b) they are of small extent, and (c) only one scene is used for parameter retrieval. However, a correction is assumed to improve accuracies when parameter retrieval methods are applied to whole scenes or subparts, as performed in Fig. 6.26.

Table 6.9 LAI, FAPAR and plant water content of the observed spring wheat and winter barley field, determined from spectral data of the HyMap imaging spectrometer and measured in the field, one day after the HyMap data take (July 17th 1999).

Retrieved Parameter	SpringWheat HyMap July 16th 1999	Spring Wheat Measured July 17th 1999	Winter Barley HyMap July 16th 1999	Winter Barley Measured July 17th 1999
LAI mean []	2.33	2.13	0.32	0.41
FAPAR mean []	0.75	0.78	0.18	-
Plant Water mean [%]	50.38	59.04	17.94	20.36

The application of plant water content determination from stepwise multiple linear regression using the regressor wavelengths and coefficients of a joint data set of both spring wheat and winter barley, as given in Tab. 6.8, is demonstrated in Fig. 6.26 for a subpart of the HyMap scene, that was recorded on July 16th 1999. The area under investigation is situated between Ober- and Unterramsern, in the central part of the Limpach valley. The two test fields can

be located in the data set. As can be seen from the true color composite, the wheat and barley fields are at the phenological stages between *milk development* and *ripening*. Some fields are already harvested. Green fields are mainly pasture land, corn and sugar beet. Plant water content determination from stepwise multiple linear regression is based on ground truth data of spring wheat and winter barley. It could be demonstrated in Chapter 6.5.1, that the data of both cultivars can be used as one data set in order to determine the regression wavelengths and corresponding regression coefficients. As a consequence, plant water content of both cultivars can be mapped simultaneously across the data set.

However, the regression equation does not apply to other agricultural fields, like pasture land, corn- or sugar beet fields, and forest. The applied method of plant water content retrieval is crop-type dependent, which is obvious for a range of other cultivars present in the subscene. Plant water content of black areas exceeds 100% and can be found in cultivars of corn, sugar beet and pasture land. As a consequence, regression equations should be developed for each cultivar over a cropping cycle in order to accurately retrieve its respective plant water content. Such a data base would be a prerequisite for crop-dependent plant water retrieval over a phenological period, based on a spectroscopy data set of pre-classified cultivars, in order to apply the corresponding retrieval equations from stepwise multiple linear regression analysis.

The same remarks also apply to the semi-empirical and empirical retrieval of LAI and FAPAR of different crop types over a vegetation period.

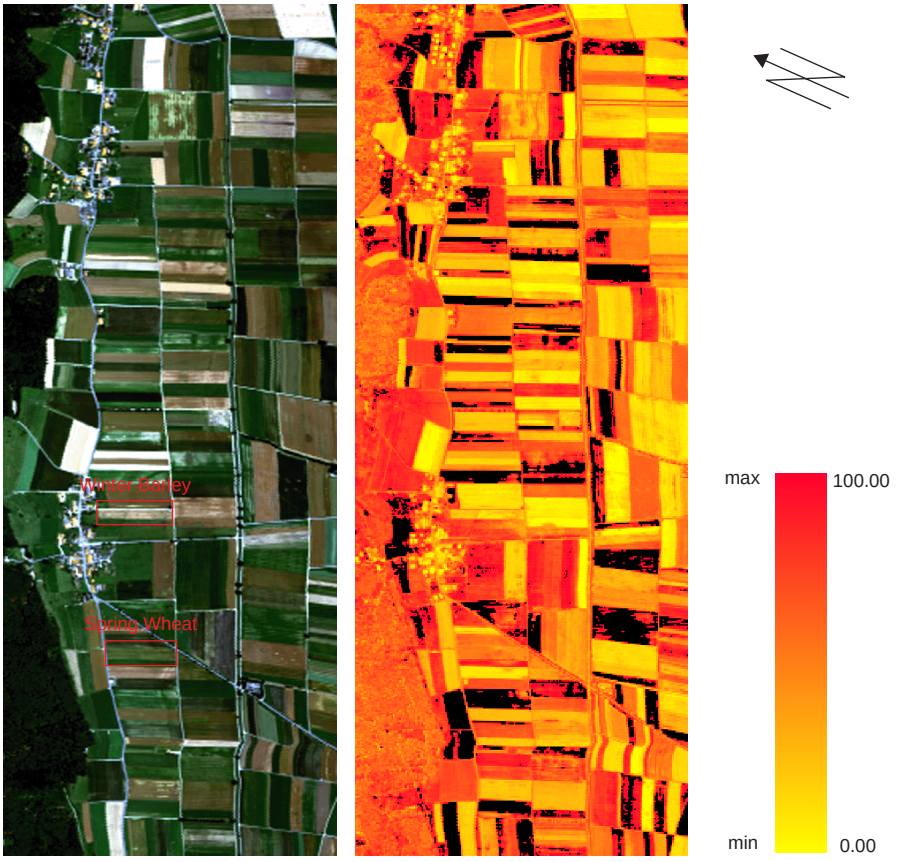

Figure 6.26 Partial HyMap scene (recorded July 16th, 1999) over the Limpach valley, near the village of Oberramsern. Left: True color composite showing the observed spring wheat and winter barley fields. Right: Result of plant water retrieval [%] from stepwise multiple linear regression, based on a joint data set of spring wheat and winter barley. Black areas denote plant water content values over 100%. They belong to agricultural crops other than cereals for which the used regressor wavelengths and coefficients do not apply (e.g., corn, sugar beet).

Chapter 7

Conclusions and Outlook

7.1 Conclusions

It has been the goal of this work to evaluate the potential of spectroscopy data for the retrieval of vitality-related biophysical and biochemical parameters from remote sensing data, that allow to track the main development stages of two cereals commonly grown in Switzerland. A methodology of data acquisition, characterization and processing has been developed. Information on crop growth status is important for agricultural purposes and the emerging needs of precision crop management. The methods applied for parameter retrieval from spectroradiometric data are empirical, semi-empirical and statistical ones. Conclusions are drawn on this work's main goal and its major methodological components as outlined in Chapter 1.

7.1.1 Selection of Vitality-Related Vegetation Parameters

A parameter's ability to track the phenological development of a plant is dependent on detectable gradients of the observed data over time. Reflectance measurements from a remote sensing device must ascertain them. In addition, the measurement of the parameters should be possible using widely accepted and operational methods, both in the field and the laboratory. The parameters chosen in this work are considered to be the main canopy structural parameter (LAI), the main leaf characteristics parameters (chlorophyll content, water content) and FAPAR, being a key input parameter to growth models.

7.1.2 Parameter Retrieval from Spectroscopy Data

A number of approaches for the retrieval of biophysical and biochemical parameters from spectroscopy data has been applied to the collected data sets of spring wheat and winter barley in order to assess their capability of determining the parameters under investigation from spectral data of the observed phenological stages. Many of these methods to be found in literature were (a) developed under laboratory conditions or from modelling approaches, (b) reported to work on leaf level, (c) applied to canopies other than cereals or (d) never used for parameter retrieval over a whole range of phenological stages.

A short compilation of this work's major findings is subsequently given for each of the four vitality-related vegetation parameters investigated.

7.1.2.1 LAI Determination

Determination of LAI from spectroradiometric data using a semi-empirical approach proposed by Clevers can be performed best when treating *growing* and *senescing phase* separately. LAI determination during the *growing phase* results in a relative rms error around 20% for spring wheat and around 23% for winter barley. A relative rms error around 13% is achieved for LAI determination of spring wheat in the *senescing phase*. LAI determination of winter barley in the *senescing phase* is not successful due to heavy weed infestation and the LAI-2000 Plant Canopy Analyzer's measurement design. Especially in the case of winter barley, field measured LAI values are overestimated for the *senescing phase*, resulting in large rms errors when compared to corresponding values calculated from the inverse exponential relation as implemented in the applied semi-empirical approach. Nevertheless, the LAI data of this work shows clear trends with phenology, except for the stages of the *reproducive phase*. The selected approach of LAI determination from background corrected spectral data results in reduced rms errors compared to the use of non-corrected data, especially when applied to low closure canopies.

7.1.2.2 FAPAR Determination

Determination of FAPAR over a cropping cycle is carried out following an exponential relation with LAI. Based on a joint data set of both cultivars over the whole cropping cycle, a relative rms error around 8% is calculated. Retrieved FAPAR values are believed to be slightly overestimated towards the end of the *senescing phase* due to the ceptometer's measurement design. Since FAPAR determination is performed from LAI data, almost any additional information on crop phenology can be gained from concurrent retrieval of both parameters.

7.1.2.3 Chlorophyll Content Determination

Tracking leaf chlorophyll content over a cropping cycle by the use of wavelengths ratios that involve the visible and near-infrared spectral region turns out not to be successful. The spectral response of a vegetation canopy in the region around the main chlorophyll a absorption feature is mainly driven by green biomass (green LAI), not chlorophyll. Since plant physiology strongly varies during a cropping cycle, canopy structural effects dominate a vegetation spectrum in the abovementioned wavelength region. Chlorophyll

determination methods based on the transitional region between visible and near-infrared wavelengths work either on canopies of uniform LAI or, given canopy structure and LAI are not changing, when applied to spectral data of a range of phenological stages. In the case of cereals, however, physiological changes during the growth stages are very strong.

7.1.2.4 Water Content Determination

Retrieval of plant water content from absolute reflectance data over a phenological cycle using stepwise multiple linear regression has worked out to be possible at relative rms errors between 3% and 8% for both separate and joint data sets of the two cultivars under investigation. The rms errors calculated by using normalized band depths from continuum removed reflectance data as input into stepwise multiple linear regression lie within the same range as in the case of absolute reflectance data. Predictive wavelengths selected by multiple regression are located (a) in the green region of the electomagnetic spectrum, (b) around the red edge or at its inflection point, or (c) in a number of leaf water absorption regions. These wavelengths are both casually or indirectly related to plant water content, but equally used in the regression analysis.

Determination of leaf water content from spectroradiometric data is less accurate, since canopy structural effects cause different optical properties in the case of a vegetation canopy, as seen by a remote sensing device, compared to a single leaf.

Under the absence of precipitation, a strong linear relation between plant and grain water content is found for the phenological stages between *caryopsis water ripe* (DC 71) and *caryopsis hard* (DC 92). This bears the potential of estimating grain water content, being an indicator of harvest ripeness, from remote sensing data. However, the data sets of spring wheat and winter barley must be treated separately as a consequence of a slower drying process due to larger, bearded ears, in the case of winter barley.

7.1.3 Field and Laboratory Data Acquisition

The acquisition of accurate data sets is a prerequisite for the successful retrieval of quantitative information of plant parameters from spectral data. A field measurement plan incorporating temporal and spatial sampling considerations is presented. Time requirements of the various activities, the optimal timing within a measurement day and phenological durations over the cropping cycle determine the structure of data acquisition. A spatial sampling strategy is mandatory in order to guarantee the representativeness of a data set. It is composed of the sampling scheme and the sample size. The sampling

scheme should be kept uniform during the whole phase of data acquisition. Required sample sizes depend on the desired probability Q and the uncertainty δ of the confidence interval. They vary during a crop's development, being at their maximum in periods when successive phenological changes occurr within short time, causing maximum infield variability. In reality, an ideal measurement plan is subject to relativization due to meteorological conditions and the availability of measurement equipment and manpower.

Theoretically, sample collection for laboratory measurements is driven by the same sampling strategy considerations as they apply to field measurements. However, the complexity of many laboratory analyses often prevents from performing a statistically representative number of laboratory measurements. A single determination of leaf chlorophyll content, as performed in this work, takes approximately 30 minutes.

The use of commonly available instruments for field measurements of vegetation parameters such as LAI (using an LAI-2000 Plant Canopy Analyzer) or FAPAR (using a ceptometer) must not keep its user from being aware of what is how measured by these instruments. Both instruments are based on radiation interception techniques by the canopy. As a consequence, light is increasingly intercepted by non-photosynthetic components during the *reproductive phase*. Unless the strict definition of (green) LAI is extended to include the whole range of standing litter material, stems and ears, both LAI and FAPAR from field measurements are likely to be overestimated. The presence of weed is an additional factor that disturbs spectroradiometric measurements and acquisition of crop canopy parameters.

7.1.4 Suitability of Parameters for Phenological Observation

This work is based on a large set of empirical data, collected following a field- and laboratory measurement plan that is designed to assure accuracy and representativeness of the data set. The measurement accuracy is mainly influenced by the instruments' performance and measurement design, as well as by the operator's data acquisition skills. The data's statistical representativeness is driven by sampling strategy considerations. Whereas the acquisition and processing of representative data sets of LAI, FAPAR and water content measurements are possible on a typical measurement day, the laboratory determination of leaf chlorophyll content is the most time consuming work to be accomplished. The use of a handheld chlorophyll meter, as calibrated in this work, is a possibility for fast and numerous collection of chlorophyll data within specified accuracies. Concerning the measurement accuracy of the instruments used, awareness of the measurement

design is important in the case of LAI and FAPAR acquisition. They are affected by radiation interception of not only green leaves, but also stem and standing litter material, especially during the *senescing phase*. Unless leaf area index is redefined as an index of both (green) leaves and non-photosynthetic vegetation parts, it is subject to overestimation by such field measurements.

LAI is undoubtedly a key parameter to track plant vitality. It can therefore be used to monitor crop phenology. However, to calibrate the applied semi-empirical method of LAI determination to retrieve green LAI from a remote sensing device, it would be necessary to acquire data from destructive techniques like harvesting of leaves, which is very time consuming and labor intensive. Besides, LAI measurements using an LAI-2000 Plant Canopy Analyzer are best performed under diffuse sky conditions, which is not the case for spectroradiometric measurements and ceptometer readings.

Field acquisition of FAPAR data using a ceptometer is subject to the same drawbacks of the instrument's light interception technique as in the case of LAI. As FAPAR determination from spectral data is based on an exponential relation with LAI, the measurement accuracy of LAI readings has a direct impact on modelled FAPAR. Nevertheless, both FAPAR and LAI field measurements and their modelling from remote sensing data show clear trends between phenological stages.

Although the retrieval of chlorophyll content from spectral data of single leaves on the one hand, or of plant canopies of distinct phenological stages on the other hand, is reported as being possible using the applied methods, their application to spectral data of crop canopies over a phenological cycle is not successful. Canopy structural effects and LAI, being subject to fundamental physiological changes with time, dominate leaf scale effects in the spectral regions investigated. In addition, the representativeness of laboratory determination of leaf chlorophyll content most often suffers from a limited number of samples due to time intensity of the extraction procedure.

Plant water content can be judged the most promising vegetation parameter to be used for phenological studies. Acquisition of field sample data and its processing is fast and easy. The availability of spectroscopy data favorites the use of stepwise multiple linear regression for plant water retrieval over a vegetation period. While canopy structural effects reduce the accuracy of leaf water content retrieval, grain water content can be correlated to plant water content during the *reproductive phase*, given the absence of precipitation. The phenological stages of the *reproductive phase* are characterized by the grains' water content, which is important as a ripeness and harvest indicator.

Drawing conclusions on the main goal of this work, the following remarks can be made:

- Tracking the main development stages of cereals using key vegetation parameters is possible.
- Data collection is subject to the limitations of acquisition techniques (i.e., sampling strategy, instruments).
- Parameter retrieval from spectroscopy data in this work is based on empirical, semi-empirical and statistical approaches with their respective accuracies. As a consequence, several phenological stages following each other may often be assigned to a single retrieved parameter, especially in the case of LAI and FAPAR.
- Plant water content is judged the most promising vegetation parameter to track crop phenology, followed by LAI and FAPAR. The determination of leaf chlorophyll content is not successful to track growth stages, using the applied methods.
- Since all methods of parameter retrieval for phenological tracking of spring wheat and winter barley are empirical, semi-empirical or statistical, the results and accuracies achieved apply in the first place to the investigated data sets. However, as a number of methods and coefficients can equally be applied to joint data sets of both cultivars, they may be transferrable to any spring wheat or winter barley field. Given the fact, that a whole number of other cereals belongs to the *Poaceae* family as well, the methods may even work on phenology considerations of these cultivars. In this case, the specific coefficients are likely to be determined from corresponding field- and laboratory data, whereas the technique of data acquisition, characterization and processing remains the same.

7.2 Outlook

The availability of timely and reliable information on vegetation status is of growing importance in an ecological, political as well as economical sense. Image based hyperspectral remote sensing bears the capability of providing such data. Article 2 of the Kyoto Protocol [81], whose sufficient ratification was missed in The Hague in November 2000, demands sustainable forms of agriculture in light of climate change considerations. Article 3 addresses direct human-induced land use changes, that result in net changes of greenhouse gas emissions (e.g., CO_2) in their sources and sinks. Since agricultural practices like CO_2- and N-fertilization affect biosphere functioning, the article's issue is related to precision farming which bears the potential of a more economical and ecological agricultural production. Variable rate application techniques, being of growing importance in the future, heavily rely on precise determination of plant nutrient status at distinct phenological stages. Data integration into growth models, as well as monitoring of crop ripening are equally dependent on phenological information.

The determination of crop vitality parameters from remote sensing data needs both, sensors capable of collecting the required spectral data, and methods of fast and accurate parameter retrieval. A widespread acceptance of remote sensing techniques in agricultural management depends on operationalization, successful realization of user requirements, system specifications and straightforward integration of the data into decision support systems.

An emerging fleet of spaceborne imaging spectrometers, designed for specific applications with a reduced number of small spectral bands, in combination with high spatial resolution multispectral systems will provide data sets for precision agriculture applications. In addition, airborne systems, like APEX, will continue to be widely operated because of their flexible use.

Phenological monitoring of crop stands is highly dependent on meteorological conditions, as are all applications of remote sensing in the solar reflective domain of the electromagnetic spectrum. A temporal sampling interval of eight to ten days is considered adequate to cover most phenological stages of cereals, except for the periods between *booting* and *anthesis*, where a sampling interval of four to six days is recommended due to faster completion of these growth stages. Given a realistic repetition rate of spaceborne sensors for agricultural applications around three days, cloud cover becomes a problem in many of the temperate regions of the world. The joint determination of fractional cloud cover must be included in future remote sensing systems. In addition, precipitation, even hours after it occurred, has an

impact on vegetation parameters (e.g., water content) especially during *senescence*. The impact of meteorological conditions on phenological studies is very obvious from this work.

The application of the methodology of phenological characterization to other agricultural products (e.g., corn, sugar beet, potatoes) remains a challenge. Corn production is a main agricultural activity in several countries. In the case of sugar beet and potatoes, phenological information could help to assess the conditions of the potential harvest products that are actually hidden in the soil. Accurate data for use as a driving variable, for updating a state variable or for forcing or recalibration of a crop growth model is needed for many agricultural products. Imaging data can provide such information at a regional extent.

More research has to be done into the separation of a crop stand's spectral signal resulting both, from leaf chlorophyll and canopy structure (e.g., LAI). In this work, the determination of chlorophyll content, being a key vitality parameter, was not successful over a cropping cycle due to superimposed canopy structural effects in the observed spectral region. The use of different spectral regions or analytical modelling approaches, that incorporate radiation interaction on both leaf and canopy level, together with scaling considerations, may help to solve this problem.

Appendix

a) Field Treatment and Harvest Parameters[1)]

Table 7.1 Fertilizer- and pestizide treatment of the observed spring wheat field.

Date	Product Applied	Amount	Effect
presowing	Dung	n.a.	Fertilizer
April 6th 1999	Ammonium nitrate (27.5%)	1.4 kg a^{-1}	Mineral fertilizer
May 3rd 1999	Ammonium nitrate (27.5%)	1.0 kg a^{-1}	Mineral fertilizer
May 18th 1999	Duplosan	1.5 l ha^{-1}	Weed-killer
May 18th 1999	Express	20 g ha^{-1}	Weed-killer (thistle)
June 25th 1999	Allegro	1 l ha^{-1} in 300 l of water	Controlling of fungal and mildew infestation, leaf rust and septoria

Table 7.2 Fertilizer and pestizide treatment of the observed winter barley field.

Date	Product Applied	Amount	Effect
presowing	Artificial Fertilizer	400 kg	Fertilizer
April 6th 1999	Ammonium nitrate (27.5%)	2.5 kg a^{-1}	Mineral fertilizer
April 6th 1999	Isoproturon	3 l ha^{-1}	Weed-killer
April 6th 1999	Ally Class	50 g ha^{-1}	Weed-killer (thistle)

Table 7.3 Harvest parameters of the observed winter barley and spring wheat fields.

Parameter	Winter Barley (Lyric)	Spring Wheat (Balmi)
Harvest date	August 4th 1999	August 22nd 1999
Grain moisure	12.5% (optimal 15%)	18% (optimal 15%)
Hectoliter weight	65 kg hl^{-1}	76 kg hl^{-1} ($\geq$76 kg hl^{-1} required for bread making)
Yield (Mean yield expected)	40 kg a^{-1} (50-60 kg a^{-1})	41 kg a^{-1} (60-70 kg a^{-1})
Designation	Fodder cereals	Fodder cereals (due to reduced grain quality and premature germination)

1) Data source: personal communication with farmer

b) Crop Growth Scales

Table 7.4 The development of cereals characterized by three crop growth scales[1].

	Growth Stage	Development Stage	Large [84]	Keller et al. [75]	Zadoks et al. [137]
Vegetative Phase	Germination	Sowing			00
	Seedling growth	1st leaf emergence	1	A	10
		1st leaf unfolded		B	11
		2 leaves unfolded		C	12
		3 leaves unfolded		D	13
	Tillering	Main shoot, 1 tiller	2	E	21
		Main shoot, 5 tillers	3	F	25
		Tillering completed	4	G	29
Generative Phase	Stem elongation	Pseudo stem erection	5	H	30
		1st node detectable	6	I	31
		2nd node detectable	7	J	32
		Flag leaf just visible	8	K	37
		Flag leaf ligule visible	9	L	39
	Booting	First awns visible	10	M	49
	Inflorescence emergence	1st spikelet of inflorescence just visible	10.1	N	51
		Emergence of inflorescence completed	10.5	O	59
	Anthesis (flowering)	Beginning of anthesis	10.5.1	P	61
		Anthesis complete	10.5.3	Q	69
Reproductive Phase	Milk development	Caryopsis water ripe	10.5.4	R	71
		Medium milk	11.1	S	75
	Dough development	Soft dough	11.2	T	85
		Hard dough		U	87
	Ripening	Caryopsis hard (16% water)	11.3	V	91
		Caryopsis hard (<16% water)	11.4	W	92

[1] normalized to the scale of Large [84]

c) Factory Specifications of the Used Field- and Laboratory Instruments

Table 7.5 ASD FieldSpec Pro FR manufacturer specifications [4].

Parameter	Description
Spectral range	350-2500 nm
Spectral resolution	3 nm @ 700 nm 10 nm @ 1400 nm & 2100 nm
Sampling interval	1.4 nm @ 350-1000 nm 2.0 nm @ 1000-2500 nm
Channels	1512 (prior to interpolation)[1)]
Detectors	1 Si photodiode array (350-1000 nm) 2 InGaAs arrays, thermoelectronically cooled (1000-2500 nm)
Scanning time	0.1 s (entire spectral range)
Field of view (FOV)	25° (fiber optic) 8° (optional fore-optic)
Wavelength accuracy / repeatability	± 1 nm / ± 0.3 nm within ± 10° C of calibration temperature
Spectrum averaging	Yes, user defined
Dark current correction	Automatic, based on user defined measurement prior to data take
Weight	7.2 kg instrument & 2.2 kg battery pack
Dimensions	35 x 29 x 13 cm

[1)] Each spectrum is resampled to 1 nm steps after its acquisition by software. These data values, as they are interpolated, are not the instrument's spectral resolution [3].

Table 7.6 LAI-2000 Plant Canopy Analyzer manufacturer specifications [86].

Parameter	Description
Spectral range	320-490 nm
Detectors	5 Si photodiodes, arranged in concentric rings of nominal angular coverage, ranging from 0° (nadir view) to 74° off-nadir view
Radiation rejection	< 1% (490-650 nm) < 0.1% (>650 nm)
Lens coating	MgF_2 for improved transmission at high oblique angles

Table 7.6 LAI-2000 Plant Canopy Analyzer manufacturer specifications [86].

Parameter	Description
View caps	0°, 45°, 90°, 180°, 270°, providing azimuthal masking into quadrants
Operating mode	1 & 2 sensor mode
Data averaging	Yes, user defined
Weight	1.8 kg control unit & 0.85 kg optical sensor
Dimensions	21 x 11 x 7 cm control unit 61 x 3 x 3 cm optical sensor handle
Operating environment	0-100% humidity / -15° to 50° C

Table 7.7 Sunfleck Ceptometer manufacturer specifications [44].

Parameter	Description
Spectral range	400-700 nm
Detectors	80 GaAsP photodiodes arranged on a probe
Dimensions	108 cm probe length
Weight	0.9 kg
Operating environment	0-100% humidity / 0°-50° C

Table 7.8 CADAS-100 Spectrophotometer manufacturer specifications [83].

Parameter	Description
Spectral range	200-900 nm
Light source	UV: deuterium lamp VIS, NIR: halogen lamp
Scan speed	220 nm/min @ 1 nm resolution 930 nm/min @ 5 nm resolution
Operating mode	extinction, concentration, absorption
Spectral resolution	5 nm
Wavelength accuracy / repeatability	± 1 nm / < 0.1 nm
Weight	21 kg
Dimensions	50.5 x 15 x 45 cm

Table 7.9 LI-COR LI-3100 Area Meter manufacturer specifications [88].

Parameter	Description
Light source	15 W fluorescent tube
Resolution	1 mm^2 0.1 mm^2 (for small samples < 1 cm^2)
Accuracy	± 1% of 10 cm^2 @ 1 mm^2 resolution ± 2% of 5 cm^2 @ 1 mm^2 resolution ± 0.5% of 10 cm^2 @ 0.1 mm^2 resolution ± 1% of 5 cm^2 @ 0.1 mm^2 resolution
Conveyor belt speed	8.0 cm s^{-1} @ 60 Hz, 6.7 cm s^{-1} @ 50 Hz
Weight	43 kg
Dimensions	25 x 60 x 73 cm
Operating environment	15°-55° C

Table 7.10 SPAD-502 Chlorophyll Meter manufacturer specifications [118].

Parameter	Description
Light source	2 LEDs with peak wavelengths @ 650 nm and 940 nm
Detector	1 Si photodiode
Units range	0-199[1)]
Repeatability	± 0.3 units
Measuement area of the detector	2 x 3 mm
Data memory	30 data sets

[1)] The SPAD values display arbitrary units of the ratio of leaf transmittance at 650 nm and 940 nm. The amount of light present at the photodiode detector is inversely proportional to the amount of chlorophyll in the light path.

References

[1] Allen, W. A., Gausman, H. W., Richardson, A. J., and Thomas J. R.: "Interaction of Isotropic Light With a Compact Plant Leaf", *Appl. Opt.*, 59(10):1376-1379, 1969

[2] Allen, W. A., Gausman, H. W., and Richardson, A. J.: "Willstatter-Stoll Theory of Leaf Reflectance Evaluated by Ray Tracing", *Appl. Opt.*, 12:2448-2454, 1973

[3] Analytical Spectral Devices, Inc.: "FieldSpec^{TM}, User's Guide", *Analytical Spectral Devices, Inc.*, Boulder, CO, pp. 81, 1997

[4] Analytical Spectral Devices, Inc.: "Portable Accurate Solutions from Light", *<http://www.asdi.com>*, September 20, 2001

[5] Asner, G. P.: "Biophysical and Biochemical Sources of Variability in Canopy Reflectance", *Remote Sens. Environ.*, 64:234-253, 1998

[6] Bahrenberg, G. and Giese, E.: "Statistische Methoden und ihre Anwendung in der Geographie", Teubner, Stuttgart, pp. 233, 1990

[7] Baret, F., Guyot, G., and Major, D.: "TSAVI: a Vegetation Index Which Minimizes Soil Brightness Effects on LAI and APAR Estimation", in: *Proc. IGARSS'89*, pp. 1355-1358, 1989

[8] Baret, F. and Guyot, G.: "Potentials and Limits of Vegetation Indices for LAI and APAR Assessment", *Remote Sens. Environ.*, 35:161-173, 1991

[9] Baret, F. and Jacquemoud, S.: "Modeling Canopy Spectral Properties to Retrieve Biophysical and Biochemical Characteristics", in: *Imaging Spectrometry - a Tool for Environmental Observations*, eds. J. Hill and J. Mégier, Kluwer Academic Publishers, pp. 145-167, 1994

[10] Baret, F. and Fourty, T.: "The Limits of a Robust Estimation of Canopy Biochemistry", in: *Proc. 7th Int. Symp. Physical Measurements and Signatures in Remote Sensing*, Courchevel (F), pp. 413-420, 1997

[11] Baret, F., "Potentiel de la télédétection pour l'agriculture de précision", in: *L'enjeu français de l'agriculture de précision*, pp. 8-11, 1998

[12] Barnes, E. M., Qi, J., and Pinter, P. J.: "Integration of Remote Sensing and Growth Models to Assist in Precision Crop Management", *<http://www.uswcl.ars.ag.gov/publicat/index/FMD4.htm>*, March 15, 2001

[13] Bauer, M. E., Anuta, P. E., Swain, P. H., MacDonald, R. B., and Mroczynski R. P.: "Detection of Southern Corn Leaf Blight by Remote Sensing", in: *Proc. 7th Int. Symp. on Remote Sensing of Environment, Ann Arbor, MI*, pp. 693-704, 1971

[14] Bauer, M. E.: "Spectral Inputs to Crop Identification and Condition Assessment", *Proc. IEEE*, 73(6), pp. 1071-1085, 1985

[15] Beisl, U.: "Correction of Bidirectional Effects in Imaging Spectrometer Data", Ph.D. Thesis, *Remote Sensing Series*, Vol. 37, Dept. of Geography, University of Zurich, pp. 189, 2001

[16] Bizzell, R., Hall, F., Feiveson, A., Bauer, M., Davis, B, Malia, W., and Rice, D.: "Results from Crop Identification Assessment for Remote Sensing (CITARS) Project", in: *Proc. 9th Int. Symp. on Remote Sensing of Environment, Ann Arbor, MI*, pp. 39, 1974

[17] Blackburn, G. A.: "Spectral Indices for Estimating Photosynthetic Pigment Concentrations: A Test Using Senescent Tree Leaves", *Int. J. Remote Sens.*, 19(4):657-675, 1998

[18] Blackburn, G. A.: "Quantifying Chlorophylls and Carotenoids at Leaf and Canopy Scales: An Evaluation of Some Hyperspectral Approaches", *Remote Sens. Environ.*, 66:273-285, 1998

[19] Brown, C.: "Practical Commercial Remote Sensing Applications in the Ontario Precision Agriculture Marketplace", in: *2nd Int. Conference on Geospatial Information in Agriculture and Forestry*, I-1-I-13, 2000

[20] Boochs, F., Kupfer, G., Dockter, K., and Kübauch, W.: "Shape of the Red Edge as Vitality Indicator for Plants", *Int. J. Remote Sens.*, 11:1741-1753, 1990

[21] Bundesamt für Landwirtschaft: "Getreiderechnung 1999, Bern, pp.15, 2000

[22] Bundesamt für Landwirtschaft: "Evaluation der Ökomassnahmen und Tierhaltungsprogramme", *Dritter Zwischenbericht*, Bern, pp.14, 2000

[23] Bunnik, N. J. J.: "The Multispectral Reflectance of Shortwave Radiation by Agricultural Crops in Relation With Their Morphological and Optical Properties", Thesis, *Meded. Landbouwhogeschool Wageningen*, 78-1, pp. 175, 1978

[24] Carlson, R. E., Yarger, D. N., and Shaw, R. H.: "Factors Affecting the Spectral Properties of Leaves With Special Emphasis on Leaf Water Status", *Agronomy Journal*, 63:486-489, 1971

[25] Changyong, C. and Lam, N. S.: "Understanding the Scale and Resolution Effects in Remote Sensing and GIS", in: *Scale in Remote Sensing and GIS*, eds. Quattrochi, D. A., and Goodchild, M. F., Lewis Publishers, ISBN 1-56670-104-X, pp. 57-72, 1997

[26] Chappelle, E. W., Kim, M. S., and McMurtrey III, J. E.: "Ratio Analysis of Reflectance Spectra (RARS): An Algorithm for the Remote Estimation of the Concentrations of Chlorophyll A, Chlorophyll B, and Carotenoids in Soybean Leaves", *Remote Sens. Environ.*, 39: 239-247, 1992

[27] Clevers, J. G. P. W.: "The Derivation of a Simplified Reflectance Model for the Estimation of Leaf Area Index", *Remote Sens. Environ.*, 25:53-69, 1988

[28] Clevers, J. G. P. W.: "The Application of a Weighted Infrared-Red Vegetation Index for Estimating Leaf Area Index by Correcting for Soil Moisture", *Remote Sens. Environ.*, 29:25-37, 1989

[29] Clevers, J. G. P. W.: "Application of the WDVI in Estimating LAI at the Generative Stage of Barley", *ISPRS J. Photogramm. Remote Sensing*, 46(1):37-47, 1991

[30] Clevers, J. G. P. W., Büker, C., Van Leeuwen, H. J. C., and Bouman, B. A. M.: "A Framework for Monitoring Crop Growth by Combining Directional and Spectral Remote Sensing Information", *Remote Sens. Environ.*, 50:161-170, 1994

[31] Cocks, T., Jenssen, R., Stweart, I. W., and Shields, T.: "The HyMap^{TM} Airborne Hyperspectral Sensor: The System, Calibration and Performance", in: *Proc. 1st EARSeL Workshop on Imaging Spectroscopy*, Zurich, Switzerland, pp. 37-42, 1998

[32] Combal, B. and Baret, F.: "Estimation of Chlorophyll Content from Remote Sensing Measurements and Signatures in Remote Sensing", in: *Proc. 8th Int. Symp. Physical Measurements and Signatures in Remote Sensing*, Aussois (F), pp. 461-471, 2001

[33] Condit, H. R.: "The Spectral Reflectance of American Soils", *Photogramm. Eng. and Rem. Sens.*, 36:955-966, 1970

[34] Congalton, R. G.: "A Comparison of Sampling Schemes Used in Generating Error Matrices for Assessing the Accuracy of Maps Generated from Remotely Sensed Data", *Photogramm. Eng. and Rem. Sens.*, 54(5):593-600, 1988

[35] Curran, P.: "Remote Sensing of Foliar Chemistry", *Remote Sens. Environ.*, 35(1):271-278, 1989

[36] Curran, P. J., Dungan, J. L., Macler, B. A., Plummer, S. E., and Peterson, D. L.: "Reflectance Spectroscopy of Fresh Whole Leaves for the Estimation of Chemical Concentration", *Remote Sens. Environ.*, 39:153-166, 1992

[37] Curran, P. J., Dungan, J. L., and Peterson, D. L.: "Estimating the Foliar Biochemical Concentration of Leaves With Reflectance Spectrometry. Testing the Kokaly and Clark Methodologies", *Remote Sens. Environ.*, 76:349-359, 2001

[38] Danson, F. M., Steven, M. D., Malthus, T. J., and Clark, J. A.: "High-spectral Resolution Data for Determining Leaf Water Content", *Int. J. Remote Sens.*, 13(3):461-470, 1992

[39] Datt, B.: "Remote Sensing of Chlorophyll a, Chlorophyll b, Chlorophyll a+b, and Total Carotenoid in Eucalyptus Leaves", *Remote Sens. Environ.*, 66:111-121, 1998

[40] Daughtry, C. S. T., Gallo, K. P., Goward, S. N., Price, S. D., and Kustas, W. P.: "Spectral Estimates of Absorbed Radiation and Phytomass Production in Corn and Soybean Canopies", *Remote Sens. Environ.*, 39:141-152, 1992

[41] Daughtry, C. S. T., Walthall, C. L., Kim, M. S., Brown de Colstoun, E., and McMurtrey III, J. E.: "Estimating Corn Leaf Chlorophyll Concentration from Leaf and Canopy Reflectance", *Remote Sens. Environ.*, 74:229-239, 2000

[42] Defila, C.: "45 Years Phytophenological Observations in Switzerland, 1951-1995", in: *Proc. 14th Int. Congress of Biometeorology*, Ljubljana, Slovenia, pp. 175-183, 1996

[43] Delécolle, R., Maas, S. J., Guérif, M., and Baret, F.: "Remote Sensing and Crop Production Models: Present Trends", *ISPRS Journal of Photogrammetry and Remote Sensing*, 47:145-161, 1992

[44] DELTA-T-DEVICES LTD: "Sunfleck Ceptometer User Manual", *Decagon Devices Inc*., Cambridge England, pp. 28, 1989

[45] Deschamps, P. Y., Breon, F.-M., Leroy, M., Podaire, A., Bricaud, A., Buriez, J.-C., and Seze, G.: "The POLDER Mission: Instrument Characteristics and Specific Objectives", *IEEE Trans. Geosc. Rem. Sens*., 32:598-615, 1994

[46] Eidg. Forschungsanstalt für landw. Pflanzenbau: "Bodenkarte Lyss mit Erläuterungen", *LK 1:25'000*, Blatt 1146, Zürich Reckenholz, 1984

[47] ESA: "The Four Candidate Earth Explorer Core Missions - Land-Surface Processes and Interactions", Reports for Mission Selection, ESA-SP-1233 (2), *ESA*, pp. 211, 1999

[48] ESA: "The Five Candidate Earth Explorer Core Missions - SPECTRA - Surface Processes and Ecosystem Changes Through Response Analysis", Reports for Assessment, ESA-SP-1257 (5), *ESA*, pp. 123, 2001

[49] Everitt, J. H. and Nixon, P. R.: "Canopy Reflectance of Two Drought Stressed Shrubs", *Photogramm. Eng. and Rem. Sens.*, 52:1189-1192, 1986

[50] FAO: "Faostat Database", <*http://apps.fao.org/*>, February 15, 2001

[51] Filella, I., Peñuelas, J.: "The Red Edge Position and Shape as Indicators of Plants Chlorophyll Content, Biomass and Hydric Status", *Int. J. Remote Sens*., 15(7):1459-1470, 1994

[52] Fourty, Th., Baret, F., Jacquemoud, S., Schmuck, G., and Verdebout, J.: "Leaf Optical Properties With Explicit Description of its Biochemical Composition: Direct and Inverse Problems", *Remote Sens. Environ.*, 56:104-117, 1996

[53] Gates, D. M., Keegan, H. J., Schleter, J. C., and Weidner, V. R.: "Spectral Properties of Plants", *Appl. Opt*., 4(1):11-20, 1965

[54] Gausman, H. W., Allen, W. A., and Escobar, D. E.: "Refractive Index of Plant Cell Walls", *Appl. Opt.*, 9(3):545-552, 1970

[55] Gausman, H. W.: "Plant Leaf Optical Properties in Visible and Near-Infrared Light", *Graduate Studies No. 29*, Texas Technical University, Lubbock, Texas, pp. 78, 1985

[56] Gitelson, A. A. and Merzlyak, M., N.: "Remote Estimation of Chlorophyll Content in Higher Plant Leaves", *Int. J. Remote Sens.*, 18(12):2691-2697, 1997

[57] Goel, N. S.: "Models of Vegetation Canopy Reflectance and Their Use in Estimation of Biophysical Parameters from Reflectance Data", *Remote Sensing Rev.*, 4:1-212, 1988

[58] Goward, S. N. and Huemmerich, K. F.: "Vegetation Canopy PAR Absorptance and the Normalized Difference Vegetation Index: An Assessment Using the SAIL Model", *Remote Sens. Environ.*, 39:119-140, 1992

[59] Grant, L.: "Diffuse and Specular Characteristics of Leaf Reflectance", *Remote Sens. Environ.*, 22:309-322, 1987

[60] Grossman, Y. L., Ustin, S. L., Jacquemoud, S., Sanderson, E. W., Schmuck, G., and Verdebout, J.: "Critique of Stepwise Multiple Linear Regression for the Extraction of Leaf Biochemistry Information from Leaf Reflectance Data", *Remote Sens. Environ.*, 56:182-193, 1996

[61] Haboudane, D., Miller, J. R., Tremblay, N., Zarco-Tejeda, P. L., and Dextraze, L.: "Integration of Hyperspectral Vegetation Indices for Prediction of Crop Chlorophyll Content for Application to Precision Farming", *submitted to Remote Sens. Environ.*, April 2001

[62] Haggett, P., Cliff, A. D., and Frey, A.: "Locational Analysis in Human Geography", Edwards Arnold, London, pp. 605, 1977

[63] Harrison, P. A., Porter, J. R., Downing, T. E.: "Scaling-up the AFRCWHEAT-2 Model to Assess Phenological Development for Wheat in Europe", *Agricultural and Forest Meteorology*, 101:167-186, 2000

[64] Hipps, L. E., Asrar, G., and Kanemasu, E. T.: "Assessing the Interception of Photosynthetically Active Radiation in Winter Wheat", *Agricultural and Forest Meteorology*, 28:253-259, 1983

[65] Holben, B. N., Schutt, J., B., and McMurtrey, III, Jr.: "Leaf Water Stress Detection Utilizing Thematic Mapper Bands 3, 4 and 5 in Soybean Plants", *Int. J. Remote Sens*., 4(2):289-297, 1983

[66] Horler, D. N. H., Dockray, M., and Barber, J: "The Red Edge of Plant Leaf Reflectance", *Int. J. Remote Sens*., 4(2):273-288, 1983

[67] Huete, A.R., Jackson, R.D., and Post, D.F.: “Spectral Response of a Plant Canopy With Different Soil Backgrounds”, *Remote Sens. Environ.*, 17:37-53, 1985

[68] Huete, A. R.: "A Soil-Adjusted Vegetation Index (SAVI), *Remote Sens. Environ.*, 25:295-309, 1988

[69] Hurcom, S. J., Harrison, A. R., and Taberner, M.: "Assessment of Biophysical Vegetation Properties Through Spectral Decomposition Techniques", *Remote Sens. Environ.*, 56(3):203-214, 1996

[70] Jackson, R. D. and Ezra, C. E.: "Spectral Response of Cotton to Suddenly Induced Water Stress", *Int. J. Remote Sens*., 6:177-185, 1985

[71] Jacquemoud, S. and Baret, F.: "PROSPECT: A Model of Leaf Optical Properties", *Remote Sens. Environ.*, 34:75-91, 1990

[72] Jacquemoud, S., Verdebout, J., Schmuck, G., Andreoli, G., and Hosgood, B.: "Investigation of Leaf Biochemistry by Statistics", *Remote Sens. Environ.*, 54:188-188, 1995

[73] Jacquemoud, S., and Ustin, S. L.: "Leaf Optical Properties: A State of the Art", in: *Proc. 8th Int. Symp. Physical Measurements and Signatures in Remote Sensing*, Aussois (F), pp. 223-231, 2001

[74] Johannson, C. J., Carter, P. G., Morris, D. K., Ross, K., and Erickson, B.: "The Real Applications of Remote Sensing to Agriculture", in: *2nd International Conference on Geospatial Information in Agriculture and Forestry*, I-1-I-5, 2000

[75] Keller, C. and Baggiolini, M.: "Les stades repères dans la végétation du blé", *Revue Romande d’Agriculture*, 10:17-20, 1954

[76] Kim, M. S., Daughtry, C. S. T., Chappelle, E. W., McMurtrey III, J., E., and Walthall, C. L.: "The Use of High Spectral Resolution Bands for Estimating Absorbed Photosynthetically Active Radiation (APAR)", *6th Symposium on Physical Measurements and Signatures in Remote Sensing*, Val D’Isère, France, pp. 299-306, 1994

[77] Kimes, D. S., Markham, B. L., Tucker, C. J., and McMurtrey III, J. E.: "Temporal Relationships Between Spectral Response and Agronomic Variables of a Corn Canopy", *Remote Sens. Environ.*, 11:401-411, 1981

[78] Kokaly, R. F. and Clark, R. N.: "Spectroscopic Determination of Leaf Biochemistry Using Band-Depth Analysis of Absorption Features and Stepwise Multiple Linear Regression", *Remote Sens. Environ.*, 67(3):267-287, 1998

[79] Kolbe, W.: "Studies on the Course of Development of Cereals (1968-1984) in Relation to Sowing Time", *Pflanzenschutz-Nachrichten Bayer*, 37:337-423, 1984

[80] Kumar, R. and Silva, L.: "Ray Tracing Through a Leaf Cross Section", *Appl. Opt.*, 12:2950-2954, 1973

[81] Kyoto Protocol to the United Nations Framework Convention on Climate Change: <*http://www.unfccc.de/resource/docs/convkp/kpeng.pdf,* September 15, 2001

[82] Lacaze, R. and Roujean, J.-L.: "Retrieval of Biophysical Parameters Over Land Based on Polder Directional and Hot Spot Measurements", in: *Proc. 8th Int. Symp. Physical Measurements and Signatures in Remote Sensing*, Aussois (F), pp. 487-492, 2001

[83] Lange, B., GMBH: "Spektralphotometer CADAS 100, Bedienungsanleitung", *Lange GMBH, Berlin*, pp. 59, 1990

[84] Large, E. C.: "Growth Stages in Cereals, Illustration ot the Feekes Scale", *Plant Pathology*, 3:128-129, 1952

[85] Lichtenthaler, H. K. "Chlorophylls and Carotenoids: Pigments of Photosynthetic Biomembranes", *Methods in Enzymology*, 148:350-382, 1987

[86] LI-COR: "LAI-2000 Plant Canopy Analyzer", *LI-COR Inc*., Lincoln, Nebraska, pp. 14, 1990

[87] LI-COR: "LAI-2000 Plant Canopy Analyzer", Instruction Manual, *LI-COR Inc.*, Lincoln, Nebraska, 1992

[88] LI-COR: "Area Meters", *LI-COR Inc.*, Lincoln, Nebraska, pp. 6, 1994

[89] Lieth, H.: "Phenology and Seasonality Modelling", *Ecological Studies*, Vol. 8, pp. 444, Springer, 1974

[90] Lu, Y.-C., Daughtry, C., Hart, G., and Watkins, B.: "The Current State of Precision Farming", *Food Rev. Int.*, 13(2):141-162, 1997

[91] Maas, S. J.: "Use of Remotely-Sensed Information in Agricultural Crop Growth Models", in: *Ecological Modelling*, 41:655-662, 1988

[92] Maas, S. J., "Remote Sensing Resources for Agriculture in the Next Decade", in: *Proc. Beltwide Cotton Conferences*, pp. 36-38, 1998

[93] MacDonald, R. B. and Hall, F. G.: "Global Crop Forecasting", *Science*, 208:670-679, 1980

[94] Markwell, J., Osterman, J. C., and Mitchell J. L.: "Calibration of the Minolta SPAD-502 Leaf Chlorophyll Meter", *Photosynthesis Research*, 46:467-472, 1995

[95] McMurtrey, J., Doraiswamy, P., Schepers, J., Zara, P., Stern, A., and Corp, L.: "Evaluation of Hyperspectral Algorithms and Methods to Detect Changes in the Primary Plant Pigments for Nitrogen Management in Field Corn", in: *2nd International Conference on Geospatial Information in Agriculture and Forestry*, II-395-II-401, 2000

[96] Menzi, M., Weilenmann, F., Anders, M., Winzeler, M., Schachermayr, G., Streckeisen, Ph. and Arnold, A.: "Nationaler Getreide-Sortenkatalog 2000", *Eidgenössische Forschungsanstalt für Agrarökologie und Landbau (FAL)*, Zürich-Reckenholz, pp. 7, 2000

[97] Meteo Swiss: "Phänologische Auswertetabelle Jegenstorf und Oeschberg", *Courtesy of Meteo Swiss, C. Defila*, February 16, 2001

[98] Moran, M. S., Inoue, Y., and Barnes, E. M.: "Opportunities and Limitations for Image-Based Remote Sensing in Precision Crop Management", *Remote Sens. Environ.*, 61:319-346, 1997

[99] Moran, M. S.: "Image-Based Remote Sensing for Agricultural Management. Perspectives of Image Providers, Research Scientists and Users", in: *2nd International Conference on Geospatial Information in Agriculture and Forestry*, I-23-I-30, 2000

[100] Moulin, S., Bondeau, A., and Delécolle, R.: "Combining Agricultural Crop Models and Satellite Observations from Field to Regional Scales", in *Int. J. Remote Sens.*, 19(6):1021-1036, 1998

[101] Naef, C.: "Der Blattflächenindex ermittelt aus Feldspektrometerdaten", Diplomarbeit, *Geographisches Institut Universität Zürich*, pp. 54, 2000

[102] Porter, J. R.: "AFRCWHEAT-2: A Model of the Growth and Development of Wheat Incorporating Responses to Water and Nitrogen", *Eur. J. Agron.*, 2:69-82, 1993

[103] Richardson, A.J. and Wiegand, C.L.: “Distinguishing Vegetation from Soil Background Information”, *Photogramm. Eng. Rem. Sens.*, 43:1541-1552, 1977

[104] Richter, R.: "Atmospheric / Topographic Correction for Wide FOV Airborne Imagery: Model ATCOR4", *DLR*, IB 552-05/00, pp. 62, 2000

[105] Robert, P. C., Rust, R. H., and Larson, W. E.: Preface, in: *Proc. Site-Specific Management for Agricultural Systems*, pp. xiii-xiv, 1994

[106] Rollin, E. M. and Milton, E. J.: "Processing of High Spectral Resolution Reflectance Data for the Retrieval of Canopy Water Content Information", *Remote Sens. Environ.*, 65:86-92, 1998

[107] Rondeaux, G., Steven, M., and Baret, F.: "Optimization of Soil-Adjusted Vegetation Indices", *Remote Sens. Environ.*, 55:95-107, 1996

[108] Russell, G.: "Barley Knowledge Base", *Commission of the European Communities*, Luxembourg, EUR 13040 EN, pp. 135, 1990

[109] Russell, G. and Wilson, G. W.: "An Agro-Pedo-Climatological Knowledge-Base of Wheat in Europe", *Commission of the European Communities*, Luxembourg, EUR 15789 EN, pp. 160, 1994

[110] Schaepman, M. E.: "Calibration of a Field Spectroradiometer", PhD. Thesis, *Remote Sensing Series*, Vol. 32, Dept. of Geography, University of Zurich, pp. 126, 1998

[111] Schaepman, M. E. and Itten, K.: "APEX - Airborne PRISM Experiment: An Airborne Imaging Spectrometer Serving as a Precursor Instrument of the Future ESA Land Surface Processes Interactions Mission", *Proc. ISPRS*, 22(7):31-37, 1998

[112] Schaepman, M. and Kneubühler, M.: "Kalibrierung HyMap", in: *Pro-Smart Endbericht*, DaimlerChrysler Aerospace, Vol. 2, Dok-No.: EB-DSS-REP-0001, 1999

[113] Schaepman, M. E., Schläpfer, D., and Itten, K. I.: "APEX - A New Pushbroom Imaging Spectrometer for Imaging Spectroscopy Applications: Current Design and Status", *Proc. IGARSS*, pp. 828-830, 2000

[114] Schweizerischer Bauernverband: "Statistische Erhebungen und Schätzungen über Landwirtschaft und Ernährung", *SBV, Abt. Statistik und Dokumentation*, Brugg, 2000

[115] Schweizerische Vereinigung integriert produzierender Bauern und Bäuerinnen: "IP-Suisse Label für Getreide", *IP-Suisse*, Zollikofen, 2000

[116] Sinclair, T. R., Hoffer, R. M., and Schreiber, M. M.: "Reflectance and Internal Structure of Leaves from Several Crops During a Growing Season", *Agronomy Journal*, 63:864-867, 1971

[117] Sinclair, T. R., Schreiber, M. M., and Hoffer, R. M.: "Diffuse Reflectance Hypothesis for the Pathway of Solar Radiation Through Leaves", *Agronomy Journal*, 65:276-283, 1973

[118] Spectrum Technologies: "Minolta SPAD-502 Meter", *<http://www.specmeters.com/Plant_Chlorophyll_Meters/Minolta_SPAD_502_Meter.html>*, June 15, 2001

[119] Spitters, C., Van Keulen, H., and Van Kraalingen, D. W. G.: "A Simple and Universal Crop Growth Simulator: SUCROS87", in: *Simulation and Systems Management in Crop Protection*, eds. R. Rabbinge, S. A. Ward, H. H. Van Laar, Simulation Monographs, PUDOC, Wageningen, pp. 147-181, 1989

[120] Storrer, H. H.: "Einführung in die mathematische Behandlung der Naturwissenschaften", Band II, Vorlesung Sommersemester 1993, *Mathematisches Institut der Universität Zürich*, pp. 241, 1993

[121] Strobl, P.: "Entwicklung von Verfahren zur Datenaufbereitung und Kalibrierung eines abbildenden Spektrometers am Beispiel des DAIS 7915", Scientific Technical Report STR00/12, *Geoforschungszentrum Potsdam*, pp. 142, 2000

[122] Suits, G. W.: "The Calculation of the Directional Reflectance of a Vegetation Canopy", *Remote Sens. Environ.*, 2:117-125, 1972

[123] Swinton, S. M. and Jones, K. Q.: "From Data to Information: Adding Value to Site-Specific Data", in: *Proc. 4th International Conference on Precision Agriculture*, Part B, pp. 1681-1692, 1998

[124] Thenkabail, P. S., Smith, R. B., and De Pauw, E.: "Hyperspectral Vegetation Indices and Their Relationships With Agricultural Crop Characteristics", *Remote Sens. Environ.*, 71:158-182, 2000

[125] Thomas, J. R., Namken, L. N., Oerther, G. F., and Brown, R. G.: "Estimating Leaf Water Content by Reflectance Measurements", *Agronomy Journal*, 63:845-847, 1971

[126] Thomas, J. R. and Gausman, H. W.: "Leaf Reflectance vs. Leaf Chlorophyll and Carotenoid Concentrations for Eight Crops", *Agronomy Journal*, 69:799-802, 1977

[127] Verdebout, J. S., Jacquemoud, S., and Schmuck, G.: "Optical Properties of Leaves: Modelling and Experimental Studies", in: *Imaging Spectrometry - a Tool for Environmental Observations*, eds. J. Hill and J. Mégier, Kluwer Academic Publishers, pp. 169-191, 1994

[128] Verhoef, W.: "Light Scattering by Leaf Layers With Application to Canopy Reflectance Modelling: The SAIL Model", *Remote Sens. Environ.*, 16:125-141, 1984

[129] Verhoef, W.: "Theory of Radiative Transfer Models Applied in Optical Remote Sensing of Vegetation Canopies", *National Aerospace Laboratory NLR*, NLR-TP-98025, pp. 320, 1998

[130] Verstraete, M. M.: "Retrieving Canopy Properties from Remote Sensing Measurements", in: *Imaging Spectrometry - A Tool for Environmental Observations*, eds. J. Hill and J. Mégier, Kluwer Academic Publishers, pp. 109-123, 1994

[131] Welles, J. M. and Norman, J. M.: "Instrument for Indirect Measurement of Canopy Architecture", *Agronomy Journal*, 83(5):818-825, 1991

[132] Wessman, C. A.: "Evaluation of Canopy Biochemistry", in: *Remote Sensing of Biosphere Functioning*, eds. R. Hobbs, and H. Mooney, Ecological Studies, 79:135-156, 1990

[133] Weiss, M. and Baret, F.: "Evaluation of Canopy Biophysical Variable Retrieval Performances from the Accumulation of Large Swath Satellite Data", *Remote Sens. Environ.*, 70:293-306, 1999

[134] Wiegand, C. L., Richardson, A. J., Escobar, D. E., and Gerbermann, A. H.: "Vegetation Indices in Crop Assessments", *Remote Sens. Environ.*, 35:105-119, 1991

[135] Willstätter, R. and Stoll, A.: "Untersuchungen über die Assimilation der Kohlensäure", Springer, Berlin, pp. 122, 1918

[136] Yoder, B. and Pettigrew-Crosby, R.: "Predicting Nitrogen and Chlorophyll Content and Concentration from Reflectance Spectra (400-2500 nm) at Leaf and Canopy Scales", *Remote Sens. Environ*., 53:199-211, 1995

[137] Zadoks, J. C., Chang, T. T., and Konzak, C. F.: "A Decimal Code for the Growth Stages of Cereals", *Weed Research*, 14:415-421, 1974

[138] Zur, Y., Gitelson, A. A., Chivkunova, O. B., and Merzlyak M. N.: "The Spectral Contribution of Carotenoids to Light Absortion and Reflectance in Green Leaves", in: *2nd International Conference on Geospatial Information in Agriculture and Forestry*, II-17-II-23, 2000

Acknowledgements

I would like to acknowledge the following persons for their highly appreciated support during the time of this work:

- Prof. Dr. Klaus I. Itten for his continuous support and interest in this work on the one hand, and his generous way of unconstrained research activities on the other hand.
- The Co-Investigator, Prof. Dr. Karl Staenz from CCRS in Ottawa, Canada, for the proof-reading and his interest in my work.
- Michael Schaepman (RSL), for many hints and inspiring discussions, especially during long overland trips to the Middle East and the Sahara, his ongoing encouragements and proof-reading of this work.
- Daniel Schläpfer (RSL), for his active role in the weekly progress- and discussion meetings, his support in methodology and implementation, and his assistance in the proof-reading of this work,
- My colleagues at RSL, Anko Börner (now at DLR Berlin), Stephan Bojinski, Stefan Dangel, Sandra Eckert, Tobias Kellenberger, Peter Keller (now with MeteoSwiss), Cornelia Naef, Roman Schurter and Gabi Strub, for supporting me in the extensive field- and laboratory work, answering my questions, and for their interest in my work.
- Erich Meier und Daniel Nüesch for their support in organizing flight-campaigns, and for many entertaining discussions during coffee breaks.
- Uli Beisl, Andrea Hausold, Andreas Müller and Rolf Richter, our friends at DLR Oberpfaffenhofen (Germany), for fruitful collaboration and memorable meetings in Munich.
- Markus Egli, Christian Hitz, Bruno Kägi, Ivan Woodhatch (GIUZ), and René Husi (Institute of Environmental Sciences, University of Zurich) for helping me with the laboratory work.
- Leo Arni of Oberramsern (Swiss Canton of Solothurn) and his family, who allowed me to take as many measurements and samples on their fields as necessary. They generously shared their experience and knowledge in crop growth with me, answering to dozens of questions arising from my side over time.